

Heat stored in the Earth system 1960-2020: Where does the energy go?

Authors: [Karina von Schuckmann](#)¹, [Audrey Minère](#)¹, [Flora Gues](#)^{1,2}[Gues](#)^{2,1}, [Francisco José Cuesta-Valero](#)^{3,364}, [Gottfried Kirchengast](#)⁴[Kirchengast](#)^{5,6}, [Susheel Adusumilli](#)⁵, [Fiamma Straneo](#)⁵[Adusumilli](#)⁷, [Fiammetta Straneo](#)⁷, [Michael Ablain](#)⁸, [Richard P. Allan](#)⁶[Allan](#)⁹, [Chris Atkinson](#)¹⁰, [Paul M. Barker](#)⁷[Barker](#)¹¹, [Hugo Beltrami](#)^{8,51}[Beltrami](#)¹², [Alejandro Blazquez](#)¹³, [Tim Boyer](#)⁹[Boyer](#)¹⁴, [Lijing Cheng](#)^{10,11}[Cheng](#)^{15,16}, [John A. Church](#)⁷[Church](#)¹⁷, [Damien Desbruyeres](#)¹²[Desbruyeres](#)¹⁸, [Han Dolman](#)¹³[Dolman](#)¹⁹, [Catia M. Domingues](#)¹⁴[Domingues](#)²⁰, [Almudena García-García](#)^{3,364}, [Donata Giglio](#)¹⁵[Giglio](#)²¹, [John E. Gilson](#)⁵[Gilson](#)⁷, [Maximilian Gorfer](#)^{16,4}[Gorfer](#)^{5,22}, [Leopold Haimberger](#)¹⁷[Haimberger](#)²³, [Maria Z. Hakuba](#)²⁴, [Stefan Hendricks](#)¹⁸[Hendricks](#)²⁵, [Shigeki Hosoda](#)¹⁹[Hosoda](#)²⁶, [Gregory C. Johnson](#)²⁰[Johnson](#)²⁷, [Rachel Killick](#)²¹[Killick](#)¹⁰, [Brian King](#)¹⁴[King](#)²⁸, [Nicolas Kolodziejczyk](#)²²[Kolodziejczyk](#)²⁹, [Anton Korosov](#)²³[Korosov](#)³⁰, [Gerhard Krimmer](#)²⁴[Krimmer](#)³¹, [Mikael Kuusela](#)²⁵[Kuusela](#)³², [Felix W. Landerer](#)²⁴, [Moritz Langer](#)^{26,27}[Langer](#)^{33,34}, [Thomas Lavergne](#)²⁸[Lavergne](#)³⁵, [Isobel Lawrence](#)²⁹[Lawrence](#)³⁶, [Yuehua Li](#)³⁰[Li](#)³⁷, [John Lyman](#)²⁰[Lyman](#)²⁷, [Florence Marti](#)⁸, [Ben Marzeion](#)²¹[Marzeion](#)³⁸, [Michael Mayer](#)^{17,31}[Mayer](#)^{23,39}, [Andrew H. MacDougall](#)³²[MacDougall](#)⁴⁰, [Trevor McDougall](#)⁷[McDougall](#)¹⁷, [Didier Paolo Monselesan](#)³³[Monselesan](#)⁴¹, [Jan Nitzbon](#)^{26,34}[Nitzbon](#)^{42,43}, [Inès Otosaka](#)³⁵[Otosaka](#)⁴⁴, [Jian Peng](#)^{3,364}, [Sarah Purkey](#)⁵[Purkey](#)^{7,45}, [Dean Roemmich](#)⁵[Roemmich](#)^{7,45}, [Kanao Sato](#)¹⁹[Sato](#)²⁶, [Katsunari Sato](#)³⁷[Sato](#)⁴⁶, [Abhishek Savita](#)³⁸[Savita](#)⁴⁷, [Axel Schweiger](#)³⁹[Schweiger](#)⁴⁸, [Andrew Shepherd](#)¹³⁵[Shepherd](#)⁴⁴, [Sonia I. Seneviratne](#)⁴⁰[Seneviratne](#)⁴⁹, [Leon Simons](#)⁴¹[Simons](#)⁵⁰, [Donald A. Slater](#)⁴²[Slater](#)⁵¹, [Thomas Slater](#)³⁵, [Noah Smith](#)⁴³[Slater](#)⁴⁴, [Andrea Steiner](#)⁵[Steiner](#)⁵, [Toshio Suga](#)^{44,19}[Suga](#)^{52,26}, [Tanguy Szekely](#)⁴⁵[Szekely](#)⁵³, [Wim Thiery](#)⁴⁶[Thiery](#)⁵⁴, [Mary-Louise Timmermans](#)⁴⁷[Timmermans](#)⁵⁵, [Inne Vanderkelen](#)⁴⁶, [Vanderkelen](#)⁵⁴, [Susan E. Wijffels](#)^{33,48}[Wijffels](#)^{41,56}, [Tonghua Wu](#)⁴⁹[Wu](#)⁵⁷, [Michael Zemp](#)⁵⁰[Zemp](#)⁵⁸

Corresponding author: Karina von Schuckmann, karina.von.schuckmann@mercator-ocean.fr

¹Mercator Ocean International, Toulouse, France

²CELAD, Toulouse, France

³Department of Remote Sensing, Helmholtz Centre for Environmental Research, Leipzig, 04318, Germany

⁴Wegener Remote Sensing Centre for Earth System Research, Leipzig University, Leipzig, Germany

⁵Wegener Center for Climate and Global Change and Institute, University of Graz, Graz, Austria

⁶Institute of Physics, University of Graz, Graz, Austria

⁷Scripps Institution of Oceanography, University of California San Diego, San Diego, California, USA

⁸MAGELLUM, Ramonville St.-Agne, France

⁹Department of Meteorology and National Centre for Earth Observation, University of Reading, Reading, UK

¹⁰Met Office Hadley Centre, Exeter, UK

¹¹University of New South Wales, Sydney, Australia

¹²Climate & Atmospheric Sciences Institute and Department of Earth Sciences, St. Francis Xavier University, Antigonish, B2G 2W5, Canada

¹³NOAA's LEGOS, Université de Toulouse, CNES, CNRS, IRD, UPS, Toulouse, France

¹⁴NOAA's National Centers for Environmental Information, Silver Spring, Maryland, USA

¹⁵Institute of Atmospheric Physics, Chinese Academy of Sciences, Beijing, China

¹⁶Center for Ocean Mega-Science, Chinese Academy of Sciences, Qingdao, 266071, China

¹⁷University of New South Wales, Sydney, Australia

¹⁸Ifremer, University of Brest, CNRS, IRD, Laboratoire d'Océanographie Physique et Spatiale, Brest, France

¹⁹Netherlands Institute for Sea Research, Den Burg, Texel, Netherlands

- 51 | 14 National²⁰National Oceanographic Centre, Southampton, UK
52 | 15 University²¹University of Colorado, Boulder, Boulder, Colorado, USA
53 | 16 Center²²Center for Climate Systems Modeling, ETH Zurich, Zurich, Switzerland
54 | 17 Department²³Department of Meteorology and Geophysics, University of Vienna, Vienna, Austria
55 | 18 Alfred²⁴Jet Propulsion Laboratory, California Institute of Technology, Pasadena, USA
56 | 25 Alfred Wegener Institute Helmholtz Centre for Polar and Marine Research, Bremerhaven, Germany
57 | 19 Japan²⁶Japan Marine-Earth Science and Technology (JAMSTEC), Japan
58 | 20 NOAA²⁷NOAA, Pacific Marine Environmental Laboratory, Seattle, USA
59 | 21 Met Office Hadley²⁸National Oceanographic Centre, Exeter Southampton, UK
60 | 22 University²⁹University of Brest, CNRS, IRD, Ifremer, Laboratoire d'Océanographie Physique et Spatiale,
61 | IUEM, Brest, France
62 | 23 Nansen³⁰Nansen Environmental and Remote Sensing Center, Bergen, Norway
63 | 24 Institut³¹Institut des Géosciences de l'Environnement, CNRS, Université Grenoble Alpes, Grenoble, France
64 | 25³²Department of Statistics and Data Science, Carnegie Mellon University, PittsburghPittsburgh, PA, USA
65 | 26³³Permafrost Research Section, Alfred Wegener Institute Helmholtz Centre for Polar and Marine Research,
66 | Permafrost Research Section, Potsdam, Germany
67 | 27 Humboldt-Universität zu Berlin, Geography Department, Berlin, Germany
68 | 28 Norwegian³⁴Department of Earth Sciences, Vrije Universiteit Amsterdam, Amsterdam, The Netherlands
69 | 35Norwegian Meteorological Institute, Oslo, Norway
70 | 29 European³⁶European Space Agency, ESRIN, Via Galileo Galilei, 1, 00044 Frascati RM, Italy
71 | 30³⁷School of Earth Sciences, Yunnan University, Kunming, China
72 | 38Institute of Geography and MARUM - Center for Marine Environmental
73 | Sciences, University of Bremen, Germany
74 | 31 European³⁹European Centre for Medium-Range Weather Forecasts (ECMWF), Reading, UK
75 | 32 Climate⁴⁰Climate & Environment Program, St. Francis Xavier University Antigonish, Nova Scotia, Canada
76 | B2G 2W5
77 | 33 CSIRO⁴¹CSIRO Oceans and Atmosphere, Hobart, Tasmania, Australia
78 | 34⁴²Permafrost Research Section, Alfred Wegener Institute Helmholtz Centre for Polar and Marine Research,
79 | PaleoclimatePotsdam, Germany
80 | 43Paleoclimate Dynamics Section, Alfred Wegener Institute Helmholtz Centre for Polar and Marine Research,
81 | Bremerhaven, Germany
82 | 35 Centre⁴⁴Centre for Polar Observation and Modelling, University of Leeds, UK
83 | 36 Remote Sensing Centre for Earth System Research, Leipzig University, 04103, Leipzig, Germany
84 | 37 Japan⁴⁵University of California San Diego, San Diego, California, USA
85 | 46Japan Meteorological Agency, Japan
86 | 38 GEOMAR⁴⁷GEOMAR, Kiel, Germany
87 | 39 Polar⁴⁸Polar Science Center, Applied Physics Laboratory, University of Washington, Seattle, WA, USA
88 | 40 Institute⁴⁹Institute for Atmospheric and Climate Science, ETH Zurich, Zurich, 8092, Switzerland
89 | 41 The⁵⁰The Club of Rome, The Netherlands Association, 's-Hertogenbosch, The Netherlands
90 | 42 Glaciology⁵¹Glaciology and Oceanography, Univ. of Edinburgh, UK
91 | 43 Department of Mathematics, University of Exeter, Exeter, United Kingdom
92 | 44 Tohoku⁵²Tohoku University, Japan
93 | 45 Ocean⁵³Ocean Scope, Brest, France
94 | 46 Department⁵⁴Department of Hydrology and Hydraulic Engineering, Vrije Universiteit Brussel, Brussels,
95 | 1050, Belgium
96 | 47 Department⁵⁵Department of Earth and Planetary Sciences, Yale University, New Haven, Connecticut, USA
97 | 48 Woods⁵⁶Woods Hole Oceanographic Institution, Massachusetts, USA
98 | 49 Cryosphere⁵⁷Cryosphere Research Station on Qinghai-Xizang Plateau, State Key Laboratory of
99 | Cryospheric Science, Northwest Institute of Eco-Environment and Resources (NIEER), Chinese Academy of
100 | Sciences (CAS), Lanzhou, 730000, China
101 | 50 Department⁵⁸Department of Geography, University of Zurich, Switzerland
102 | 51 Département des sciences de la Terre et de l'atmosphère, Université du Québec à Montréal, Montréal, Québec,
103 | Canada
104 | -

107 **Abstract.** The Earth climate system is out of energy balance and heat has accumulated
 108 continuously over the past decades, warming the ocean, the land, the cryosphere and the
 109 atmosphere. According to the 6th Assessment Working Group I Report of the Intergovernmental
 110 Panel on Climate Change, this planetary warming over multiple decades is human-driven and
 111 results in unprecedented and committed changes to the Earth system, with adverse impacts for
 112 ecosystems and human systems. The Earth heat inventory provides a measure of the Earth
 113 energy imbalance, (EEI), and allows for quantifying how much heat has accumulated in the
 114 Earth system, and where the heat is stored. Here we show that ~~380 ± 62 ZJ of heat has~~
 115 ~~accumulated in the Earth~~Earth's system has continued to accumulate heat, with 381 ± 61 ZJ from
 116 ~~1971 to 2020, at. This is equivalent to a heating rate (i.e., the EEI) of 0.48 ± 0.1 W m⁻², with,~~
 117 ~~The majority, about 89 ± 17%%, of this heat is stored in the ocean, followed by about 6 ± 0.1%~~
 118 ~~on land, 4 ± 1% in the cryosphere and 1 ± 0.2 % 1 % in the atmosphere, and about 4 % is~~
 119 ~~available for melting the cryosphere.~~ Over the most recent decade (period 2006-2020), the Earth
 120 ~~heat inventory shows increased warming at rate of 0.48 ± 0.3 W m⁻²/decade, and, the Earth~~
 121 ~~climate system is out of energy balance by EEI amounts to 0.76 ± 0.2 Wm⁻².~~ The Earth heat
 122 ~~inventory~~Energy Imbalance is the most fundamental global climate indicator that the scientific
 123 community and the public can use as the measure of how well the world is doing in the task of
 124 bringing anthropogenic climate change under control. Moreover, this indicator is highly
 125 complementary to other established ones like global mean surface temperature as it represents a
 126 robust measure of the rate of climate change, and its future commitment. We call for an
 127 implementation of the Earth ~~heat inventory~~energy imbalance into the Paris agreement's global
 128 stocktake based on best available science. The Earth heat inventory in this study, updated from
 129 von Schuckmann et al.,² 2020, is underpinned by worldwide multidisciplinary collaboration and
 130 demonstrates the critical importance of concerted international efforts for climate change
 131 monitoring and community-based recommendations ~~as coordinated by the Global Climate~~
 132 ~~Observing System (GCOS).~~ We and we also call for urgently needed actions for enabling
 133 continuity, archiving, rescuing and calibrating efforts to assure improved and long-term
 134 monitoring capacity of the ~~relevant GCOS Essential Climate Variables (ECV) for the Earth heat~~
 135 ~~inventory~~global climate observing system.

136

137

138 Introduction

139 -

140 ~~Since a recent international quantification of the Earth heat inventory (von Schuckmann et al.,~~
 141 ~~2020), three main reports of the 6th assessment cycle of the Intergovernmental Panel for Climate~~
 142 ~~Change (IPCC)¹ have been published. The IPCC report of Working Group III (WGIII) 'Climate~~
 143 ~~Change 2022: Mitigation of Climate Change'² (IPCC, 2022b) states that 'options available now in~~
 144 ~~every sector that can at least halve emissions by 2030' and that 'accelerated climate action is~~
 145 ~~critical to sustainable development'². The IPCC report of Working Group II (WGII) 'Climate~~
 146 ~~Change 2022: Impacts, Adaptation and Vulnerability'³ (IPCC, 2022a) offers solutions, while~~
 147 ~~pointing out that 'every small increase in warming will result in increased risks', and that 'it is~~
 148 ~~essential to make rapid, deep cuts in greenhouse gas emissions to keep the maximum number of~~
 149 ~~adaptation options open'³. The IPCC report of Working Group I (WGI) 'Climate Change 2022:~~

8 1 — <https://www.ipeec.ch/>

9 2 — https://report.ipeec.ch/ar6wg3/pdf/IPCC_AR6_WGIII_PressConferenceSlides.pdf

10 3 — https://report.ipeec.ch/ar6wg2/pdf/IPCC_AR6_WGII_PressConferenceSlides.pdf

150 The Physical Science Basis' (IPCC, 2021) concluded that '*recent human-induced changes in the*
 151 *climate are widespread, rapid, and intensifying, and unprecedented in thousands of years*', and
 152 *'that there is no going back from some changes in the climate system, from which some changes*
 153 *could be slowed and others could be stopped by limiting warming*²⁴.

154
 155
 156 The Earth energy imbalance (EEI) is the most fundamental indicator for climate change, as it
 157 tells us if, how much, how fast and where the Earth climate is warming, and how this warming
 158 evolves in the future (Hansen et al., 2011, 2005; von Schuckmann et al., 2016). The EEI is given
 159 by the difference between incoming solar radiation and outgoing radiation, which determines the
 160 net radiative flux at the Top Of the Atmosphere (TOA). Today, the Earth climate system is out of
 161 energy balance, and consequently, heat has accumulated continuously over the past decades,
 162 warming the ocean, the land, the cryosphere and the atmosphere, determining the Earth heat
 163 inventory (Fig. 1, von Schuckmann et al., 2020). This planetary warming is human-driven and
 164 results in unprecedented and committed changes to the Earth system (Fig. 1) (Forster et al.,
 165 2022), with adverse impacts for ecosystems and human systems (IPCC, 2022a). As long as this
 166 imbalance persists, or even increases, planet Earth will keep gaining energy, increasing planetary
 167 warming (Hansen et al., 2005; 2017). Today the EEI can be best estimated from the
 168 quantification of the Earth heat inventory, complemented by direct measurements from space
 169 (von Schuckmann et al., 2016; Loeb et al., 2021). In addition, the Earth heat inventory as derived
 170 from multiple sources of measurements and models also allows to unravel where the energy –
 171 mostly in the form of heat – is stored in the Earth system across all components (von
 172 Schuckmann et al., 2020). Results of the first internationally driven initiative on the Earth heat
 173 inventory (von Schuckmann et al., 2020) do not only show how much and where heat has
 174 accumulated in the Earth system, but have also shown for the first time that the Earth energy
 175 imbalance has increased over the recent decade. This increase is expected to have fundamental
 176 implications for Earth climate, and several potential drivers have been discussed recently
 177 (Hakuba et al., 2021; Kramer et al., 2021; Loeb et al., 2021).

178
 179 ~~These assessment outcomes further emphasize the need to extend the Global Climate Observing~~
 180 ~~System (GCOS) beyond the strict scientific observation of the climate state to also supporting~~
 181 ~~policy and planning (GCOS, 2021). The GCOS was established in 1992 to aid in developing and~~
 182 ~~coordinating a GCOS that supported scientific understanding of climate change. More recently it~~
 183 ~~has broadened its focus to include policy development, public information and planning for~~
 184 ~~adaptation and mitigation (GCOS, 2016). GCOS started assessments of the Earth's heat~~
 185 ~~inventory in 2018, and the carbon and the water cycles, to identify potential gaps and~~
 186 ~~inconsistencies in existing observation systems (Crisp et al., 2022; Dorigo et al., 2021; von~~
 187 ~~Schuckmann et al., 2020). The first call for concerted international collaboration on the Earth's~~
 188 ~~energy imbalance and the associated Earth heat inventory had been established in a perspective~~
 189 ~~paper in 2016 (von Schuckmann et al., 2016), initiating a research focus activity under~~
 190 ~~WCRP/CLIVAR⁵. One of the outcomes was the development of an internationally and~~
 191 ~~multidisciplinary driven publication on the Earth heat inventory, now under the auspices of~~
 192 ~~GCOS (von Schuckmann et al., 2020), which further continues with this study. With this second~~

14 4 — <https://www.ipcc.ch/report/ar6/wg1/resources/presentations-and-multimedia>

15 5 — <https://www.clivar.org/research-foci/heat-budget>

193 study we aim to contribute to a more frequent and regular update of the state of the Earth heat
 194 inventory as an important indicator of climate change.

195
 196 The Earth heat inventory provides a quantitative measure of the heat accumulated in the Earth
 197 system, which results from the anthropogenically perturbed planetary radiation budget—i.e., a
 198 positive Earth Energy Imbalance (EEI) forced by increasing atmospheric concentrations of
 199 radiatively active greenhouse gases from human-induced emissions (Forster et al., 2022;
 200 Hansen et al., 2011) (Fig. 1). Estimates of the Earth heat inventory can be obtained by analyzing
 201 several Essential Climate Variables (ECVs) of GCOS, complemented by model and reanalysis
 202 outputs to fill the gaps, through the quantification of increases in heat content of the ocean, the
 203 land, the atmosphere, and the heat used to melt ice (Forster et al., 2022; von Schuckmann et al.,
 204 2020). This assessment allows for evaluating the total heat accumulated in the Earth system and
 205 where and how much heat is stored in the different Earth system components (Fig. 1). The
 206 derivative of the Earth heat inventory over time provides then an estimate of the global heating
 207 rate, and hence, the absolute value of the EEI (Loeb et al., 2012; Trenberth et al., 2016). A recent
 208 quantification of the Earth heat inventory (von Schuckmann et al., 2020) revealed a consistent
 209 long-term Earth system heat gain over the period 1971–2018, with a total heat gain of 358 ± 37
 210 ZJ, which is equivalent to a global heating rate of $0.47 \pm 0.1 \text{ W m}^{-2}$. Over the period 1971–2018,
 211 the majority of heat gain is reported for the global ocean, with 89 % of the excess heat in the
 212 climate system stored there, and for 2010–2018 that was 90%. 52 % of the excess heat was
 213 stored in the upper 700 m of the ocean for both time periods, with 28 % stored in the 700–2000 m
 214 depth layer and 9 % below 2000 m depth for 1971–2018 (30% in the 700–2000 m layer and 8%
 215 below 2000 m for 2010–2018). For 1971–2018, heat gain by the land amounts to 6 % of the total,
 216 4 % is used for the melting of grounded and floating ice, and 1 % goes to atmospheric warming.
 217 Those fractions are 5%, 3%, and 2% respectively for 2010–2018. The results are consistent
 218 within uncertainty ranges with the assessment outcomes as obtained in the recent IPCC report
 219 (Forster et al., 2022).

220
 221 The rate of change in the Earth heat inventory, and hence, the EEI, is the portion of the forcing
 222 that the Earth has not yet realized as warming (Hansen et al., 2005). The Earth system responds
 223 to an imposed radiative forcing through a number of feedbacks, which operate on various
 224 different timescales. Earth's radiative response is complex, comprising a variety of climate
 225 feedbacks (e.g., water vapor feedback, cloud feedbacks, ice-albedo feedback) (Forster et al.,
 226 2022). Conceptually, the relationships between EEI, radiative forcing and surface temperature
 227 change can be expressed as (Gregory & Andrews, 2016):

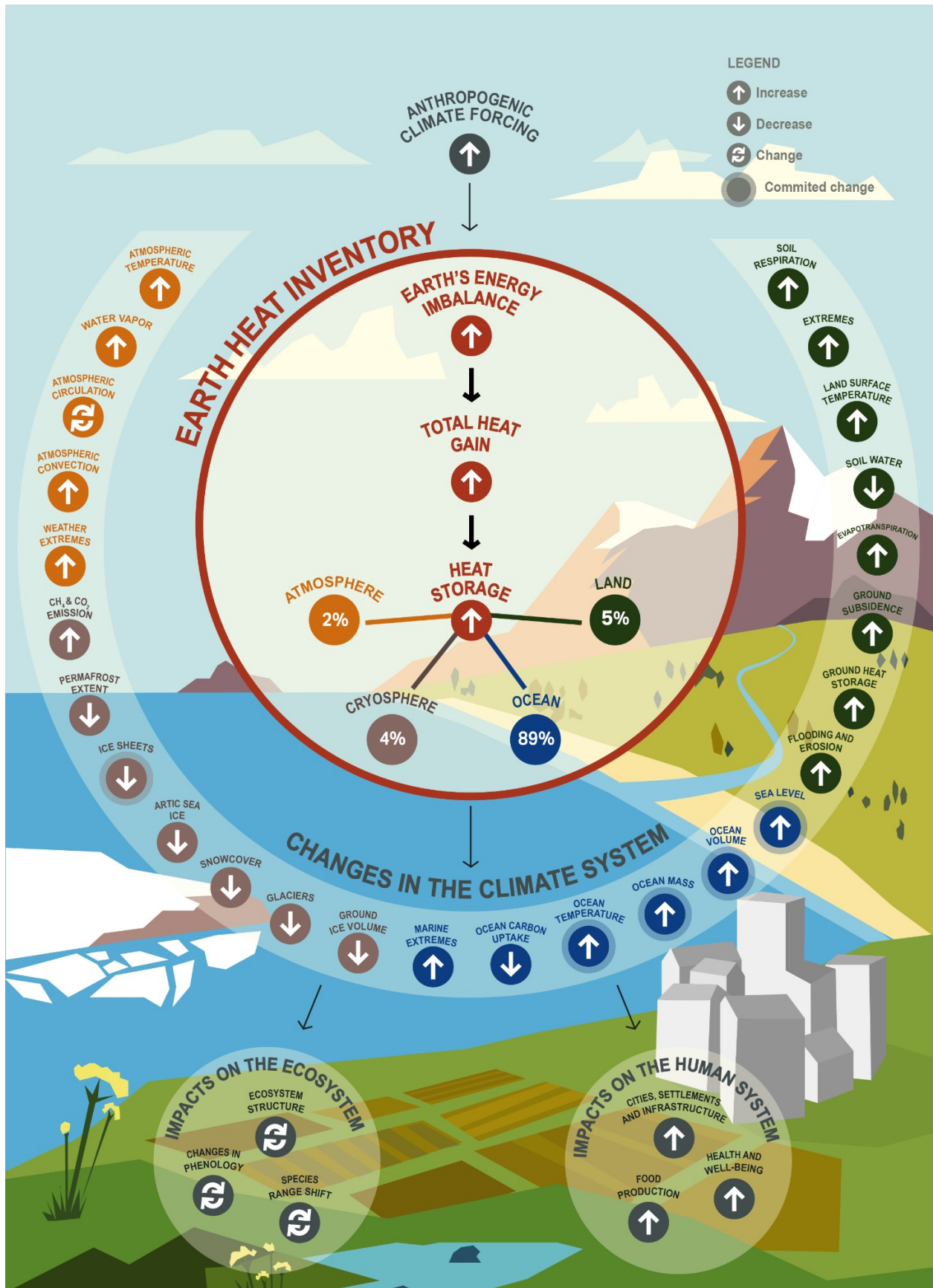
$$228 \quad \Delta N_{\text{TOA}} = \Delta F_{\text{ERF}} - |\alpha_{\text{FP}}| \Delta T_{\text{S}}, \quad (1)$$

229
 230 where ΔN_{TOA} is the Earth's net energy imbalance at ~~the Top Of the Atmosphere (TOA)~~ TOA (in
 231 W m^{-2}), ΔF_{ERF} is the effective radiative forcing (W m^{-2}), ΔT_{S} is the global surface temperature
 232 anomaly (K) relative to the equilibrium state and α_{FP} is the net total feedback parameter (W m^{-2}
 233 K^{-1}), which represents the combined effect of the various climate feedbacks. Essentially, α_{FP} in
 234 Eq. (1) can be viewed as a measure of how efficient the system is at restoring radiative
 235 equilibrium for a unit surface temperature rise. Thus, ΔN_{TOA} represents the difference between
 236 the applied radiative forcing and Earth's radiative response through climate feedbacks associated
 237 with surface temperature increase (e.g., Hansen et al., 2011). Observation-based estimates of

239 ΔN_{TOA} are therefore crucial both to our understanding of past climate change and for refining
240 projections of future climate change (Gregory & Andrews, 2016; Kuhlbrodt & Gregory, 2012).
241 The long atmospheric lifetime of carbon dioxide means that ΔN_{TOA} , ΔF_{ERF} and ΔT_{S} will remain
242 positive for centuries, even with substantial reductions in greenhouse gas emissions, and lead to
243 substantial sea-level rise, ocean warming and ice shelf loss (~~Cheng et al., 2019; Forster et al.,~~
244 ~~2022; Hansen et al., 2017; IPCC, 2021; Nauels et al., 2017~~)(Cheng et al., 2019; Forster et al.,
245 ~~2022; Hansen et al., 2017; IPCC, 2021; Nauels et al., 2017~~). In other words, warming will
246 continue even if atmospheric greenhouse gas (GHG) amounts are stabilized at today's level, and
247 the EEI defines additional global warming that will occur without further change in forcing
248 (Hansen et al., 2017). The EEI is less subject to decadal variations associated with internal
249 climate variability than global surface temperature and therefore represents a robust measure of
250 the rate of climate change; and its future commitment (~~Cheng et al., 2017; Forster et al., 2022;~~
251 ~~Palmer & McNeall, 2014; von Schuckmann et al., 2016~~)(Cheng et al., 2017; Forster et al., 2022;
252 ~~Loeb et al., 2018; Palmer & McNeall, 2014; von Schuckmann et al., 2016~~).

253

254



256 **Fig. 1:** Schematic overview on the central role of the Earth heat inventory and its linkage to
 257 anthropogenic emissions, the Earth energy imbalance, change in the Earth system and
 258 implications for ecosystems and human systems. The Earth heat inventory plays a central role
 259 for climate change monitoring as it provides information on the absolute value of the Earth
 260 energy imbalance, the total Earth system heat gain, and how much and where heat is stored in
 261 the different Earth system components. Examples of associated global-scale changes in the Earth
 262 system as assessed in (Gulev et al., 2021) are drawn, together with major implications for the
 263 ecosystem and human systems (IPCC, 2022e)-(IPCC, 2022b). Upward arrows indicate
 264 increasing change, downward arrows indicate decreasing change, and turning arrows indicate
 265 change in both directions. The % for heat stored in the Earth system are provided over the
 266 period 2006-2020 (see section 6).

267
 268 The heat gain in the Earth system from a positive EEI results in directly and indirectly triggered
 269 changes in the climate system, with a variety of implications for the environment and human
 270 systems (Fig. 1). One of the most direct implications from a positive EEI is the rise of Global
 271 Mean Surface Temperature (GMST). The accumulation and storage of surplus anthropogenic
 272 heat leads to ocean warming and thermal expansion of the water column, which together with
 273 terrestrial ice melt leads to sea level rise (WCRP Global Sea Level Budget Group, 2018).
 274 Moreover, there are various facets of impacts from ocean warming such as on climate extremes,
 275 which are provided in more detail in a recent review (Cheng et al., 2022)-(Cheng et al., 2022a).
 276 The heat accumulation in the Earth system also leads to warming of the atmosphere, particularly
 277 to a temperature increase in the troposphere, leading to water vapor increase and changes in
 278 atmospheric circulation (Gulev et al., 2021).

279
 280 On land, the heat accumulation leads to an increase in ground heat storage, which in turn triggers
 281 an increase in ground surface temperatures that may increase soil respiration, and may lead to a
 282 decrease in soil water, depending on the climatic and meteorological conditions and factors such
 283 as land cover and soil characteristics (Cuesta-Valero et al., 2022a; Gulev et al., 2021). Moreover,
 284 inland water heat storage increases, leading to increases in lake water temperatures that may
 285 result in algal blooms and lake stratification, and typically leads to a decrease in ice cover. Heat
 286 gain in the Earth system also induces an increase in permafrost heat content, which in turn leads
 287 to disruptive changes in ground morphology, CH₄ and CO₂ emissions, and a decrease in
 288 permafrost extent and ground ice volume. More details are synthesized in (Cuesta-Valero et al.,
 289 2022). In the cryosphere associated changes include a loss of glaciers, ice sheets and Arctic sea
 290 ice (IPCC, 2019, 2021a). These human-induced changes have already impacted terrestrial,
 291 freshwater and ocean ecosystems, and have adverse impacts on human systems (Fig.1).
 292 Particularly, they have emerged for ecosystem structure, species ranges and phenology (timing of
 293 life cycles), and include adverse impacts such as for water security and food production, health
 294 and wellbeing, cities, settlements and infrastructures (IPCC, 2022c, see their Fig. SPM.2).

295
 296 Regularly assessing, quantifying and evaluating the Earth heat inventory creates a unique
 297 opportunity to support the call of action and solution pathways as assessed during the 6th
 298 assessment cycle of the IPCC. Moreover, the Earth heat inventory allows for a regular stock
 299 taking of the implementation of the Paris Agreement⁶ while monitoring progress towards
 300 achieving the purpose of the agreement and its long-term goals based on best available science.

28 ⁶ <https://unfccc.int/process-and-meetings/the-paris-agreement/the-paris-agreement>

301 These assessment outcomes further emphasize the need to extend the Global Climate Observing
 302 System (GCOS) beyond the strict scientific observation of the climate state to also supporting
 303 policy and planning (GCOS, 2021). Science-driven studies driven by an Earth system view and
 304 backboned by concerted multidisciplinary and international collaborations play here a critical
 305 role to support these objectives (Crisp et al., 2022; Dorigo et al., 2021; von Schuckmann et al.,
 306 2020). On land, the heat accumulation leads to an increase in ground heat storage, which in turn
 307 triggers an increase in ground surface temperature that may increase soil respiration, and
 308 evaporation, and may lead to a decrease in soil water, depending on the climatic and
 309 meteorological conditions and factors such as land cover and soil characteristics (Cuesta-Valero
 310 et al., 2022; Gulev et al., 2021). Moreover, inland water heat storage increases, which in turn
 311 leads to increases in lake water temperature that may result in algal blooms and lake
 312 stratification, and typically leads to a decrease in ice cover. Heat gain in the Earth system also
 313 induces an increase in permafrost heat content, which in turn increases ground subsidence, CH₄
 314 and CO₂ emissions, and a decrease in permafrost extent and ground ice volume. More details are
 315 synthesized in (Cuesta-Valero et al., 2022). In the cryosphere associated changes include a loss
 316 of glaciers, ice sheets and Arctic sea ice (IPCC, 2019)With this second study we aim to
 317 contribute to a more frequent and regular science-driven update of the state of the Earth heat
 318 inventory as an important indicator of climate change.

319 These human-induced changes have already impacted terrestrial, freshwater and ocean
 320 ecosystems, and have adverse impacts on human systems (Fig.1). Particularly, they have
 321 emerged for ecosystem structure, species ranges and phenology (timing of life cycles), and
 322 include adverse impacts such as for water security and food production, health and wellbeing,
 323 cities, settlements and infrastructures as assessed in detail in the recent IPCC Working Group II
 324 report (IPCC, 2022e, see their Fig. SPM.2).

325
 326 In summary, the Earth heat inventory is a global climate indicator integrating fundamental
 327 aspects of the Earth system under global warming. Particularly, the global climate indicator of
 328 the Earth heat inventory

- 329
- 330 • provides the best available current estimate of the absolute value of the Earth Energy
 331 Imbalance (Cheng et al., 2017; Cheng et al., 2019; Hakuba et al., 2021; Hansen et al.,
 332 2011; Loeb et al., 2012, 2022; Trenberth et al., 2016; von Schuckmann et al., 2020);
 333
- 334 • enables an integrated view of the effective radiative climate forcing, Earth's surface
 335 temperature response and the climate sensitivity (Forster et al., 2022; Hansen et al., 2011;
 336 Hansen et al., 2005; Palmer & McNeall, 2014; Smith et al., 2015);
 337
- 338 • informs about the status of global warming in the Earth system as it integrates the heat 'in
 339 the pipeline' that will ultimately warm the deep ocean and melt ice sheets in the long
 340 term (Hansen et al., 2011; Hansen et al., 2005; IPCC, 2021);
 341
- 342 • reveals how much and where surplus anthropogenic heat is available for melting the
 343 cryosphere and warming the ocean, land and atmosphere, which in turn allows for an
 344 evaluation of associated changes in the climate system and is essential to improve
 345 seasonal-to-decadal climate predictions and projections on century timescales to enable

improved planning for and adaptation to climate change (Hansen et al., 2011; von Schuckmann et al., 2016, 2020);

- provides a tool for assessing the status of the GCOS, the identification of its strength and gaps, and the development of crucial recommendations of its future evolution (GCOS, 2021; von Schuckmann et al., 2020);
- creates an opportunity for a safe climate pathway while evaluating an atmospheric CO₂ reduction amount to bring Earth back towards energy balance (Hansen et al., 2000; von Schuckmann et al., 2020);
- Enables concerted international and multidisciplinary collaboration and advancements in climate science.

Hence, regularly assessing, quantifying and evaluating the Earth heat inventory creates a unique opportunity to support the call of action and solution pathways as assessed during the 6th assessment cycle of the IPCC. Moreover, the Earth heat inventory allows for a regular stock taking of the implementation of the Paris Agreement⁷ while monitoring progress towards achieving the purpose of the agreement and its long-term goals based on best available science.

Based on the quantification of the Earth heat inventory published in 2020 (von Schuckmann et al., 2020), we will present the updated results of the Earth heat inventory over the period 1960-2020, along with the long-term Earth's system heat gain over this period, and the partitions of where the heat goes for the ocean, atmosphere, land and cryosphere. Section 2 provides the updates for ocean heat content, which is based on improved evaluations (e.g., [trend evaluation method](#)) and the addition of further international data products of subsurface temperature. Updated estimates and refinements for atmospheric heat content are discussed in Section 3. For the land component in section 4, an improved uncertainty framework is proposed for the ground heat storage estimate, and new evaluations for inland freshwater heat storage and thawing of permafrost have been included (Cuesta-Valero et al., 2022). [Heat2022a](#). An update of the heat available to melt the cryosphere is described in section 5 [based on reenforced international collaboration](#). In section 6, the updated Earth heat inventory is established and discussed based on the results of sections 2-5. In the final section, challenges and recommendations for future improved estimates are discussed for each Earth system component, with associated recommendations for future evolutions of the [GCOS observing system](#).

2. Heat stored in the ocean

[Estimating global](#) Global Ocean Heat Content (OHC) [can be estimated](#) directly [depends on](#) from [subsurface temperature measurements](#), which is one of the variables of the in situ component of the Global Ocean Observing System (GOOS)⁸, and which has continued to evolve during the past century (Abraham et al., 2013; Gould et al., 2013; Moltmann et al., 2019). Many global OHC estimates for the historical period start from about the 1950s and 1960s, i.e., when shipboard Nansen bottle and mechanical bathythermograph (MBT) instruments, conductivity-

⁷ <https://unfccc.int/process-and-meetings/the-paris-agreement/the-paris-agreement>

⁸ <https://www.goosocean.org/>

390 temperature–depth (CTD) instruments and the expendable bathythermograph (XBT) became
 391 available (Abraham et al., 2013; Goni et al., 2019). In the 1980s and 1990s, the GOOS (GOOS,
 392 2019) started to further evolve, including programs for moored arrays in the tropical ocean
 393 basins, and the international World Ocean Circulation Experiment (WOCE) (Gould et al., 2013;
 394 King et al., 2001). Estimates of global OHC are, however, challenged by various factors, such as
 395 limited global coverage and data quality. The international community, especially under the
 396 auspices of the International quality-controlled Ocean Database project (IQuOD⁹), works together
 397 to face these obstacles through data and meta-data recovery and improved observational
 398 uncertainty specification, bias correction methods, and data processing techniques (Boyer et al.,
 399 2016; Castelao, 2020; Castelão, 2021; Cheng et al., 2018; Cowley et al., 2021; Goni et al., 2019;
 400 Gouretski & Cheng, 2020; Leahy et al., 2018; Mieruch et al., 2021; Palmer et al., 2018; Savita et
 401 al., 2022). Satellite altimeter measurements of sea surface height began in 1993 and are used to
 402 complement in situ-derived OHC estimates, either for validation purposes (Cabanes et al., 2013)
 403 or for establishing global gridded ocean temperature fields (Guinchut et al., 2012; Willis et al.,
 404 2004). Indirect estimates of OHC from remote sensing through the global sea-level budget
 405 became possible with satellite-derived ocean mass information in 2002 (Dieng et al., 2017;
 406 Hakuba et al., 2021; Llovel et al., 2014; Marti et al., 2022; Meyssignae et al., 2019), and should
 407 be considered in future establishments of the Earth heat inventory.

408 -
 409 From the year 2000 onwards, the in situ component of the GOOS was revolutionized with the
 410 implementation of an international program of profiling floats targeting global hydrographic
 411 measurements of the upper 2000m depth (Riser et al., 2016; Roemmich et al., 2019) — a target
 412 which was largely reached in 2005 for the ocean area between 60°S–60°N and fully realized in
 413 2006 (Riser et al. 2016). The opportunity for improved OHC estimates provided by Argo is
 414 tremendous and has led to major advancements in climate science, particularly on the discussion
 415 of the EEI (Cheng et al., 2019; Forster et al., 2022; Hansen et al., 2011; Johnson et al., 2016;
 416 Loeb et al., 2012, 2021; Trenberth & Fasullo, 2010). The near global coverage of the Argo
 417 network also provides an excellent test bed for the long-term OHC reconstruction extending back
 418 well before the Argo period (Allison et al., 2019; Cheng, Trenberth, Fasullo, Boyer, et al., 2017).
 419 Moreover, these evaluations inform further observing system recommendations for global
 420 climate studies, i.e., gaps in the deep ocean layers below 2000m depth, in marginal seas, in shelf
 421 areas and in the polar regions (von Schuckmann et al., 2016; 2020). Gap implementations are
 422 underway, for example, for the deep Argo array (Johnson et al., 2019). Different research groups
 423 have developed gridded products of subsurface temperature fields using different processing
 424 methodologies, and an exhaustive list can be found in (Abraham et al., 2013; Boyer et al., 2016;
 425 Savita et al., 2022; Cheng et al., 2022; Gulev et al., 2021). (Abraham et al., 2013; Gould et al.,
 426 2013; Moltmann et al., 2019). The evolution of the ocean observing system for subsurface
 427 temperature measurements is provided for example in Cheng et al. (2022a), leveraging the
 428 transition from historical measures to modern autonomous techniques, which achieved near-
 429 global coverage in the year 2006 (the so-called golden Argo era). Different research groups have
 430 developed gridded products of subsurface temperature fields and ocean heat content using
 431 different processing methodologies, and an exhaustive list can be found for example in
 432 (Abraham et al., 2022; Boyer et al., 2016; Cheng et al., 2022; Gulev et al., 2021; Li et al., 2022;
 433 Savita et al., 2022). Additionally, specific Argo-based products are listed on the Argo web page
 434 (<http://www.argo.ucsd.edu/>, last access: 12 July 2022). Albeit the tremendous improvement of in

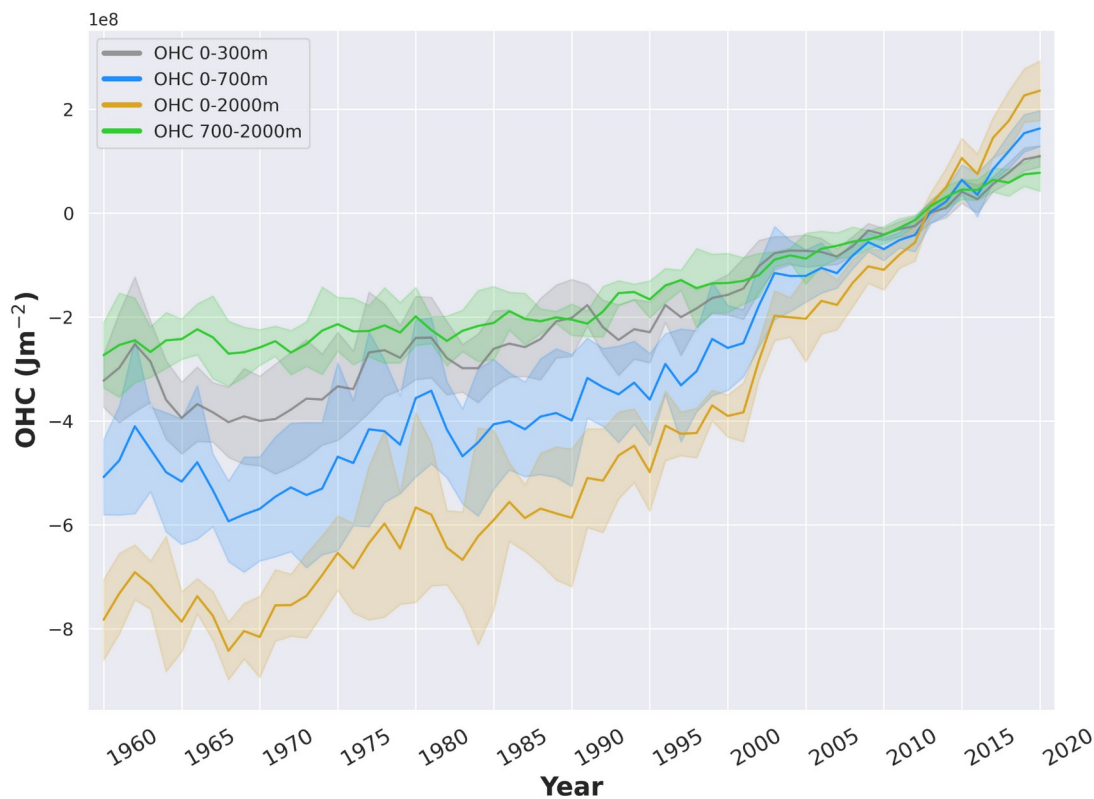
40 9 — www.iquod.org

435 ~~situ subsurface temperature measurements over time, estimates of global OHC remain an area of~~
 436 ~~active research to minimize effects from different data processing techniques of the irregular in~~
 437 ~~situ database, the choice of the climatology used in the mapping process, and data bias~~
 438 ~~corrections, which today induce discrepancies between the different estimates (Boyer et al.,~~
 439 ~~2016; Cheng et al., 2019; Good, 2017; Gouretski & Cheng, 2020; Savita et al., 2022))~~Near-global
 440 OHC can also be indirectly estimated from spatial geodetic measurements by combining sea
 441 surface height from altimetry and ocean mass from gravimetry to solve the sea-level budget
 442 equation (Dieng et al., 2017; Llovel et al., 2014; Meyssignac et al., 2019). Spatial geodetic OHC
 443 is available since 2002 and provides full depth OHC variations (Hakuba et al., 2021; Marti et al.,
 444 2022). Ocean reanalysis systems have also been used to deliver estimates of near-global OHC
 445 (Trenberth et al., 2016; von Schuckmann et al., 2018), and their international assessments show
 446 increased agreement with increasing in situ data availability for the assimilation, particularly
 447 after ~~2005~~2006, i.e. when Argo had achieved nearly global scale data sampling (Fig. 2) (Palmer
 448 et al., 2017; Storto et al., 2018, 2019). (Palmer et al., 2017; Storto et al., 2018, 2019; Meyssignac
 449 et al., 2019).

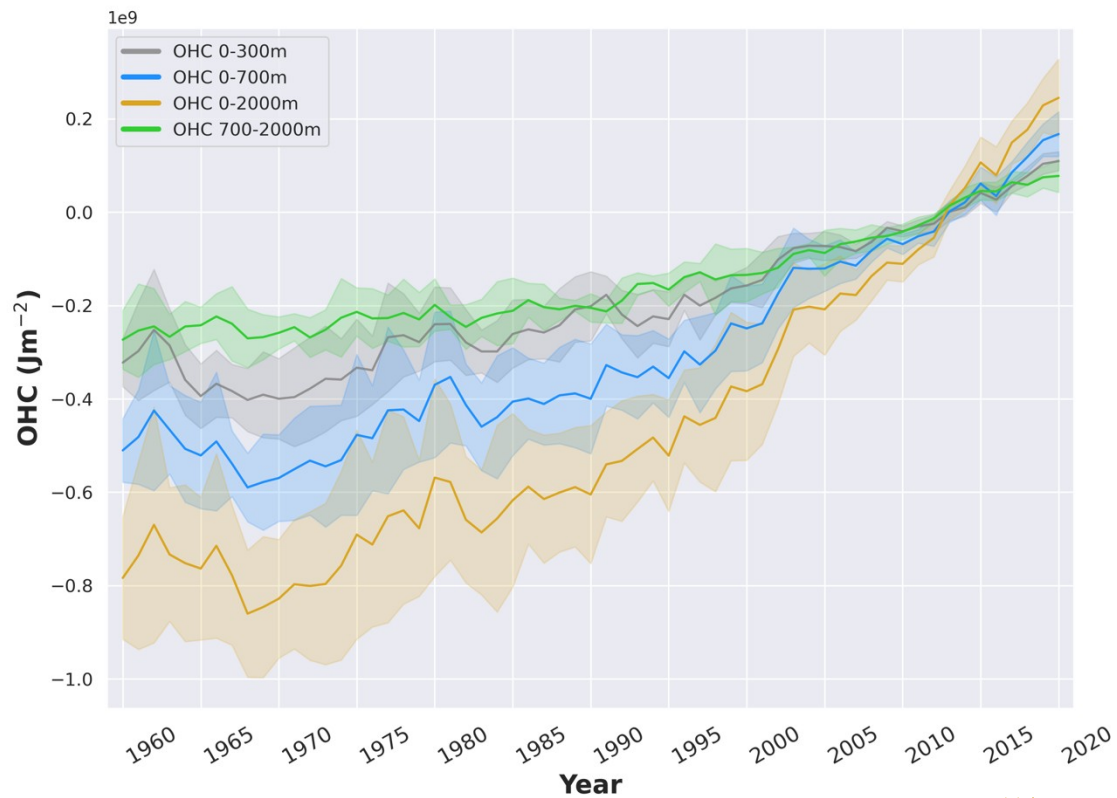
450 -
 451 This initiative relies on the availability of regular updates of data products, their temporal
 452 extensions and direct interactions with the different research groups. A complete view of all
 453 subsurface ocean temperature products can be only achieved through a concerted international
 454 effort and over time, particularly accounting for the continued development of new or improved
 455 OHC products. In this study, we do not achieve a holistic view of all available products but
 456 present a starting point for future international regular assessments of global OHC. A first
 457 established international ensemble mean and standard deviation of near global OHC up to 2018
 458 was established in von Schuckmann et al. (2020), which has now been updated up to 2020, and
 459 further extended with the addition of 45 new products (Fig. 3). The ensemble spread gives an
 460 indication of the agreement among products and can be used as a proxy for uncertainty.
 461 Compared to the results in von Schuckmann et al. (2020), the spread has increased by about 0.1
 462 W m⁻² the recent period 2006-2020 for the 0-2000m and 700-2000m integration depth
 463 layers, which can be referred back to the additional use of data products, the impact of year-to-
 464 year variations, and the refined use of the ensemble spread approach (see below).

465
 466 Albeit the tremendous improvement of in situ subsurface temperature measurements over time,
 467 estimates of global OHC remain an area of active research to minimize the major effects from
 468 different data processing techniques of the irregular (in space and time) in situ database and
 469 associated sampling characteristics, followed by the choice of the climatology used in the
 470 mapping process, and data bias corrections, which today induce discrepancies between the
 471 different estimates (Allison et al., 2019; Boyer et al., 2016; Cheng et al., 2014, 2018; Good,
 472 2017; Gouretski & Cheng, 2020; Savita et al., 2022). Concerns about common errors in the
 473 products remain. Accurate understanding of the uncertainties of the product is an essential
 474 element in their use. So far, a basic assumption is that the error distribution for the observations
 475 is Gaussian with a mean of zero, which has been approximated by an ensemble of various
 476 products. However, a more complete understanding of any apparent trends requires
 477 determination of systematic errors (e.g., systematic calibration errors), or the impacts of
 478 changing observation densities, and of instrument technologies (Wong et al., through a synthetic
 479 profile approach (Allison et al., 2019), and of instrument technologies (Wong et al., 2020). These
 480 elements can result in biases across the ensemble, or produce artificial changes in the energetics

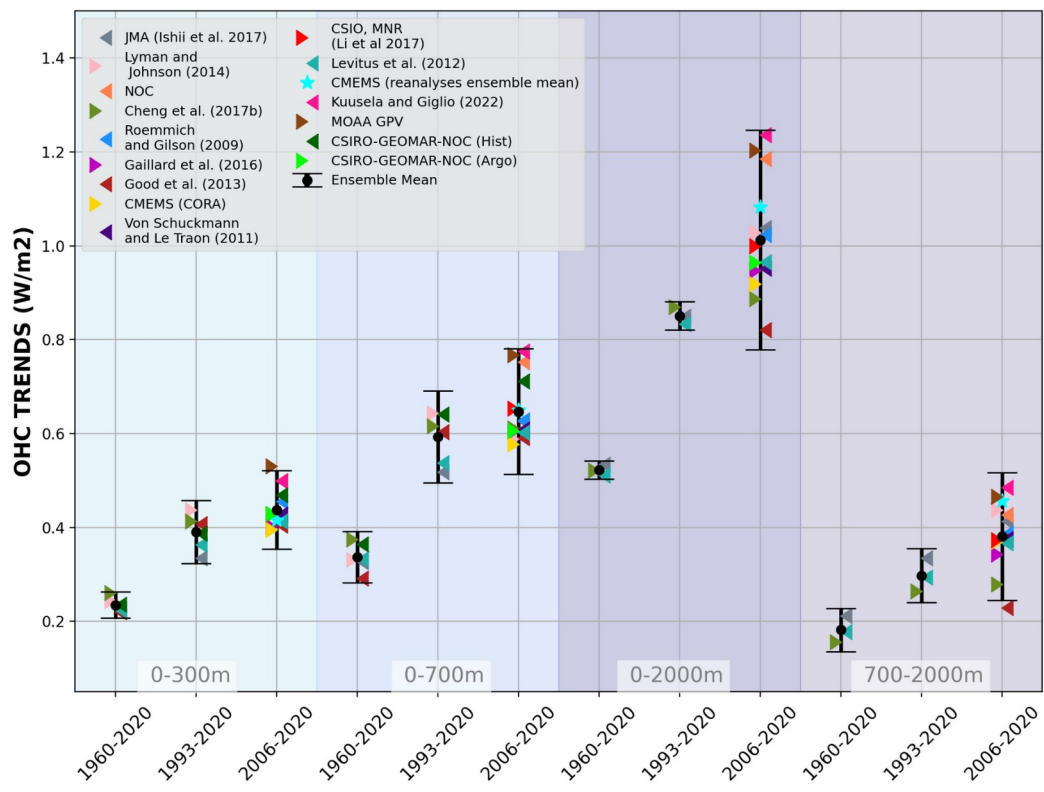
481 of the system (Wunsch, 2020). For example, Li et al. (2022) estimated that assuming linear
 482 vertical interpolation with sparse historical vertical profiles results is an underestimation of
 483 global ocean heat content (and ocean thermal expansion) trends since the 1950s of order 14%
 484 compared with more a sophisticated vertical interpolation scheme (Barker & McDougall, 2020;
 485 Li et al., 2022), with the greatest systematic underestimates at latitudes 15-20°N and S. Li et al.
 486 (2022) also found that interannual differences between various XBT corrections were similar to
 487 the differences when only higher quality hydrographic data were included, implying the need for
 488 improved time dependent XBT corrections. The uncertainty can also be estimated in other ways
 489 including some purely statistical methods (Cheng et al., 2019; Levitus et al., 2012; MacIntosh et
 490 al., 2017) or methods explicitly accounting for the error sources (Gaillard et al., 2016; Lyman &
 491 Johnson, 2014; von Schuckmann & Le Traon, 2011)(Gaillard et al., 2016; Lyman & Johnson,
 492 2014; von Schuckmann & Le Traon, 2011). Each method has its caveats; for example, the error
 493 covariances are mostly unknown, and must be estimated a priori. For this study, adopting a
 494 straightforward method with a “data democracy” strategy (i.e., all OHC estimates have been
 495 given equal weights) has been chosen as a starting point, differently from the ensemble approach
 496 adopted in AR6 (Forster et al., 2022).
 497



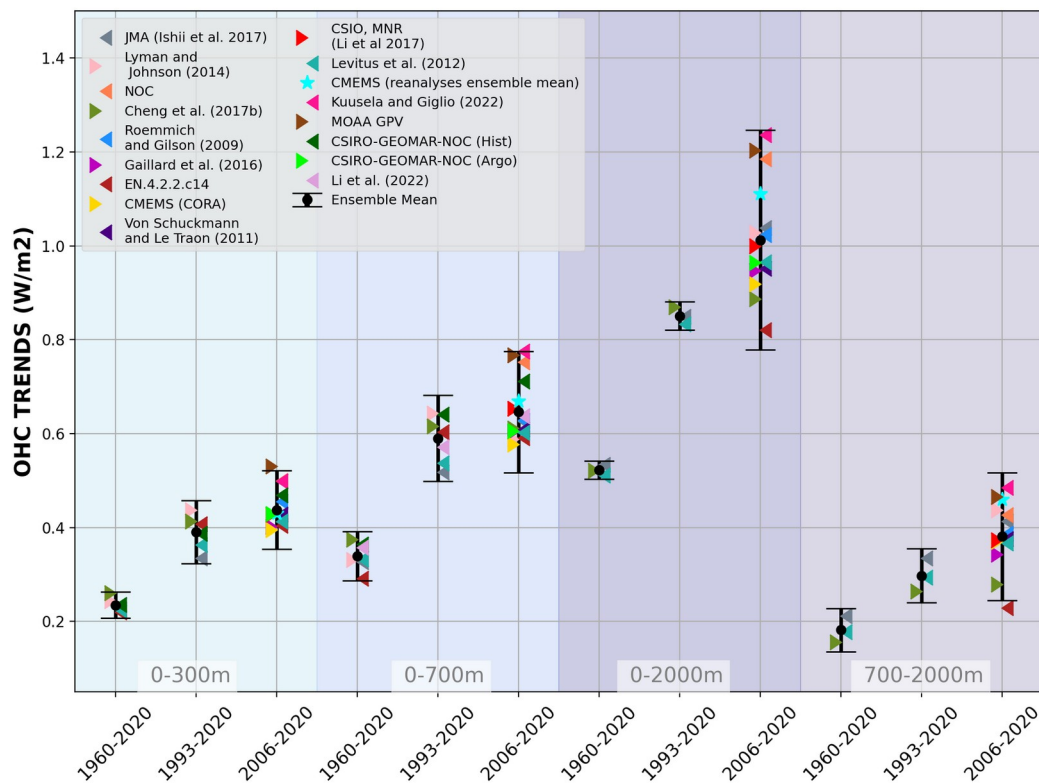
498



499 *Figure 2. Ensemble mean time series and ensemble standard deviation (shaded) of*
 500 *global ocean heat content (OHC) anomalies relative to the 2005–2020 climatology for the 0–*
 501 *300m (gray), 0–700m (blue), 0–2000m (yellow) and 700–2000m depth layer (green). The*
 502 *ensemble mean is an outcome of an international assessment initiative, and all products used are*
 503 *referenced in the legend of Fig. 3. The trends derived from the time series are given in Table 1.*
 504 *Note that values are given for the ocean surface area between 60°S and 60°N and are limited to*
 505 *the 300m bathymetry of each product.*
 506
 507



508



509
 510 *Figure 3. Trends of global ocean heat content (OHC) as derived from different products (colors),*
 511 *and using LOWESS (see text for more details). References are given in the figure legend, except,*
 512 *CMEMS (CORA—~~and~~—ARMOR-3D, [http://marine.copernicus.eu/science-learning/ocean-](http://marine.copernicus.eu/science-learning/ocean-monitoring-indicators)*
 513 *monitoring-indicators, last access: 28 June 2022), Copernicus Marine Ocean Monitoring*
 514 *Indicator, <http://marine.copernicus.eu/science-learning/ocean-monitoring-indicators>, last*
 515 *access: 28 June 2022), EN.4.2.2.c14 (Good et al., 2013b) with (Cheng et al., 2015) XBT and*
 516 *(Gouretski & Cheng, 2020) MBT bias corrections, and the method of (Palmer et al., 2007).*
 517 *CSIRO-GEOMAR-NOC (Argo) (Domingues et al., 2008; Roemmich et al., 2015; Wijffels et al.,*
 518 *2016), CSIRO-GEOMAR-NOC (hist) (Church et al., 2011; Domingues et al., 2008), NOC*
 519 *(National Oceanographic Institution) (Desbruyères et al., 2017) and the Argo dataset MOAA*
 520 *GPV (Hosoda et al., 2008). The ensemble mean and standard deviation (2σ) are indicated in*
 521 *black. Results from the Copernicus Marine reanalysis ensemble mean have been added as well*
 522 *(CMEMS, 2022) for comparison, but are not considered for the ensemble mean in Fig. 1. The*
 523 *ensemble mean and standard deviation (95% confidence interval) are indicated in black. The*
 524 *shaded areas show trends from different depth layer integrations, i.e., 0–300m (light turquoise),*
 525 *0–700m (light blue), 0–2000m (purple) and 700–2000m (light purple). For each integration*
 526 *depth layer, trends are evaluated over the three study periods, i.e., historical (1960–2020),*
 527 *altimeter era (1993–2020) and golden Argo era (2006–2020). See text for more details on the*
 528 *international assessment criteria. Note that values are given for the ocean surface area (see text*
 529 *for more details). References as indicated in the legend include (Cheng, Trenberth, Fasullo,*
 530 *Boyer, et al., 2017; Gaillard et al., 2016; Good et al., 2013; Ishii et al., 2017; Kuusela & Giglio,*
 531 *2022; Levitus et al., 2012; Li et al., 2017; Lyman & Johnson, 2014; Roemmich & Gilson, 2009;*

532 [von Schuckmann & Le Traon, 2011](#) ([Cheng et al., 2017](#); [Gaillard et al., 2016](#); [Good et al., 2013a](#);
533 [Ishii et al., 2017](#); [Kuusela & Giglio, 2022](#); [Levitus et al., 2012](#); [Li et al., 2017](#); [Li et al., 2022](#);
534 [Lyman & Johnson, 2014](#); [Roemmich & Gilson, 2009](#); [von Schuckmann & Le Traon, 2011](#)).

535
536 The continuity of this activity will help to further expand international collaboration and to
537 unravel uncertainties due to the community’s collective efforts on data quality as well as on
538 detecting and reducing processing ~~errors (e.g., IQuOD)-uncertainties~~. It also provides up-to-date
539 scientific knowledge of ocean warming. Products used for this assessment are referenced in the
540 caption of Fig. 3. Estimates of OHC have been provided by the different research groups under
541 ~~largely~~ homogeneous criteria. ~~All~~: all estimates use a coherent ocean volume limited by the
542 300m isobath ([700m for Li et al. 2022](#)) of each product and are limited to 60°S–60°N since most
543 observational products exclude high latitude ocean areas because of the low observational
544 coverage, and only annual averages have been used. The ocean areas within 60°S–60°N includes
545 91% of the global ocean surface area, and limiting to the 300m isobath neglects the contributions
546 from coastal and shallow waters, so the resultant OHC trends will be underestimated if these
547 ocean regions are warming. For example, neglecting shallow waters is ~~discussed~~ ~~estimated~~
548 to account for more than 10% for 0–2000m OHC trends ([Savita et al., 2022](#); [von Schuckmann et](#)
549 [al., 2014](#)), and about 4% for the Arctic area (~~Mayer et al., 2021~~)-(Mayer et al., 2021a). The
550 assessment is based on three distinct periods to account for the evolution of the observing
551 system, i.e., 1960–2020 (i.e., “historical”), 1993–2020 (i.e., “altimeter era”) and 2006–2020 (i.e.,
552 “golden Argo era”). All time series go up to 2020 – which was one of the principal limitations
553 for the inclusion of some products. Our final estimates of OHC for the 0-300m, 0-700m, 700-
554 2000m and 0-2000 m depth layers are the ensemble average of all products, with the uncertainty
555 range defined by the standard deviation (2σ , [95% confidence interval](#)) of the corresponding
556 ~~estimates~~ ~~ensemble~~ used (Fig. 2).

557
558 For the trend evaluation we have followed the most recent study of ([Cheng et al., 2022](#)), and
559 used a Locally Weighted Scatterplot Smoothing (LOWESS) approach to reduce the effect of
560 high-frequency variability (e.g., year-to-year variability), data noise or changes in the
561 [GCOS observing system](#) as it relies on a weighted regression ([Cleveland, 1979](#)) within a
562 prescribed span width of 25 years for the historical and altimeter era, and 15 years for the recent
563 period 2006-2020. The change in OHC(t) over a specific period, ΔOHC , is then calculated by
564 subtracting the first value to the last value of the fitted time series, $\text{OHC}_{\text{LOWESS}(t)}$, to obtain the
565 trend while dividing by the considered period. To obtain an uncertainty range on the trend
566 estimate, and take into account the sensitivity of the calculation to interannual variability, we
567 implement a Monte-Carlo simulation to generate 1000 surrogate series $\text{OHC}_{\text{random}}(t)$, under the
568 assumption of a given mean (our “true” time series $\text{OHC}(t)$) ([Cheng et al., 2022](#)). Each surrogate
569 $\text{OHC}_{\text{random}}(t)$ consists of the [fitted](#) “true” time serie $\text{OHC}(t)$ plus a randomly generated residual
570 which follows a normal (Gaussian) distribution, and which is included in an envelope equal to 2
571 times the uncertainty associated to the time series. Then, a LOWESS fitted line is estimated for
572 each of the 1000 surrogates. The 95% confidence interval for the trend is then calculated based
573 on ± 2 times the standard deviation ($\pm 2\sigma$) of all 1000 trends of the surrogates. However, the use
574 of either trend estimates following a linear, or LOWESS approach, or the approach discussed in
575 ([Palmer et al., 2021](#)) lead to consistent results within uncertainties (not shown).

576

577 In agreement with (Cheng et al., 2019; Gulev et al., 2021), our results reveal a continuous
 578 increase of ocean warming over the entire study period (Fig. 2). Moreover, rates of global ocean
 579 warming have increased over the 3 different study periods, i.e., historical up to the recent decadal
 580 change. The trend values are all given in Table 1. The major fraction of heat is stored in the
 581 upper ocean (0–300 m and 0–700 m depth). However, heat storage at intermediate depth (700–
 582 2000 m) increases at a nearly comparable rate as reported for the 0–300 m depth layer (Table 1,
 583 Fig. 3). There is a general agreement among the 16 international OHC estimates (Fig. 3).
 584 However, for some periods and depth layers the standard deviation reaches maxima to about 0.3
 585 W m^{-2} . All products agree on the fact that global ocean warming rates have increased in the past
 586 decades and doubled since the beginning of the altimeter era (1993–2020 compared with 1960–
 587 2020) (Fig. 3). Moreover, there is a clear indication that heat sequestration into the deeper ocean
 588 layers below 700 m depth took place over the past 6 decades linked to an increase in OHC trends
 589 over time (Fig. 3). Ocean warming rates for the 0–2000 m depth layer reached record rates of 1.0
 590 $(0.7) \pm 0.3 \text{ W m}^{-2}$ over the period 2006–2020 for the ocean (global) area confirm a continuous
 591 increase of ocean warming over the entire study period (Fig. 2). Moreover, rates of global ocean
 592 warming have increased over the 3 different study periods, i.e., historical up to the recent decadal
 593 change. The trend values are all given in Table 1. The major fraction of heat is stored in the
 594 upper ocean (0–300 m and 0–700 m depth). However, heat storage at intermediate depth (700–
 595 2000 m) increases at a nearly comparable rate as reported for the 0–300 m depth layer (Table 1,
 596 Fig. 3). There is a general agreement among the 16 international OHC estimates (Fig. 3).
 597 However, for some periods and depth layers the standard deviation (95% confidence level)
 598 reaches maxima to about 0.3 W m^{-2} . All products agree on the fact that global ocean warming
 599 rates have increased in the past decades and doubled since the beginning of the altimeter era
 600 (1993–2020 compared with 1960–2020) (Fig. 3). Moreover, there is a clear indication that heat
 601 sequestration took place in the 700–2000m depth layer over the past 6 decades linked to an
 602 increase in OHC trends over time (Fig. 3). Ocean warming rates for the 0–2000 m depth layer
 603 reached record rates of 1.03 $(0.62) \pm 0.2 \text{ W m}^{-2}$ over the period 2006–2020 for the ocean (global)
 604 area, consistent with what had been reported in (Johnson et al., 2022).

605 -

606

	Ocean Heat Content linear trends (W/m^2)						
	0-300m	0-700m	0-2000m	700-2000m	0-bottom	0-bottom, Hakuba et al., 2021	0-bottom, Marti et al., 2022
1960-2020	0.2414 ± 0.104	0.3421 ± 0.1	0.5332 ± 0.1	0.1811 ± 0.04	0.35 ± 0.1		
1971-2020	0.3018 ± 0.1	0.4427 ± 0.1	0.6240 ± 0.1	0.2113 ± 0.03	0.43 ± 0.1		
1993-2020	0.3924 ± 0.1	0.6037 ± 0.1	0.8655 ± 0.2	0.3018 ± 0.04	0.61 ± 0.2		
2006-2020	0.4427 ± 0.1	0.6439 ± 0.1	1.00 ± 0.362 ± 0.2	0.3823 ± 0.1	0.68 ± 0.3	0.88 ± 0.24	0.87 ± 0.2

607

608 **Table 1:** OHC trends using LOWESS (Locally Weighted Scatterplot Smoothing, see text for more
 609 details) as derived from the ensemble mean (Fig. 2) for different time intervals, as well as
 610 different integration depths. The regression was done for each time period (1960 - 2020, 1971 -

2020, 1993 - 2020, 2006 -2020). A time window of 25 years was used for the periods that allowed it (1960 - 2020, 1971 - 2020, 1993 - 2020). For the period 2006 - 2020, a time window of 15 years was used. Note that values are given in Wm^{-2} relative to the ~~ocean~~ global surface-area between $60^{\circ}S$ and $60^{\circ}N$ and are limited to the 300-m bathymetry of each product. See also text and Fig. 2-3 for more details. Additionally, values for satellite-derived estimates of OHC have been added for the most recent period, updated after Hakuba et al., 2021 and Marti et al., 2022.

For the deep OHC changes below 2000 m, we adapted an updated estimate from (Purkey & Johnson, 2010) (PG10 hereinafter) from ~~1991~~1992 to 2020, which is a constant linear trend estimate (0.97 ± 0.48 ZJ yr^{-1} , 0.06 ± 0.03 W m^{-2}) derived from a global integration of OHC below 2000 m using basin scale deep ocean temperature trends from repeated hydrographic sections. Some recent studies strengthened the results in PG10 (Desbruyères et al., 2016; Zanna et al., 2019). Desbruyères et al. (2016) examined the decadal change of the deep and abyssal OHC trends below 2000 m in the 1990s and 2000s, suggesting that there has not been a significant change in the rate of decadal global deep/abyssal warming from the 1990s to the 2000s and the overall deep ocean warming rate is consistent with PG10. Using a Green's function method and ECCO reanalysis data, Zanna et al. (2019) reported a deep ocean warming rate of ~ 0.06 W m^{-2} during the 2000s, consistent with PG10 used in this study. Zanna et al. (2019) shows a fairly weak global trend during the 1990s, different from observation-based estimates. This mismatch might come from how surface-deep connections are represented in ECCO reanalysis data and the use of time-mean Green's functions in Zanna et al. (2019), as well as from the sparse coverage of the observational network for relatively short time spans. Furthermore, combining hydrographic and deep-Argo floats, a recent study (Johnson et al., 2019) reported an accelerated warming in the South Pacific Ocean in recent years, but a global estimate of the OHC rate of change over time is not available yet, and the rates of warming may vary by ocean basin. Comparison of the results in table 1 with OHC estimates derived from the space geodetic approach (Hakuba, 2019; Marti et al., 2022) shows overall agreement within uncertainties.

Before ~~1990~~1992, we assume zero OHC trend below 2000 m due to insufficient global observations below 2000m, following the methodology in some studies (Cheng et al. 2017; 2022), IPCC-AR5 (Rhein et al., 2013) and IPCC-AR6 (Forster et al., 2022; Gulev et al. 2021). The deep warming is likely driven by decadal variability in deep water formation rates, which could have been in a non-steady state mode prior to 1990, introducing additional uncertainty to the pre-1990 OHC estimates. Using surface temperature observations and assuming the heat is advected by mean circulation, Zanna et al. (2019) shows a near-zero (small cooling trend) OHC trend below 2000 m from the 1960s to 1980s, suggesting the ~~assumption of zero-trend~~ before ~~1990~~1992 might be small. The derived time following PG10 series after 1991 and zero-trend before ~~1990~~1992 is used for the Earth energy inventory in Sect. 5. A centralized (around the year 2006) uncertainty approach has been applied for the deep (>2000 m depth) OHC estimate following the method of Cheng et al. (2017), which allows us to extract an uncertainty range over the period 1993–2018 within the given [lower ($0.96-0.48$ ZJ yr^{-1}), upper ($0.96+0.48$ ZJ yr^{-1})] range of the deep OHC trend estimate. We then extend the obtained uncertainty estimate back from ~~1993~~1992 to 1960, with 0 OHC anomaly.

657

658 3. Heat available to warm the atmosphere

659

660 The heat content of the atmosphere is small in absolute terms, since its heat capacity as a gas is
 661 small compared to the one of the other Earth subsystems discussed in this paper. Yet it is by no
 662 means negligible, since in relative terms, the atmospheric heat gain is rapid over the recent
 663 decades and has a high impact on human life (Fig. 1). As for Earth's surface, widespread and
 664 rapid changes are ongoing in the atmosphere due to human-induced climate change (IPCC,
 665 2021).

666 Atmospheric observations show a warming of the troposphere and a cooling and contraction of
 667 the stratosphere since at least 1979 (Pissoft et al., 2021; Steiner et al., 2020). (Pissoft et al., 2021;
 668 Steiner et al., 2020a). In the tropics, the upper troposphere has warmed faster than the near-
 669 surface atmosphere since at least 2001, as seen with the new observation technique of GPS radio
 670 occultation (Gulev et al., 2021; Steiner et al., 2020a; 2020b) (Gulev et al., 2021; Ladstädter et al.,
 671 2023; Steiner et al., 2020a; Steiner et al., 2020b), while observations based on microwave
 672 soundings have likely underestimated tropospheric temperature trends in the past (Santer et al.,
 673 2021; Zou et al., 2021).

674 Recently, a continuous rise of the tropopause has been observed for 1980 to 2020 over the
 675 northern hemisphere (Meng et al., 2022). The increase is equally due to tropospheric warming
 676 and stratospheric cooling in the period 1980 to 2000 while the rise after 2000 resulted primarily
 677 from enhanced tropospheric heat gain. Moreover, indications exist on a widening of the tropical
 678 belt (Fu et al., 2019; Grise et al., 2019; Staten et al., 2020) as well as on changes in the seasonal
 679 cycle (Santer et al., 2022). However, changes in atmospheric circulation and conditions for
 680 extreme weather are still subject to uncertainty (Cohen et al., 2020) while the occurrence of heat-
 681 related extreme weather events has clearly increased over the recent decades (Cohen et al., 2020;
 682 IPCC, 2021), with high risks for society, economy, and the environment (Fischer et al., 2021)
 683 (Cohen et al., 2020; IPCC, 2021b), with high risks for society, economy, and the environment
 684 (Fischer et al., 2021).

685 A regular assessment of atmospheric heat content changes is hence critical for a complete
 686 overview of energy and mass exchanges with other climate components and for a complete
 687 energy budgeting of Earth's climate system.

688 3.1 Atmospheric heat content

689 In a globally averaged and vertically integrated sense, heat accumulation in the atmosphere arises
 690 from a small imbalance between net energy fluxes at the top-of-atmosphere (TOA) and the
 691 surface (denoted s). The heat energy budget of the vertically integrated and globally averaged
 692 atmosphere (indicated by the global averaging operator $\langle \cdot \rangle$) reads as follows (Mayer et al.,
 693 2017):

$$694 \quad \frac{d}{dt} \langle \rho c_p T \rangle = \langle \rho c_p T \rangle - \langle \rho c_p T \rangle$$

$$695 \quad \frac{d}{dt} \langle \rho c_p T \rangle = \langle \rho c_p T \rangle - \langle \rho c_p T \rangle$$

696 | where the vertically integrated atmospheric energy content AE per unit surface area [Jm^{-2}] reads

697 |
$$\int_{z_0}^{z_1} \left(\rho (c_v T + g z) + \frac{\rho}{g} \int_{z_0}^z (g - \frac{1}{\rho} \frac{d\rho}{dz}) dz \right) dz.$$

698 | In Equation (1), ~~formulated in mean-sea-level altitude (z) coordinates used here for integrating~~
 699 | ~~over observational data~~, N_{TOA} is the net radiation at top of the atmosphere, F_s is the net surface
 700 | energy flux defined as the sum of net surface radiation and latent and sensible heat fluxes, F_{snow}
 701 | denotes the latent heat flux associated with snowfall, and F_{PE} additionally accounts for sensible
 702 | heat of precipitation. See Mayer et al. (2017) or von Schuckmann et al. (2020) for a discussion of
 703 | the latter two terms, which are small on a global scale and hence often neglected.

704 | Equation (2), ~~formulated in mean-sea-level altitude (z) coordinates used here for integrating~~
 705 | ~~over observational data~~, provides a decomposition of AE_{A} into sensible heat energy (sum of the
 706 | first two terms, internal heat energy and gravity potential energy), latent heat energy (third term),
 707 | and kinetic energy (fourth term), where ρ is the air density, c_v the specific heat for moist air at
 708 | constant volume, T the air temperature, g the acceleration of gravity, L_e the temperature-
 709 | dependent effective latent heat of condensation L_v or sublimation L_s (the latter relevant below 0
 710 | °C), q the specific humidity of the moist air, and V the wind speed. We neglect atmospheric
 711 | liquid water droplets and ice particles as separate species, as their amounts and especially their
 712 | trends are small.

713 | In computing AE_{A} for the purpose of this update to the von Schuckmann et al. (2020) heat
 714 | storage assessment, we continued to use the formulations described therein, including that we
 715 | refer to the (geographically aggregated) AE_{A} as atmospheric heat content (AHC) in this context;
 716 | ~~acknowledging. This acknowledges~~ the dominance of the heat-related terms in Eq. (2). Briefly,
 717 | in deriving the AHC from observational datasets, we accounted for the intrinsic temperature-
 718 | dependence of the latent heat of water vapor in formulating L_e (for details see Gorfer, 2022)
 719 | while the reanalysis derivations approximated L_e by constant values of L_v , as this simplification is
 720 | typically also made in the assimilating models ~~(e.g., ECMWF-IFS, 2015)~~ ~~(e.g., ECMWF-IFS,~~
 721 | ~~2015)~~. As another small difference, the observational estimations neglected the kinetic energy
 722 | term in Eq. (2) while the reanalysis estimations accounted for it. The resulting differences in
 723 | AHC anomalies from any of these differences are negligibly small, however, especially when
 724 | considering trends over time.

725 | 3.2 Datasets and heat content estimation

726 | Turning to the actual datasets used, the AHC and its changes and trends over time can be
 727 | quantified using various data sources, observation-based and reanalyses. Reassessing possible
 728 | data sources, we extended the high-quality datasets that we used in the initial von Schuckmann et
 729 | al. (2020) assessment. In particular, we updated the time period from 2018 to 2020 and improved
 730 | the back-extension from 1980 to 1960. Specifically, the adopted datasets and the related AHC
 731 | data record preparations can be summarized as follows.

732 | Atmospheric reanalyses combine observational information from various sources (radiosondes,
 733 | satellites, weather stations, etc.) and a dynamical model in a statistically optimal way. These data
 734 | have reached a high level of maturity, thanks to continuous improvement work since the early

735 1990s (Hersbach et al., 2018). Especially reanalyzed thermodynamic state variables, like
 736 temperature and water vapor that are most relevant for AHC computation, are of high quality and
 737 suitable for climate studies, although temporal discontinuities introduced from changing
 738 observing systems continue to deserve due attention (Berrisford et al., 2011; Chiodo &
 739 Haimberger, 2010; Hersbach et al., 2020; Mayer et al., ~~2021~~2021b).

740 We use the latest generation of reanalyses, including ECMWF’s Fifth generation reanalysis
 741 ERA5 (Bell et al., 2021; Hersbach et al., 2020), JMA’s reanalysis JRA55 (Kobayashi et al.,
 742 2015), and NASA’s Modern-Era Retrospective analysis for Research and Applications version 2
 743 (MERRA2) (Gelaro et al., 2017). ERA5 and JRA55 are both available over the full joint
 744 timeframe of this heat storage assessment from 1960 to 2020, while MERRA2 complements
 745 these from 1980 to 2020. The additional JRA55C reanalysis variant of JRA55, included for
 746 initial inter-comparison in von Schuckmann et al. (2020), is no longer used since it is available to
 747 2012 only and due to its similarity to JRA55 is not adding appreciable complementary value.

748 In addition to these three reanalyses, the datasets from two climate-quality observation
 749 techniques are used, for complementary observational AHC estimates. These include the
 750 Wegener Center (WEGC) multi-satellite radio occultation (RO) data record, WEGC OPSv5.6
 751 (~~Angerer et al., 2017; Steiner et al., 2020b~~)(Angerer et al., 2017; Steiner et al., 2020b), over
 752 2002-2020 and ~~itsa~~ radiosonde (RS) data record derived from the high-quality Vaisala sondes
 753 RS80/RS92/VS41, WEGC Vaisala (~~Ladstädter et al., 2015~~)(F Ladstädter et al., 2015), covering
 754 1996-2020. These RO and RS data sets provide atmospheric profiles of temperature, specific
 755 humidity, and density that are vertically completed by collocated ERA5 profiles in domains not
 756 fully covered by the data (e.g., in the lower troposphere for RO or at polar latitudes for RS).
 757 Similar to dropping the JRA55C reanalysis variant for no longer adding appreciable further
 758 value, the simplified AHC-proxy data based on microwave sounding unit (MSU) observational
 759 data, inter-compared in von Schuckmann et al. (2020), are no longer used.

760 From the observational data, the AHC is estimated by first evaluating Eq. (2) (using all terms for
 761 total and the third term only for latent AHC) at each available profile location and subsequently
 762 deriving it as volumetric heat content, for up to global scale, from vertical integration, temporal
 763 averaging, and geographic aggregation according to the approach summarized in von
 764 Schuckmann et al. (2020) and described in detail by (Gorfer, 2022). For the reanalyses, the
 765 estimation is based on the full gridded fields. Applying the approach for crosscheck to reanalysis
 766 profiles sub-sampled at observation locations only, confirms its validity as it accurately leads to
 767 the same AHC results as from the full gridded fields.

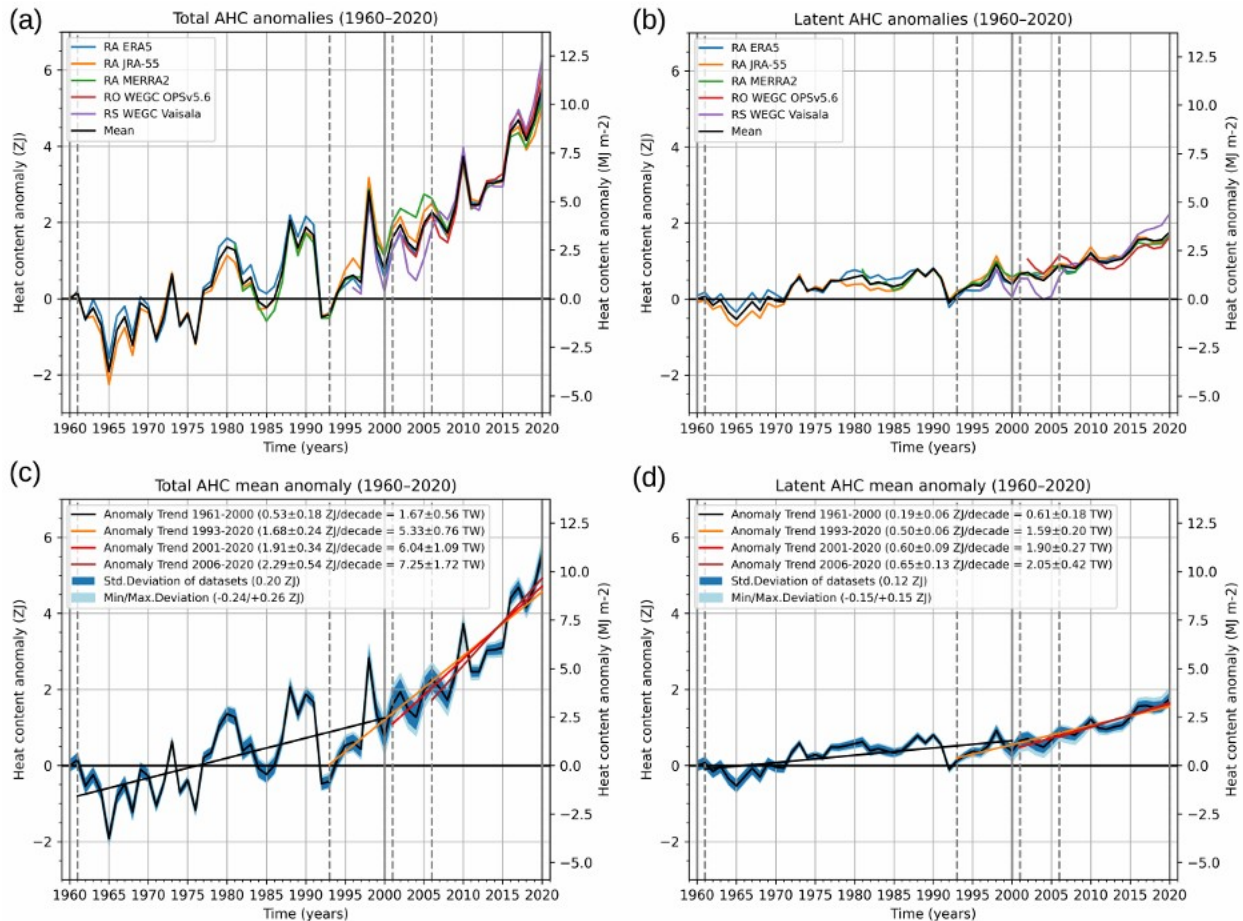
768 Overall, the ensemble spread of all the atmospheric datasets used is deemed a reasonable proxy
 769 for the uncertainty in the ensemble-mean annual AHC anomaly data, in particular since 1980
 770 during the “satellite observations era” (e.g., Hersbach et al., 2020; Steiner et al., 2020a). The
 771 uncertainties of the trend estimates, i.e., of the AHC increase rates (“AHC gain”) obtained from
 772 linear fitting to the anomaly data over periods of interest (see next Sect. 3.3), are weakly
 773 depending on these data uncertainties anyway, however, since the trend uncertainties are
 774 dominated by the inter-annual natural variability in the data, which is significantly larger than the
 775 data uncertainties expressed by the ensemble spread (see Figure 4).

776 | 3.3 Atmospheric heat content change since 1960 and its amplification

777 Figure 4 shows the resulting global AHC change inventory over 1960 to 2020 (61 years record),
778 in terms of total AHC anomalies for each data type (Fig. 4a), and for the ensemble mean with
779 trends for selected periods and uncertainty estimates (Fig. 4c). The selected trend periods align
780 with those for ocean data and with availability of atmospheric data sets (see subsection 3.2
781 above) and represent a reference trend 1961-2000 plus recent trends of the last about 30, 20, and
782 15 years, respectively. Latent AHC anomalies, a key component of the AHC (Matthews et al.,
783 2022), are also shown (Fig. 4b and 4d). Compared to von Schuckmann et al. (2020), the AHC
784 data have the ENSO signal removed (with ENSO regressed out via the Nino 3.4 Index; and
785 cross-check with non-ENSO-corrected data showing that trend differences are reasonably small).
786 Variability due to volcanic eruptions is still included, however, and may somewhat influence the
787 trends over 1993-2020, which start in the cold anomaly after the Pinatubo eruption (Santer et al.,
788 2001).

789 The latent AHC (Fig. 4b and 4d), which accounts for about one-quarter of the total AHC,
790 exhibits a qualitatively similar temporal evolution as total AHC, however with larger relative
791 uncertainty compared to the total AHC. The RO and RS data sets in Fig. 3b show some
792 differences, particularly the low latent AHC values in the 1990s and early 2000s from the RS
793 WEGC Vaisala data set likely stem from known dry biases of the RS80/RS90/RS92 humidity
794 sensors (Verver et al., 2006; Vömel et al., 2007). Estimated trends based on these RS data are
795 thus likely too high, although the overall increase in latent AHC is substantial also in the other
796 datasets.

797



798

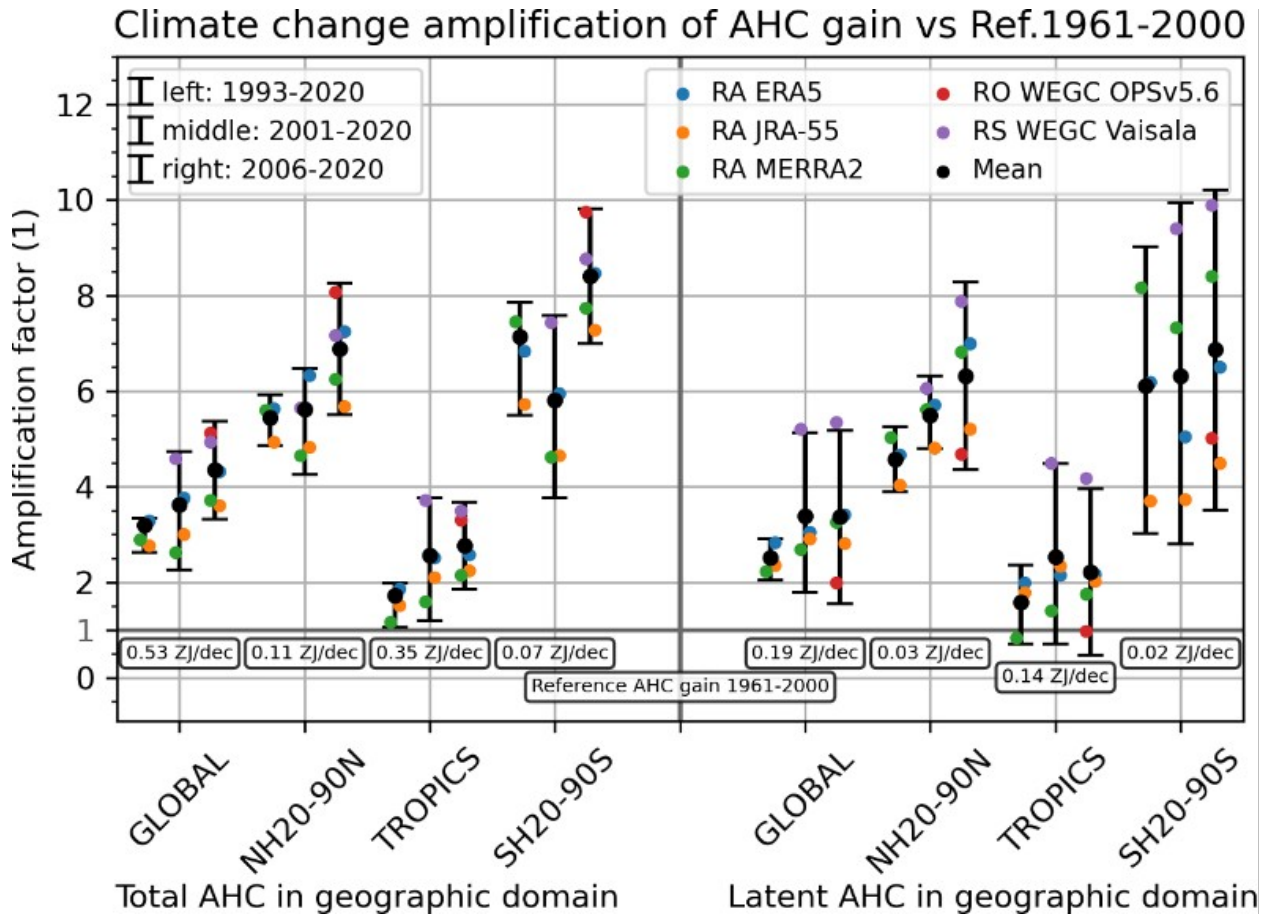
799 **Figure 4.** Annual-mean global AHC anomalies from 1960 to 2020 of total AHC (left) and latent-
 800 only AHC (right), respectively, of three different reanalyses and two different observational
 801 datasets shown together with their mean (top), and the mean AHC anomaly shown together with
 802 four representative AHC trends and ensemble spread measures of its underlying datasets
 803 (bottom). The in-panel legends identify the individual datasets (top) and the selected trend
 804 periods together with the associated trend values (plus 90 % confidence range) and ensemble
 805 spread measures (bottom), the latter including the time-average standard deviation and
 806 minimum/maximum deviations of the individual datasets from the mean.

807

808 The results clearly show that the AHC trends have increased from the earlier decades represented
 809 by the 1961-2000 trend of near 1.7 TW. We find the mean trend about 2.5 times higher over
 810 1993-2020 (about 5.3 TW) and about four times higher in the most recent two decades (about 6-
 811 7 TW), a period that is already covered also by the RO and RS records. Latent AHC trends in the
 812 most recent periods are 3 times larger than the 1961-2000 reference period. Since 1971, the heat
 813 gain in the atmosphere amounts to 5 \pm 1 ZJ (see also Fig. 8).

814 The remarkable amplification of total AHC and latent AHC trends is highlighted in Figure 45
 815 and summarized in Table 2 for the representative recent periods vs. the 1961-2000
 816 period. The 1961-2000 and 1993-2020 periods were covered by reanalysis only, while the

817 WEGC Vaisalä RS dataset additionally covers the 2001-2020 and 2006-2020 periods and the RO
 818 dataset the most recent period (see dataset descriptions in subsection 3.2). The larger diversity of
 819 recent datasets induces more spread; for example, the RS dataset shows an amplification factor
 820 of near 4.5 in the global total AHC gain for 2001-2020, while the amplification factors from the
 821 reanalyses range from 2.6 to 3.8. Amplifications are generally largest in the southern hemisphere
 822 extratropics, where also the 1961-2000 reference gain is smallest, and weakest in the tropics. In
 823 the most recent period 2006-2020, the amplification factors are strongest, with the RS and RO
 824 data sets on the high end of the spread (near factor 5 in global total AHC) and somewhat smaller
 825 but still high from the reanalyses (around factor 4).



826

827 **Figure 5.** Amplification of long-term trends in AHC anomalies (“AHC gain”) for total AHC
 828 (left) and latent-only AHC (right) in four geographic domains (global, northern-hemisphere
 829 extratropics, tropics, southern-hemisphere extratropics) for three recent time periods (legend
 830 upper-left) expressed as a ratio of the trend of each period relative to the trend in the previous-
 831 century reference period 1961-2000 (noted below the “amplification factor = 1” reference line).
 832 The amplification factor for each recent-trend case (for the four domains of both total and latent
 833 AHC) is depicted for the mean anomaly serving as best estimate (larger black circles), the
 834 related recent trends in the individual-dataset anomalies (colored circles as per upper-right
 835 legend). The related 90 % uncertainty range (black “error bar”) is estimated from the spread
 836 (standard deviation) of the individual-dataset amplification factors. The trend in the mean
 837 anomaly over 1961-2000 is used as the reference AHC gain.

838 For the latent AHC amplification factors, we see moderate values in the 1993-2020 period in the
 839 global mean and tropics. In the tropics, the lower uncertainty bound for amplification is slightly
 840 below 1 during all three recent trend periods. The spread of the amplification factors increases
 841 for the most recent periods, which is on the one hand due to the shorter period duration. The
 842 range increase is also related to the introduction of the RS and RO data sets after 1993-2020
 843 which contribute the largest and smallest latent AHC gain amplification factors. For 2006-2020,
 844 the global mean amplification factor from RO is about 2, whereas from the RS data set it is near
 845 5. Regarding latitudinal bands, the amplification factors are again strongest in the extratropics,
 846 where also the 1961-2000 reference gains are smallest, exhibiting a large spread especially in the
 847 southern extratropics. The relatively large amplification factors of the RS WEGC Vaisala data
 848 set are likely exaggerated due to the well documented dry bias of the early RS humidity sensors
 849 as noted above (Vömel, 2007; Verver et al., 2006).

850 Despite the uncertainties and spread described, the overall message from Figure 5 and Table 2 is
 851 very clear and substantially reinforcing the evidence from the initial von Schuckmann et al.
 852 (2020) assessment: the trends in the AHC, including in its latent heat component, show that
 853 atmospheric heat gain has accelerated strongly increased over the recent decades ~~at an~~
 854 unprecedented rate.

855

Domain	Time range	Total AHC Gain		Latent AHC Gain	
		Gain ZJ/decade (TW)	Amplification vs Ref.	Gain ZJ/decade (TW)	Amplification vs Ref.
GLOBAL	1993-2020	1.68±0.24 (5.33±0.76)	3.19 [2.63 to 3.34]	0.50±0.06 (1.59±0.20)	2.51 [2.05 to 2.91]
	2001-2020	1.91±0.34 (6.04±1.09)	3.62 [2.27 to 4.73]	0.60±0.09 (1.90±0.27)	3.39 [1.79 to 5.13]
	2006-2020	2.29±0.54 (7.25±1.72)	4.35 [3.33 to 5.36]	0.65±0.13 (2.05±0.42)	3.37 [1.55 to 5.18]
	Ref. 1961-2000	0.53±0.18 (1.67±0.56)	1.0	0.19±0.06 (0.61±0.18)	1.0
NH20-90N	1993-2020	0.62±0.11 (1.97±0.35)	5.44 [4.86 to 5.92]	0.16±0.02 (0.50±0.08)	4.57 [3.90 to 5.26]
	2001-2020	0.64±0.15 (2.03±0.47)	5.62 [4.26 to 6.48]	0.18±0.03 (0.58±0.11)	5.50 [4.79 to 6.31]
	2006-2020	0.79±0.25 (2.49±0.80)	6.89 [5.51 to 8.26]	0.22±0.05 (0.70±0.17)	6.32 [4.36 to 8.28]
	Ref. 1961-2000	0.11±0.08 (0.36±0.24)	1.0	0.03±0.02 (0.11±0.05)	1.0
TROPICS	1993-2020	0.60±0.13 (1.90±0.41)	1.72 [1.05 to 1.98]	0.24±0.04 (0.75±0.12)	1.58 [0.71 to 2.36]
	2001-2020	0.89±0.15 (2.82±0.47)	2.56 [1.20 to 3.77]	0.31±0.05 (1.00±0.16)	2.52 [0.70 to 4.49]
	2006-2020	0.96±0.24 (3.04±0.77)	2.76 [1.86 to 3.67]	0.31±0.07 (0.99±0.22)	2.22 [0.48 to 3.96]
	Ref. 1961-2000	0.35±0.08 (1.10±0.25)	1.0	0.14±0.03 (0.45±0.11)	1.0
SH20-90S	1993-2020	0.46±0.09 (1.46±0.29)	7.14 [5.49 to 7.86]	0.11±0.02 (0.33±0.05)	6.11 [3.02 to 9.02]
	2001-2020	0.37±0.17 (1.18±0.52)	5.80 [3.76 to 7.58]	0.10±0.03 (0.32±0.08)	6.31 [2.81 to 9.95]
	2006-2020	0.54±0.25 (1.71±0.79)	8.40 [6.99 to 9.81]	0.11±0.04 (0.36±0.12)	6.87 [3.52 to 10.22]
	Ref. 1961-2000	0.06±0.06 (0.20±0.18)	1.0	0.02±0.01 (0.05±0.05)	1.0

Domain	Time range	Total AHC Gain		Latent AHC Gain	
		Gain ZJ/decade (TW)	Amplification vs Ref.	Gain ZJ/decade (TW)	Amplification vs Ref.
GLOBAL	1993-2020	1.68±0.24 (5.33±0.76)	3.19 [2.63 to 3.34]	0.50±0.06 (1.59±0.20)	2.51 [2.05 to 2.91]
	2001-2020	1.91±0.34 (6.04±1.09)	3.62 [2.27 to 4.73]	0.60±0.09 (1.90±0.27)	3.39 [1.79 to 5.13]
	2006-2020	2.29±0.54 (7.25±1.72)	4.35 [3.33 to 5.36]	0.65±0.13 (2.05±0.42)	3.37 [1.55 to 5.18]
	Ref. 1961-2000	0.53±0.18 (1.67±0.56)	1.0	0.19±0.06 (0.61±0.18)	1.0
NH20-90N	1993-2020	0.62±0.11 (1.97±0.35)	5.44 [4.86 to 5.92]	0.16±0.02 (0.50±0.08)	4.57 [3.90 to 5.26]
	2001-2020	0.64±0.15 (2.03±0.47)	5.62 [4.26 to 6.48]	0.18±0.03 (0.58±0.11)	5.50 [4.79 to 6.31]
	2006-2020	0.79±0.25 (2.49±0.80)	6.89 [5.51 to 8.26]	0.22±0.05 (0.70±0.17)	6.32 [4.36 to 8.28]
	Ref. 1961-2000	0.11±0.08 (0.36±0.24)	1.0	0.03±0.02 (0.11±0.06)	1.0
TROPICS	1993-2020	0.60±0.13 (1.90±0.41)	1.72 [1.05 to 1.98]	0.24±0.04 (0.75±0.12)	1.58 [0.71 to 2.36]
	2001-2020	0.89±0.15 (2.82±0.47)	2.56 [1.20 to 3.77]	0.31±0.05 (1.00±0.16)	2.52 [0.70 to 4.49]
	2006-2020	0.96±0.24 (3.04±0.77)	2.76 [1.86 to 3.67]	0.31±0.07 (0.99±0.22)	2.22 [0.48 to 3.96]
	Ref. 1961-2000	0.35±0.08 (1.10±0.25)	1.0	0.14±0.03 (0.45±0.11)	1.0
SH20-90S	1993-2020	0.46±0.09 (1.46±0.29)	7.14 [5.49 to 7.86]	0.11±0.02 (0.33±0.05)	6.11 [3.02 to 9.02]
	2001-2020	0.37±0.17 (1.18±0.52)	5.80 [3.76 to 7.58]	0.10±0.03 (0.32±0.08)	6.31 [2.81 to 9.95]
	2006-2020	0.54±0.25 (1.71±0.79)	8.40 [6.99 to 9.81]	0.11±0.04 (0.36±0.12)	6.87 [3.52 to 10.22]
	Ref. 1961-2000	0.07±0.06 (0.21±0.18)	1.0	0.02±0.01 (0.05±0.03)	1.0

856

857 *Table 2. Long-term trend values in mean AHC anomalies (AHC gains; in units ZJ/decade and*
858 *TW) and amplification factors vs. the 1961-2000 reference gain (grey "Ref." lines), for total*
859 *AHC (left block) and latent-only AHC (right block) for the three recent time periods in four*
860 *geographic domains as illustrated in Figure 4. The AHC gain and amplification values are listed*
861 *together with their 90% confidence ranges.*

862

863

864 4. Heat available to warm land

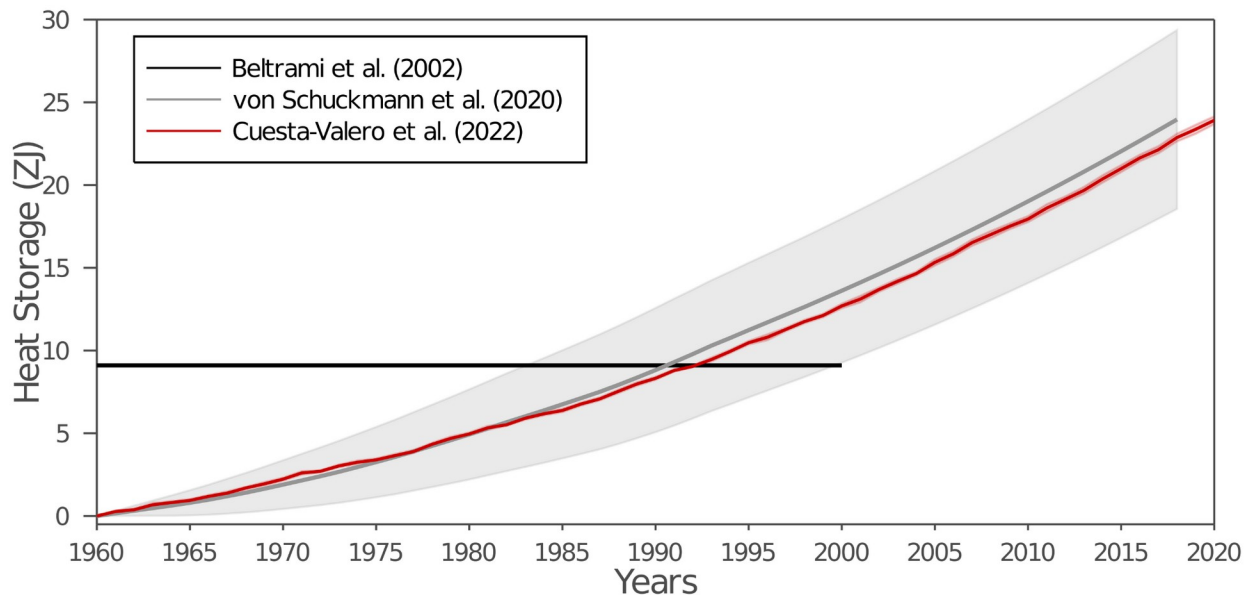
865

866 In previous studies the land term of the Earth heat inventory was considered as the heat used to
867 warm the continental subsurface (Hansen et al. 2011; Rhein et al. 2013; von Schuckmann et al.
868 2020). Temperature changes within the continental subsurface are typically retrieved by
869 analyzing the global network of temperature-depth profiles, measured mostly in the northern
870 hemisphere, southern Africa, and Australia. Each temperature profile records changes in
871 subsurface temperatures caused by the heat propagated through the ground due to alterations in
872 the surface energy balance (Cuesta-Valero et al., 2022a); (Cuesta-Valero et al., 2022b). Such
873 perturbations in the subsurface temperature profiles can be analyzed to recover the changes in
874 past surface conditions that generated the measured profile, allowing a reconstruction of the
875 evolution of ground surface temperatures and ground heat fluxes at decadal to centennial time
876 scales (Beltrami et al., 2002; Beltrami & Mareschal, 1992; Demezhko & Gornostaeva, 2015;
877 Hartmann & Rath, 2005; Hopcroft et al., 2007; Jaume-Santero et al., 2016; Lane, 1923; Pickler
878 et al., 2016; Shen et al., 1992). Although previous estimates only considered changes in ground
879 temperatures for representing the heat storage by exposed land, ground heat storage has been
880 found to be the second largest term of the Earth heat inventory accounting for 4 % to 6 % of the
881 total heat in the Earth System (von Schuckmann et al. 2020, section 6).

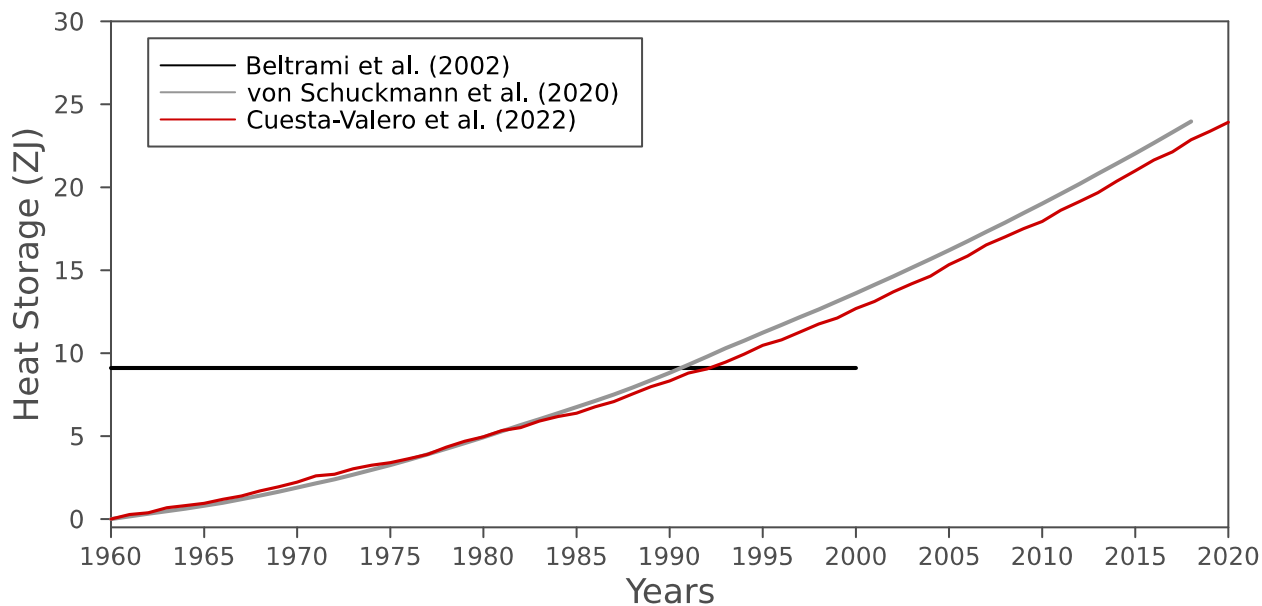
882

883 The ground heat is, nevertheless, not the only energy component of the continental landmasses.
884 Other processes with large thermodynamic coefficients, such as permafrost thawing and the
885 warming of inland water bodies, occur across large areas, leading to the exchange of large

886 amounts of heat with their surroundings over time. ~~To account for those heat exchanges, a recent~~
887 ~~study (Cuesta-Valero et al., 2022a)~~To account for those heat exchanges, a recent study (Cuesta-
888 Valero et al., 2022a) has estimated the heat uptake by permafrost thawing and the warming of
889 inland water bodies, as well as ground heat storage from subsurface temperature profiles,
890 resulting in a comprehensive estimate of continental heat storage. Therefore, our estimate is
891 different to ‘terrestrial’ or ‘land’ estimates, as we take into account the subsurface and water
892 bodies of the continental landmasses, thus not the land surface. The authors used the same global
893 network of subsurface temperature profiles as in von Schuckmann et al. (2020) to estimate
894 ground heat storage but applied an improved inversion technique to analyze the profiles. This
895 new technique is based on combining bootstrapping sampling with a widely-used Singular Value
896 Decomposition (SVD) algorithm (e.g., Beltrami et al., 1992) to retrieve past changes in surface
897 temperatures and ground heat fluxes, which also resulted in smaller uncertainty estimates for
898 global results ~~(Cuesta-Valero et al., 2022b)~~(Cuesta-Valero et al., 2022b). Heat uptake from
899 permafrost thawing was estimated using a large ensemble of simulations performed with the
900 CryoGridLite permafrost model ~~(Nitzbon et al., 2022)~~. ~~Ground stratigraphies required for this~~
901 ~~purpose, including ground ice distributions, were generated using various global ground datasets:~~
902 ~~(Nitzbon et al., 2022)~~. Ground stratigraphies required for this purpose, including ground ice
903 distributions, were generated using various global ground datasets. For soil properties, we used
904 the datasets described in (Masson et al., 2003) and (Faroux et al., 2013); for soil organic carbon,
905 the dataset described in (Hugelius et al., 2013); and for excess ground ice content (Brown et al.,
906 1997). Latent heat storage due to melting of ground ice is evaluated to a depth of 550 m over the
907 Arctic region. Uncertainty ranges are evaluated using 100 parameter ensemble simulations with
908 strongly varied soil properties and soil ice distributions. The climate forcing at the surface is
909 based on a paleoclimate simulation performed by the Commonwealth Scientific and Industrial
910 Research Organization (CSIRO) providing the initialization of the permafrost model, and data
911 from the ERA-Interim reanalysis since 1979 onwards. Heat storage by inland water bodies was
912 estimated by integrating water temperature anomalies in natural lakes and reservoirs from a set
913 of Earth System Model (ESM) simulations participating in the Inter-Sectoral Impact Model
914 Intercomparison Project phase 2b (ISIMP2b) (Frieler et al., 2017; Golub et al., 2022; Grant et al.,
915 2021). Heat storage is then computed using simulations with four global lake models following
916 the methodology presented in (Vanderkelen et al., 2020), but replacing the cylindrical lake
917 assumption in that study for a more detailed lake morphometry, which leads to a more realistic
918 representation of lake volume.
919



920



921

922

923

924

925

926

927

928

929

930

931

932

933

934

Figure 6: Continental heat storage from Beltrami et al. (2002) (black), von Schuckmann et al. (2020) (gray), and Cuesta-Valero et al. (2022a) (red). Gray and red shadows show the uncertainty range of the heat storage from von Schuckmann et al. (2020) and Cuesta-Valero et al. (2022a), respectively.

Figure 6 shows the three main estimates of heat gain by the continental landmasses since 1960. The first global estimate of continental heat storage was provided by Beltrami et al. (2002), consisting of changes in ground heat content for the period 1500-2000 as time steps of 50 years (black line in Figure 6). These estimates were retrieved by inverting 616 subsurface temperature profiles constituting the global network of subsurface temperature profiles in 2002, yielding a heat gain of 9.1 ZJ during the second half of the 20th century. A comprehensive update was included in von Schuckmann et al. (2020) using the results of (Cuesta-Valero et al., 2021) (gray line in Figure 6), with the main difference consisting in the use of a larger dataset with 1079

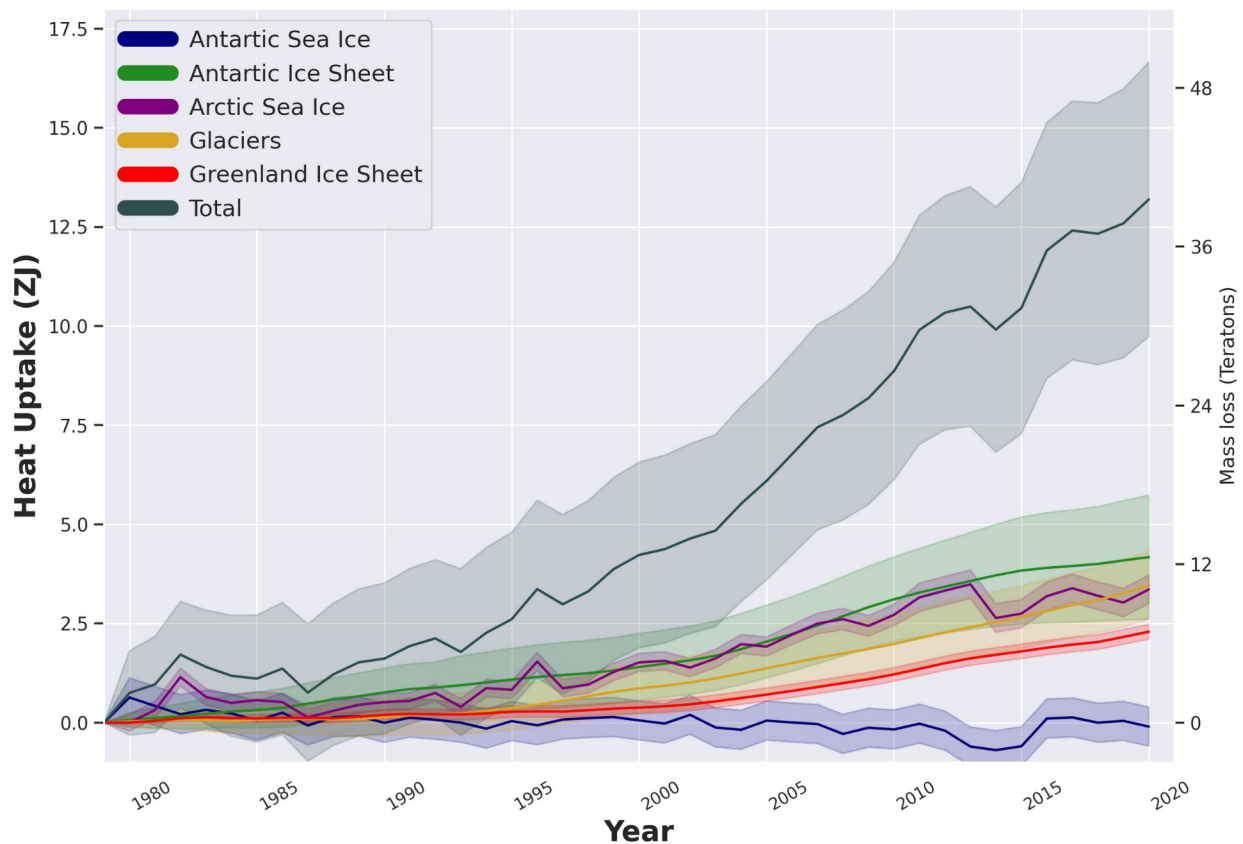
935 subsurface temperature profiles. Since many of these new profiles were measured at a later year
 936 than those in Beltrami et al. (2002), the inversions from this new data set were able to include the
 937 recent warming of the continental subsurface, yielding higher ground heat content than those
 938 from Beltrami et al. (2002). Concretely, the estimates in von Schuckmann et al. (2020) showed a
 939 heat gain of 24 ± 5 ZJ from 1960 to 2018.

940
 941 Recently, a new estimate of continental heat gain including the heat used in permafrost thawing
 942 and in warming inland water bodies was presented in Cuesta-Valero et al. (2022a) (red line in
 943 Figure 6), achieving a heat gain of 24 ± 12 ZJ since 1960, and $22 \pm 121 \pm 2$ ZJ since 1971 (see
 944 also Fig. 8). ~~Although this estimate uses the same 1079 measurement sites as~~
 945 ~~in von Schuckmann et al. (2020) and includes inland water bodies and heat stored in~~ permafrost
 946 ~~thawing, it yields similar values of heat content to those in von Schuckmann et al. (2020). These~~
 947 ~~similar results are caused by the different aggregation techniques used to derive warming of~~
 948 ~~inland water bodies, and the change in global warming of the ground, the retrieved continental~~
 949 ~~heat storage is similar to the values from ground warming in von Schuckmann et al. (2020) and~~
 950 ~~in Cuesta-Valero et al. (2022a).~~ There is a difference of ~ 3 ZJ between the average ground heat
 951 storage in Cuesta-Valero et al. (2022a) (21.6 ± 0.2 ZJ) and in von Schuckmann et al. (2020) (24
 952 ± 5 ZJ), which is similar to the heat storage in inland water bodies and the heat storage due to
 953 permafrost thawing together (see below). That is, the decrease in ground heat storage in the new
 954 estimates is compensated by the heat storage in inland water bodies and permafrost degradation.
 955 Another important result is the narrower confidence interval in estimates from Cuesta-Valero et
 956 al. (2022a), which is directly related to the new bootstrap technique used to invert the subsurface
 957 temperature profiles (Cuesta-Valero et al., 2022b). This new bootstrap technique offers a more
 958 adequate statistical framework than the technique used in von Schuckmann et al. (2020) as
 959 demonstrated in Cuesta-Valero et al. (2022a), thus we are confident in the robustness of the
 960 lower uncertainty estimate for ground heat storage presented here. Heat storage within inland
 961 water bodies has reached 0.2 ± 0.4 ZJ since 1960, with permafrost thawing accounting for 2 ± 2
 962 ZJ. Therefore, ground heat storage is the main contributor to continental heat storage (90 %),
 963 with inland water bodies accounting for 0.7 % of the total heat, and permafrost thawing
 964 accounting for 9 %. Despite the smaller proportion of heat stored in inland water bodies and
 965 permafrost thawing, several important processes affecting both society and ecosystems depend
 966 on the warming of lakes and reservoirs, and on the thawing of ground ice (Gädeke et al., 2021).
 967 Therefore, it is important to continue quantifying and monitoring the evolution of heat storage in
 968 all three components of the continental landmasses.

969 970 **5. Heat utilized to melt ice**

971
 972 Changes in Earth's cryosphere affect almost all other elements of the environment including the
 973 global sea level, ocean currents, marine ecosystems, atmospheric circulation, weather patterns,
 974 freshwater resources and the planetary albedo (Abram et al., 2019). The cryosphere includes
 975 frozen components of the Earth system that are at or below the land and ocean surface: snow,
 976 glaciers, ice sheets, ice shelves, icebergs, sea ice, lake ice, river ice, permafrost and seasonally
 977 frozen ground (IPCC, 2019). In this study, we estimate the heat uptake by the melting of ice
 978 sheets (including both floating and grounded ice), glaciers and sea ice at global scale (Fig. 7).
 979 Notwithstanding the important role snow cover plays in the Earth's energy surface budget as a
 980 result of changes in the albedo (de Vrese et al., 2021; Qu & Hall, 2007; Weihs et al., 2021), or its

981 influence on the temperature of underlying permafrost (Jan & Painter, 2020; Park et al., 2015), or
 982 on sea ice in the Arctic (Perovich et al., 2017; Webster et al., 2021) and Antarctica (Eicken et al.,
 983 1995; Nicolaus et al., 2021; Shen et al., 2022), estimates of changes in global snow cover are still
 984 highly uncertain and not included in this inventory. However, they should be considered in future
 985 estimates. Similarly, changes in lake ice cover (Grant et al., 2021) are not taken into account here
 986 and warrant more attention in the future. Permafrost is accounted for in the land component (see
 987 section 4).
 988



989
 990
 991 **Figure 7:** Heat uptake (in ZJ) and Mass Loss (Trillions of tons) for the Antarctic Ice Sheet
 992 (grounded and floating ice, green), Glaciers (orange), Arctic sea ice (purple), Greenland Ice
 993 Sheet (grounded and floating ice, red) and Antarctic sea ice (blue), together with the sum of the
 994 energy uptake within each one of its components (total, black). Uncertainties are 95%
 995 confidence intervals provided as shaded areas, respectively. See text for more details.
 996

997 We equate the energy uptake by the cryosphere (glaciers, grounded and floating ice of the
 998 Antarctic and Greenland Ice Sheets, and sea-ice) with the energy needed to drive the estimated
 999 mass loss. In doing so we assume that the energy change associated with the temperature change
 1000 of the remaining ice is negligible. As a result, the energy uptake by the cryosphere is directly
 1001 proportional to the mass of melted ice:

1002
 1003
$$E = \Delta M * (L + c * \Delta T),$$

 1004

1005 where, for any given component, ΔM is the mass of ice loss, L is the latent heat of fusion, c is the
 1006 specific heat capacity of the ice and ΔT is the rise in temperature needed to bring the ice to the
 1007 melting point. For consistency with previous estimates (Ciais et al., 2014; Slater et al., 2021; von
 1008 Schuckmann et al., 2020), we use a constant latent heat of fusion of $3.34 \times 10^5 \text{ J kg}^{-1}$, a specific
 1009 heat capacity of $2.01 \times 10^3 \text{ J/(kg } ^\circ\text{C)}$ and, a density of ice of 917 kg/m^3 . Estimating the energy
 1010 used to warm the ice to its melting point requires knowledge of the mean ice temperature for
 1011 each component. Here we assume a temperature of -15°C for floating ice in Greenland, -2°C for
 1012 the floating ice in Antarctica, $-20 \pm 10^\circ\text{C}$ for grounded ice in Antarctica and Greenland and 0°C
 1013 for sea-ice and glaciers. Although this assumption is poorly constrained, the energy required to
 1014 melt ice is primarily associated with its phase transition and the fractional energy required for
 1015 warming is a small percentage ($< 1\% \text{ } ^\circ\text{C}^{-1}$) of the total energy uptake (Slater et al., 2021).
 1016 Nevertheless, we include an additional uncertainty of $\pm 10^\circ\text{C}$ on the assumed initial ice
 1017 temperature within our estimate of the energy uptake. [An overview of all datasets used and their](#)
 1018 [availabilities are provided in Table 2, and are further described in the following.](#)
 1019

Component	Data type and information	Periods covered	Other specifications:
Antarctic Ice Sheet	Grounded ice change from IMBIE (Shepherd et al., 2018, 2019)	1992-2020;	Mean ice temperature for <ul style="list-style-type: none"> • floating ice (basal melting): $-2^\circ\text{C} \pm 10^\circ\text{C}$ • floating ice (calving): $-16^\circ\text{C} \pm 10^\circ\text{C}$ (Clough & Hansen, 1979) • grounded ice: $-20 \pm 10^\circ\text{C}$
	Grounded ice change before 1992 combining satellite and regional climate model data after Rignot et al., 2019	1972-1991	
	Floating ice change from satellite altimetry reconstructions (Adusumilli et al., 2020)	1994-2020 (extrapolated between 2017-2020); 1979-1993: zero mass loss assumed	
	Ice front retreat due to calving in the Amundsen Sea using ERS-1 radar altimetry (Adusumilli et al. 2020)	1994-2020 (linear rate of energy uptake assumed)	
	Antarctic Peninsula ice front retreat due to calving from imagery and remotely sensed data (Cook & Vaughan, 2010; Adusumilli et al. 2020)	1979-2020 (linear rate of energy uptake assumed)	
Antarctic Sea Ice	Sea ice thickness from GIOMAS (Zhang & Rothrock, 2003)	1979-2020	Mean ice temperature: $0^\circ\text{C} \pm 10^\circ\text{C}$
Arctic Sea Ice	Sea ice thickness from PIOMAS model data (Schweiger et al., 2019; Zhang & Rothrock, 2003)	1979-2011	Mean ice temperature: $0^\circ\text{C} \pm 10^\circ\text{C}$
	CryoSat-2 satellite radar altimeter measurements (Slater et al., 2021; Tilling et al., 2018)	2011-2020	
Glaciers (distinct from ice sheets)	Geodetic and in-situ glaciological observations after Zemp et al., 2019	1979-1996	Mean ice temperature: $0^\circ\text{C} \pm 10^\circ\text{C}$
	In-situ glaciological observations after Zemp et al., 2020 and WGMS, 2021	1997-2020	
Greenland Ice Sheet	Grounded ice change from IMBIE (Shepherd et al., 2018, 2019)	1992-2020;	Mean ice temperature for <ul style="list-style-type: none"> • floating ice: $-15^\circ\text{C} \pm 10^\circ\text{C}$ • grounded ice: $-20 \pm 10^\circ\text{C}$
	Grounded ice change before 1992 from satellite velocity (Mankoff et al., 2019)	1979-1991	

	and regional climate models (Mouginot et al., 2019)		
	Floating ice change (ice shelf collapse/thinning & tidewater glacier retreat) after (Moon & Joughin, 2008; Motyka et al., 2011; Mouginot et al., 2015; Münchow et al., 2014; Wilson et al., 2017; Carr et al., 2017)	1979-1996: no loss assumed	

1020
1021
1022
1023
1024
1025
1026
1027

***Table 2:** Overview on data used and their availability for the estimate of heat available to melt the cryosphere over the period 1979-2020. Backward extension to 1971 for the heat inventory is based on the assumption of negligible contribution. General specification include constant values for latent heat of fusion of $3.34 \times 10^5 \text{ J kg}^{-1}$, specific heat capacity of $2.01 \times 10^3 \text{ J/(kg } ^\circ\text{C)}$; density of ice with 917 kg/m^3 for first-year ice, and 882 kg/m^3 for multi-year ice, see also Ciais et al., 2014; Slater et al., 2021; von Schuckmann et al., 2020. Other component specification are provided in the table.*

1028
1029
1030
1031
1032
1033
1034
1035
1036
1037
1038
1039
1040

Grounded ice losses from the Greenland and Antarctic Ice Sheets from 1992 to 2020 are estimated from a combination of 50 satellite-based estimates of ice sheet mass balance produced from observations of changes in ice sheet volume, flow and gravitational attraction, compiled by the Ice Sheet Mass Balance Intercomparison Exercise (IMBIE¹⁰) (Shepherd et al., 2018, 2019). To extend those time-series further back in time, we use ice sheet mass balance estimates produced using the input-output method, which combines estimates of solid ice discharge with surface mass balance estimates. Satellite estimates of ice velocity are available from the Landsat historical archive from 1972 allowing the calculation of ice discharge before the 1990s while surface mass balance is estimated from regional climate models. We extend the IMBIE mass balance time-series backwards to 1979 for Greenland using (Mouginot et al., 2019) and (Mankoff et al., 2019) and for Antarctica from 1972 to 1991 using (Rignot et al., 2019).

1041
1042
1043
1044
1045
1046
1047
1048
1049
1050
1051
1052
1053
1054
1055
1056
1057
1058

Changes in Antarctic floating ice shelves due to thinning between 1994 and 2017 are derived from satellite altimetry reconstructions (Adusumilli et al., 2020). There were no estimates of ice shelf thinning between 1979 and 1993, therefore we assume zero mass loss from ice shelf thinning during that period. Changes in Antarctic ice shelves due to increased calving in the Antarctic Peninsula and the Amundsen Sea sector are derived from ERS-1 radar altimetry (Adusumilli et al. 2020) for 1994-2017. For the 1979-1994 period, we only have data for changes in the extent of the Antarctic Peninsula ice shelves from (Cook & Vaughan, 2010). These are converted to changes in mass using an ice shelf thickness of $140 \pm 110 \text{ m}$ ice equivalent which represents the range of ice thickness values for the portions of Antarctic Peninsula ice shelves that have collapsed since 1994 (Adusumilli et al. 2020). Once icebergs calve off large Antarctic floating ice shelves, the timescales of dissolution of the icebergs are largely unknown; therefore, we assumed a linear rate of energy uptake between 1979–2018–2020. For icebergs, we use an initial temperature of -16°C , which was the mean ice temperature in the Ross Ice Shelf J-9 ice core (Clough & Hansen, 1979). There are no large-scale observations or manifestations of significant firn layer temperature change for the Antarctic ice shelf; for example, there is no significant trend in the observationally-constrained model outputs of surface melt described in (Smith et al., 2020). Therefore, the change in temperature of any ice that does not melt is assumed to be negligible.

107 10 <https://imbie.org>

1059
 1060 Changes in the floating portions of the Greenland Ice Sheet include ice shelf collapse, ice shelf
 1061 thinning and tidewater glacier retreat. As in von Schuckmann et al. 2020, we assume no ice shelf
 1062 mass loss pre-1997 and estimate a loss of 13 Gt/yr post-1997 based on studies of Zacharie
 1063 Isstrom, C. H. Ostefeld, Petermann, Jakobshavn, 79N and Ryder Glaciers (Moon & Joughin,
 1064 2008; Motyka et al., 2011; Mouginot et al., 2015; Münchow et al., 2014; Wilson et al., 2017).
 1065 We assign a generous uncertainty of 50% to this value. ~~For tidewater glacier retreat we note a~~
 1066 ~~mean retreat rate of 37.6 m/yr during 1992-2000 and 141.7 m/yr during 2000-2010.~~ For tidewater
 1067 glacier retreat we note a mean retreat rate of 37.6 m/yr during 1992-2000 and 141.7 m/yr during
 1068 2000-2010 (Carr et al., 2017). We assume the former estimate is also valid for 1979-1991 and
 1069 the latter estimate is valid for 2011-2020. Assuming a mean glacier width of 4 km and thickness
 1070 of 400 m we estimate mass loss from glacier retreat to be 9.3 Gt/yr during 1979-2000 and 35.1
 1071 Gt/yr during 2000-2020. Based on firn modeling we assessed that warming of Greenland's firn
 1072 has not yet contributed significantly to its energy uptake (Ligtenberg et al., 2018).

1073
 1074 The contributions from both the Antarctic and Greenland Ice Sheets to the EEI are obtained by
 1075 summing the mass loss from the individual components (ice shelf mass, grounded ice mass, and
 1076 ice shelf extent) for each ice sheet separately and, given that the datasets used for each
 1077 component are independent, the uncertainties were summed in quadrature. This is then converted
 1078 to an energy uptake according to the equation above.

1079
 1080 Glaciers are another part of the land-based ice, and we here include glaciers found in the
 1081 periphery of Greenland and Antarctica, but distinct from the ice sheets, in our estimate. We build
 1082 our estimate on the international efforts to compile and reconcile measurements of glacier mass
 1083 balance, under the lead of the World Glacier Monitoring Service (WGMS¹¹). Up to 2016, the
 1084 results are based on (Zemp et al., 2019), who combine geodetic mass balance observations from
 1085 DEM differencing on long temporal and large spatial scales with in-situ glaciological
 1086 observations, which are spatially less representative, but provide information of higher temporal
 1087 resolution. Through this combination, they achieve coverage that is globally complete yet retains
 1088 the interannual variability well. For 2017 to 2021, the numbers are based on the ad-hoc method
 1089 of (Zemp et al., 2020), which corrects for the spatial bias of the limited number of recent in-situ
 1090 glaciological observations that are available with short delay (WGMS, 2021), to derive globally
 1091 representative estimates. Error bars include uncertainties related to the in-situ and spaceborne
 1092 observations, extrapolation to unmeasured glaciers, density conversion, as well as to glacier area
 1093 and its changes. For the conversion from mass loss to energy uptake, only the latent heat uptake
 1094 is considered, which is based on the assumption of ice at the melting point, due to lack of glacier
 1095 temperature data at the global scale. Moreover, since the absolute mass change estimates are
 1096 based on geodetic mass balances, mass loss of ice below floatation is neglected. While this is a
 1097 reasonable approximation concerning the glacier contribution to sea-level rise, it implies a
 1098 systematic underestimation of the glacier heat uptake. While to our knowledge there are no
 1099 quantitative estimates available of glacier mass loss below sea level on the global scale, it is
 1100 reasonable to assume that this effect is minor, based on the volume-altitude distribution of
 1101 glacier mass (Farinotti et al., 2019; Millan et al., 2022). Further efforts are under way within the
 1102 Glacier Mass Balance Intercomparison Exercise (GlaMBIE¹²), particularly to reconcile global

111 11 <https://wgms.ch>

112 12 <https://glambie.org>

1103 glacier mass changes including also estimates from gravimetry and altimetry, and to further
1104 assess related sources of uncertainties (Zemp et al., 2019).

1105
1106 Sea ice, formed from freezing ocean water, and further thickened by snow accumulation is not
1107 only another important aspect of the albedo effect (Kashiwase et al., 2017; R. Zhang et al., 2019)
1108 and water formation processes (Moore et al., 2022), but also provides essential services for polar
1109 ecosystems and human systems in the Arctic (Abram et al., 2019). Observations of sea-ice extent
1110 are available over the satellite era, i.e., since the 1970s, but ice thickness data - required to
1111 obtain changes in volume - have only recently become available through the launch of CryoSat-2
1112 and ICESat-2. For the Arctic, we use a combination of sea ice thickness estimates from ~~from~~ the
1113 Pan-Arctic Ice Ocean Modeling and Assimilation System (PIOMAS) between ~~1980~~1979 and
1114 2011 (Schweiger et al., 2019; Zhang & Rothrock, 2003) and CryoSat-2 satellite radar altimeter
1115 measurements between 2011 and 2020 when they are available (Slater et al., 2021; Tilling et
1116 al., 2018). PIOMAS assimilates ice concentration and sea surface temperature data and is
1117 validated with most available thickness data (from submarines, oceanographic moorings, and
1118 remote sensing) and against multidecadal records constructed from satellite (Labe et al., 2018;
1119 Laxon et al., 2013; Wang et al., 2016). We note that the PIOMAS domain does not extend
1120 sufficiently far south to include all regions covered by sea ice in winter (Perovich et al., 2017).
1121 Given that the entirety of the regions that are unaccounted for (e.g., the Sea of Okhotsk and the
1122 Gulf of St. Lawrence) are only seasonally ice covered since the start of the record, this should
1123 not influence the results. We convert monthly estimates of sea ice volume from CryoSat-2
1124 satellite altimetry to mass using densities of 882 and 916.7 kg/m³ in regions of multi- and first-
1125 year ice respectively (Tilling et al., 2018). During the summer months (May to September) the
1126 presence of melt ponds on Arctic sea ice makes it difficult to discriminate between radar returns
1127 from leads and sea ice floes, preventing the retrieval of summer sea ice thickness from radar
1128 altimetry (Tilling et al., 2018). As a result, we use the winter-mean (October to April) mass trend
1129 across the Arctic for both CryoSat-2 and PIOMAS estimates for consistency. According to
1130 PIOMAS, winter Arctic sea ice mass estimates are 19 Gt/yr (6 %) smaller than the annual mass
1131 trend between ~~1980~~1979 and 2011 (-324 Gt/yr) and so are a conservative estimate of Arctic sea
1132 ice mass change (Slater et al., 2021). The uncertainty on monthly Arctic sea ice volume
1133 measurements from CryoSat-2 ranges from 14.5 % in October to 13 % in April (Slater et al.,
1134 2021; Tilling et al., 2018), and is estimated as $\pm 1.8 \times 10^3$ km³ for PIOMAS (Schweiger et al.,
1135 2011).

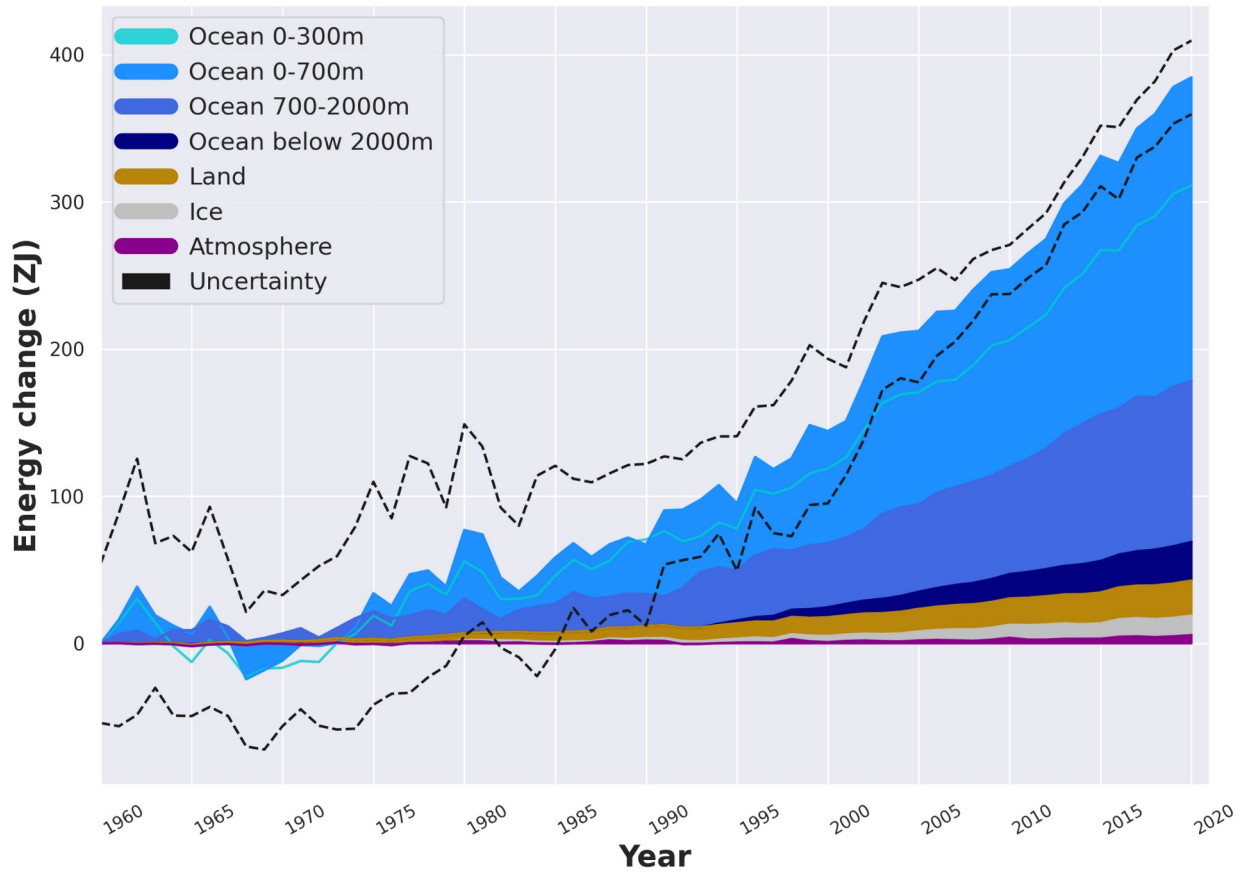
1136
1137 Satellite radar altimeter retrievals of sea ice thickness in the Southern Ocean are complicated by
1138 the presence of thick snow layers with unknown radar backscatter properties on Antarctic sea ice
1139 floes. As a result, no remote sensing estimates are available for Antarctic sea ice and we use sea
1140 ice volume anomalies from the Global Ice-Ocean Modeling and Assimilation System (GIOMAS,
1141 Zhang & Rothrock, 2003), the global equivalent to PIOMAS. GIOMAS output has been recently
1142 validated against in-situ and satellite data by (Liao et al., 2022). We compute Antarctic sea ice
1143 trends as annual averages between January and December. ~~In the absence of a detailed~~
1144 ~~characterization of uncertainties for these estimates, we attribute the same uncertainty to~~
1145 ~~GIOMAS estimates as for PIOMAS ($\pm 1.8 \times 10^3$ km³). For future updates of the GCOS~~
1146 ~~in the absence of a detailed characterization of uncertainties for these estimates, we use the uncertainty~~
1147 ~~in GIOMAS sea-ice thickness of 0.34 m (Liao et al., 2022) to estimate the uncertainty in~~
1148 GIOMAS sea-ice volume to be $\pm 4.0 \times 10^3$ km³, using an annual mean sea-ice extent of

1149 [11.9x10⁶ km² \(Lavergne et al., 2019\)](#). [One caveat to this is that the observational estimates](#)
1150 [have their own significant uncertainties \(Kern et al., 2019; Liao et al., 2022\)](#). [For future updates](#)
1151 [of the](#) Earth heat inventory, we also aim to include observation-based (remote sensing) estimates
1152 in the Southern Ocean (Lavergne et al., 2019).
1153

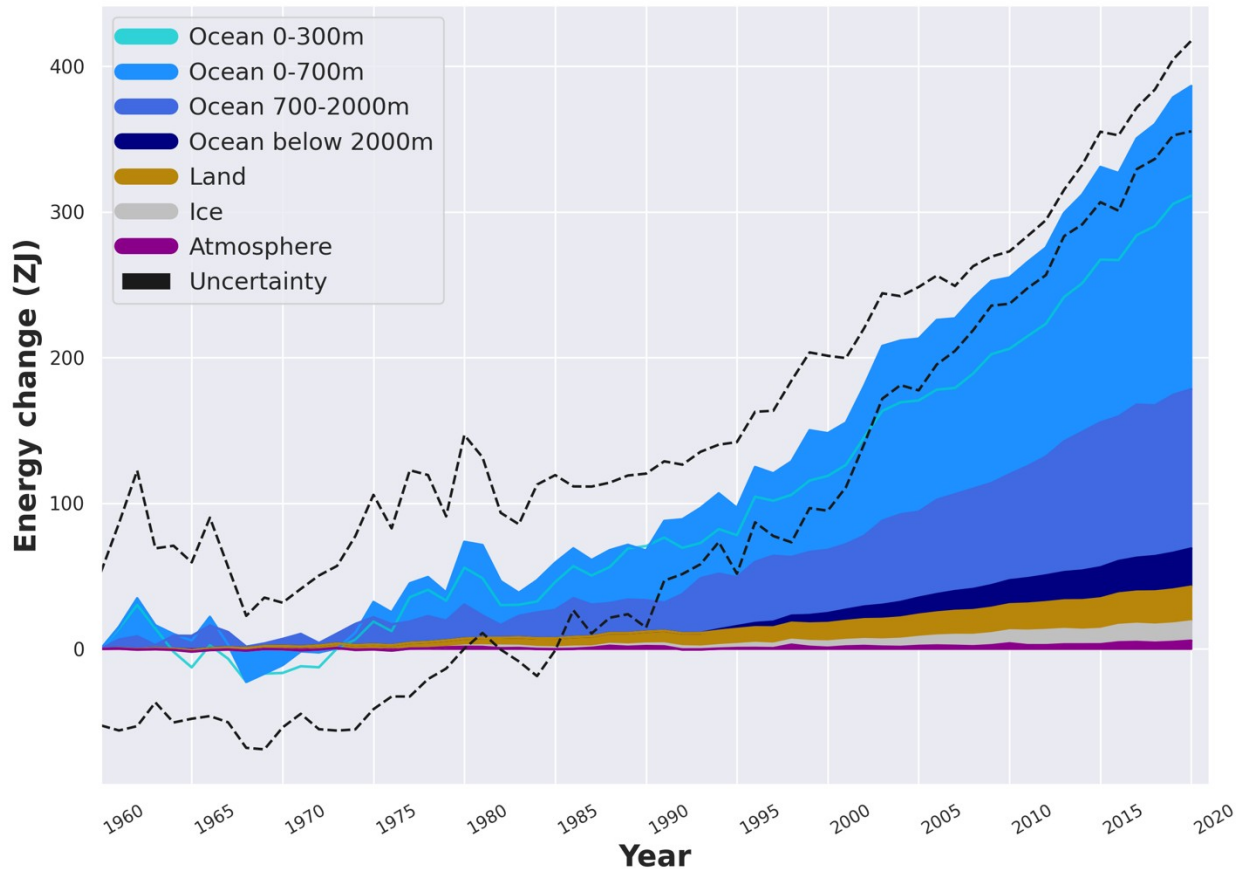
1154 Our estimate of the total heat gain in the cryosphere amounts to 14 ± 4 ZJ over the period 1971-
1155 2020 (see also Fig. 8 and section 6), (assuming negligible contribution before 1979 according to
1156 the data availability limitation), which is consistent with the estimate obtained in (von
1157 Schuckmann et al., 2020) within uncertainties. Approximately half of the cryosphere's energy
1158 uptake is associated with the melting of grounded ice, while the remaining half is associated with
1159 the melting of floating ice (ice shelves in Antarctica and Greenland, Arctic sea ice). Compared to
1160 earlier estimates, and in particular the 8.83 ZJ estimate from Ciais et al. (2013), this larger
1161 estimate is a result both of the longer period of time considered and, also, the improved estimates
1162 of ice loss across all components, especially the ice shelves in Antarctica. Contributions to the
1163 total cryosphere heat gain are dominated by the Antarctic Ice Sheet (including the floating and
1164 grounded ice, [about 33 \$\pm\$ 11%](#)) and Arctic Sea ice ([about 26 \$\pm\$ 3%](#)), directly followed by the heat
1165 utilized to melt glaciers ([about 25 \$\pm\$ 7%](#)). The Greenland Ice Sheet amounts to [about 17 \$\pm\$ 2%](#),
1166 whereas Antarctic sea ice is accounted for with a non-significant contribution of [about 0.2 \$\pm\$ 4%](#).
1167
1168

1169 **6. The Earth heat inventory: where does the energy go?**

1170
1171 Evaluations of the heat storage in the different Earth system components as performed in section
1172 2-5 allow now for the establishment of the Earth heat inventory. [Estimates for all Earth system](#)
1173 [components cover a core period of 1971-2020, except for the cryosphere where negligible](#)
1174 [contribution is assumed before 1979](#). Our results reconfirm a continuous accumulation of heat in
1175 the Earth system since our estimate begins (Fig. 8). The total Earth system heat gain in this study
1176 amounts to 380 ± 62 ZJ over the period 1971–2020. For comparison, ~~the heat gain obtained in~~
1177 IPCC AR6 obtained a total heat gain of 434.9 [324.5 to 545.5] ZJ for the period 1971-2018, and
1178 is hence consistent with our estimate within uncertainties (Forster et al., 2021). However, it is
1179 important to note that our estimate still excludes some aspects of Earth heat accumulation, such
1180 as for example the shallow areas of the ocean. ~~Although some estimates and discussions have~~
1181 ~~been provided to account for the relative contributions of these areas, these results are still~~
1182 ~~hampered by a number of assumptions and, which~~ are challenging to be quantified with respect
1183 to gaps in the observing system.
1184



1185



1186

1187

Figure 8: Total Earth system heat gain in ZJ ($1 \text{ ZJ} = 10^{21} \text{ J}$) relative to 1960 and from 1960 to

2020. The upper ocean (0–300 m, light blue line, and 0–700 m, light blue shading) accounts for

the largest amount of heat gain, together with the intermediate ocean (700–2000 m, blue

shading) and the deep ocean below 2000 m depth (dark blue shading). The second largest

contributor is the storage of heat on land (orange shading), followed by the gain of heat to melt

grounded and floating ice in the cryosphere (gray shading), and heating of the atmosphere

(magenta shading). Uncertainty in the ocean estimate also dominates the total uncertainty (dot-

dashed lines derived from the standard deviations (2σ) for the ocean, cryosphere, land and

atmosphere). See sections 2-5 for more details of the different estimates. The dataset for the

Earth heat inventory is published at the German Climate Computing Centre (DKRZ,

<https://www.dkrz.de/>) (see section 7). Consistent with von Schuckmann et al. (2020), we obtain a

total heat gain of $380 \pm 62381 \pm 61$ ZJ over the period 1971–2020, which is equivalent to a heating

rate (i.e., the EEI) of $0.48 \pm 0.1 \text{ W m}^{-2}$ applied continuously over the surface area of the Earth

($5.10 \times 10^{14} \text{ m}^2$). The corresponding EEI over the period 2006–2020 amounts to $0.76 \pm 0.2 \text{ W m}^{-2}$.

The LOWESS method and associated uncertainty evaluations have been used as described in

section 2.

The estimate of heat storage in all Earth system components not only allows for obtaining a

measure of how much and where heat is available for inducing changes in the Earth system (Fig.

1), but also to improve the accuracy of the Earth's system total heat gain. In 1971–2020 and for

the total heat gain, the ocean accounts for the largest contributor with aan about $89 \pm 17\%$

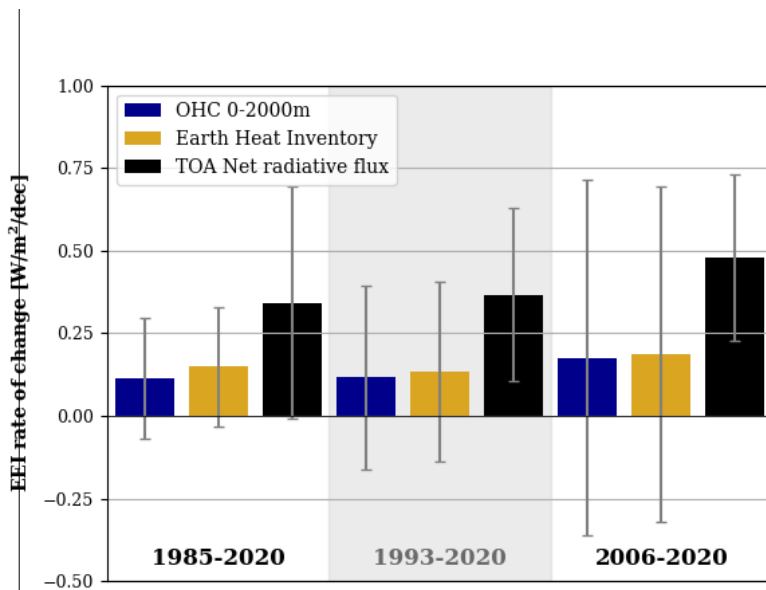
fraction of the global inventory. The second largest component in the Earth heat inventory relies

1209 on heat stored in land with a [about 6 ±0.1%](#) contribution. The cryosphere component accounts
1210 for [about 4 ±1%](#), and the atmosphere [about 1 ±0.2%](#). For the most recent era of best available
1211 GCOS data for the Earth heat inventory since the year 2006, the fractions amount to [about 89 ±](#)
1212 [20%](#) for the ocean, [about 5 ±1%](#) for land, [about 4 ±3%](#) for the cryosphere, and [about 2 ±0.4%](#)
1213 for the atmosphere.

1214
1215 The change of the Earth heat inventory over time allows for an estimate of the absolute value of
1216 the Earth energy imbalance. Our results of the total heat gain in the Earth system over the period
1217 1971-2020 is equivalent to a heating rate of $0.48 \pm 0.1 \text{ W m}^{-2}$, and is applied continuously over the
1218 surface area of the Earth ($5.10 \times 10^{14} \text{ m}^2$). For comparison, the heat gain obtained in IPCC AR5
1219 amounts to $274 \pm 78 \text{ ZJ}$ and 0.4 W m^{-2} over the period 1971–2010 (Rhein et al., 2013). In IPCC
1220 AR6, the total heat rate has been assessed by $0.57 [0.43 \text{ to } 0.72] \text{ W m}^{-2}$ for the period 1971-2018,
1221 [and 0.79 \[0.52 to 1.06\] \$\text{Wm}^{-2}\$ for the period 2006-2018](#) (Forster et al., 2021). ~~We~~[Consistently, we](#)
1222 further infer a total heating rate of $0.76 \pm 0.2 \text{ W m}^{-2}$ for the most recent era 2006-2020.

1223
1224 Thus, the ~~numberrate~~ of ~~how fast~~ heat ~~has been accumulated in~~[accumulation across](#) the Earth
1225 system has increased during the most recent era as compared to the long-term estimate – an
1226 outcome which reconfirms the earlier finding in von Schuckmann et al. (2020), and which had
1227 then been concurrently and independently confirmed in Foster et al. (2021), Hakuba et al. (2021),
1228 Loeb et al. (2021), [Liu et al. \(2020\)](#) and Kramer et al. (2021). The drivers of a larger EEI in the
1229 2000s than in the long-term period since 1971 are still unclear, and several mechanisms are
1230 discussed in literature. For example, Loeb et al. (2021) argue for a decreased reflection of energy
1231 back into space by clouds ([including aerosol cloud interactions](#)) and sea-ice, and increases in
1232 well-mixed greenhouse gases (GHG) and water vapor to account for this increase in EEI.
1233 (Kramer et al., 2021) refers to a combination of rising concentrations of well-mixed GHG and
1234 recent reductions in aerosol emissions accounting for the increase, and (Liu et al., 2020)
1235 addresses changes in surface heat flux together with planetary heat re-distribution and changes in
1236 ocean heat storage. Future studies are needed to further explain the drivers of this change,
1237 together with its implications for changes in the Earth system.

1238



1239
1240
1241
1242
1243
1244
1245
1246
1247
1248

Figure 9: Decadal scale rate of change for the Earth Energy Imbalance (EEI) in $Wm^{-2}/decade$ as derived from the Earth heat inventory in Fig. 8 (yellow), OHC of the 0-2000m depth layer (blue; see section 2) and net flux at the top of the atmosphere (TOA, black) based on the estimates of Liu et al. (2020) and Loeb et al. (2021) for three different periods, 1985-2020 (i.e., the full available net flux at TOA estimate), 1993-2020 (i.e., the altimeter era) and 2006-2020 (i.e., the GCOS golden period for the Earth heat inventory). See Liu et al. (2020) and Loeb et al. (2021) on more details of the uncertainty estimate, and note that satellite instrument drift error is not considered. A linear regression has been applied to obtain the rate of change.

1249
1250
1251
1252
1253
1254
1255
1256
1257
1258
1259
1260
1261

With respect to the current status of the GCOS, we further want to emphasize the fact that today the Earth heat inventory is the best estimate for the absolute value of the Earth energy imbalance. This is explained by the fact that satellite derived measurements for the net flux at the top of the atmosphere (TOA) have to be anchored by an absolute value, which is done through the use of the Earth heat inventory, and for which mostly global OHC is used (Loeb et al., 2012; 2021; Liu et al., 2020). However, the temporal change of the EEI can be best estimated from the net flux at TOA from remote sensing data as these are superior in terms of temporal stability. To further discuss the temporal change of the EEI, we compare our results of the Earth heat inventory with the satellite derived net flux at TOA. Consistent with the results of Loeb et al. (2021), the net flux estimates at TOA show a change in the EEI at a significant rate of $0.48 \pm 0.3 Wm^{-2}/decade$ during the period 2006-2020. In 1985-2020 (1993-2020), the value amounts to $0.3 \pm 0.4 Wm^{-2}/decade$ ($0.4 \pm 0.3 Wm^{-2}/decade$) (Fig. 9).

1262
1263
1264
1265
1266
1267
1268

For the Earth heat inventory, the results show that uncertainties for estimating temporal changes of the EEI are still too large to obtain significant results, even during the GCOS ‘golden period’ for the Earth heat inventory in 2006-2020 (Loeb et al., 2022). In other words, this comparison highlights the strength of the complementary use of different independent GCOS components. But the results also show that the current status of the GCOS does not allow for unraveling the rate of change of heat stored in the Earth system components, which is critical information to further understand associated changes in the Earth system (Fig. 1), and to validate climate

1269 ~~models for improving projections of these changes into the future. Hence, these results further~~
 1270 ~~underpin the need for sustaining and further extending the GCOS for improving our knowledge~~
 1271 ~~and monitoring capacity of estimates for how much and where heat is stored in the Earth system.~~
 1272

1273 Besides heat, which is the focus of this study, Earth also stores energy chemically through
 1274 photosynthesis in living and dead biomass with plant growth. **Recent studies** (Crisp et al., 2022;
 1275 Denning, 2022; Friedlingstein et al., 2022) on the Global Carbon Budget and cycle show that
 1276 approximately 25% of the added anthropogenic CO₂ is removed from the atmosphere by
 1277 increased plant growth, which is a result of fertilization by rising atmospheric CO₂ and Nitrogen
 1278 inputs and of higher temperatures and longer growing seasons in northern temperate and boreal
 1279 areas (Friedlingstein et al., 2022). This significant increase in carbon uptake by the biosphere
 1280 indicates that more energy is stored inside biomass, together with the stored carbon. The
 1281 quantification of the additional amount of energy stored inside the biosphere is outside the scope
 1282 of this study.
 1283

1284 7. Data availability

1285
 1286 The time series of the Earth heat inventory are published at DKRZ (<https://www.dkrz.de/>, last
 1287 access: ~~20 July 2024~~ January 2023) under [https://www.wdc-climate.de/ui/entry?](https://www.wdc-climate.de/ui/entry?acronym=GCOS_EHI_1960-2020)
 1288 [acronym=GCOS_EHI_1960-2020](https://www.wdc-climate.de/ui/entry?acronym=GCOS_EHI_1960-2020), more precisely for:

- 1289 • ~~(von Schuckmann et al., 2022); data for ocean heat content (section 2), and the total heat~~
 1290 ~~inventory as presented in section 6 are integrated.~~
- 1291 • ~~(Kirchengast et al., 2022); data for (von Schuckmann et al., 2023) data for ocean heat~~
 1292 ~~content (section 2), and the total heat inventory as presented in section 6 are integrated.~~
- 1293 • ~~(Kirchengast et al., 2022); data for the atmospheric heat content are distributed (section~~
 1294 ~~3).~~
- 1295 • ~~(Cuesta Valero et al., 2022e); data for the ground heat storage, together with the total~~
 1296 ~~continental heat gain are provided (section 4)~~
- 1297 • ~~(Cuesta-Valero et al., 2023) data for the ground heat storage, together with the total~~
 1298 ~~continental heat gain are provided (section 4)~~
- 1299 • ~~(Vanderkelen et al., 2022); data for inland freshwater heat storage is included (section 4)~~
- 1300 • (Nitzbon et al., 2022b); data for permafrost are delivered (section 4).
- 1301 • (Adusumilli et al., 2022); data for the cryosphere heat inventory are provided.
- 1302
- 1303

1304 ~~Persistent identifiers (PIDs)~~ The Digital Object Identifiers (DOIs) for ~~the specific~~ data access are
 1305 provided in Table 23.
 1306

Earth heat inventory component	<u>PHDOI</u>	Reference
Ocean heat content; Total Earth heat inventory	https://hdl.handle.net/21.14106/9b2fddbe4637e3bb9fbf2414e55e6aad0e3923b0 https://doi.org/10.26050/WDCC/GCOS_EHI_1960-2020_OHC_v2	von Schuckmann et al., 2022 <u>2023</u>
Atmospheric heat content	https://hdl.handle.net/21.14106/2e4c7216177feb742f324cae2792e43faf8361f1 https://doi.org/10.26050/WDCC/GCOS_EHI_1960-2020_AHC	Kirchengast et al., 2022
Continental heat content	https://hdl.handle.net/21.14106/302a4aedadcabf09d5f432003361275e9102a48a https://doi.org/10.26050/WDCC/GCOS_EHI_1960-2020_CHC	Cuesta Valero et al., 2022e <u>2023</u>

	doi.org/10.26050/WDCC/GCOS_EHI_1960-2020_CoHC_v2	
Inland water heat content	https://hdl.handle.net/21.14106/e095f83398baa6e5b355ba88ae97ed7dedd008dehttps://doi.org/10.26050/WDCC/GCOS_EHI_1960-2020_IWHC	Vanderkelen et al., 2022
Heat available to melt permafrost	https://hdl.handle.net/21.14106/a9654e3d10e0002da4dde3ef080f6503e2decbf5https://doi.org/10.26050/WDCC/GCOS_EHI_1960-2020_PHC	Nitzbon et al., 2022b
Heat available to melt the cryosphere	https://hdl.handle.net/21.14106/b9829ba3230f0631d3545a66a88e1e89803510eehttps://doi.org/10.26050/WDCC/GCOS_EHI_1960-2020_CrHC	Adusumilli et al., 2022

1307

1308

1309

1310

1311

1312

1313

Table 23: Overview on *persistent identifiers (PIDs)* *Digital Object Identifier (DOI)* for data access for *each component—the components* of the Earth heat inventory-, *and associated references*. The results are presented in Fig. 8.

8. Conclusion

1314

1315

1316

1317

1318

1319

1320

1321

1322

1323

1324

1325

1326

1327

1328

1329

1330

1331

1332

1333

This study builds on the first internationally and multidisciplinary driven Earth heat inventory in 2020 (von Schuekmann et al., 2020) and provides an update on total Earth system heat accumulation, heat storage in all Earth system components (ocean, land, cryosphere, atmosphere) and the Earth energy imbalance up to the year 2020. Moreover, this study succeeded to improve estimates, to further extent and foster international collaboration, and to continue to move towards a more complete view on where and how much heat is stored in the Earth system through the addition of new estimates such as for permafrost thawing, inland freshwater (section 4) and Antarctic sea ice (section 5). Results obtained reveal a total Earth system heat gain of 380 ± 62 ZJ over the period 1971–2020, with an associated total heating rate of 0.48 ± 0.1 W m⁻²: 89 ± 17 % of this heat stored in the ocean, 6 ± 0.1 % on land, 4 ± 1 % in the cryosphere and 1 ± 0.2 % in the atmosphere (Fig. 8, 11). The analysis additionally reconfirms an increased heating rate which amounts to 0.76 ± 0.2 W/m² for the most recent era 2006–2020. These results are consistent with previous estimates, which is again demonstrated through a comprehensive assessment of estimates for the EEI published in peer-reviewed literature (Fig. 10). Albeit the drivers for this change still need to be elucidated and most likely reflect the interplay between natural variability and anthropogenic change (Loeb et al., 2021; Kramer et al., 2021; Liu et al., 2020), their implications for changes in the Earth system are reflected in the many record levels of change in the 2000s reported elsewhere, e.g., (Cheng et al., 2022; Forster et al., 2022; Gulev et al., 2021; WMO, 2022).

1334

1335

1336

1337

1338

1339

1340

The recent Glasgow Climate Pact (UNFCCC, 2021) is ‘*Acknowledging that climate change is a common concern of humankind ...*’ and ‘*Recognizing ... the importance of international cooperation in addressing climate change and its impacts ...*’, and ‘*Recognizes the importance of the best available science for effective climate action and policy making*’. The UN 2030 Agenda for Sustainable Development¹³ states that climate change is “*one of the greatest challenges of our time ...*” and warns “*... the survival of many societies, and of the biological support systems of the planet, is at risk*”. The outcome document of the Rio+20 Conference, The Future We Want¹⁴,

137

138

139

13 — <https://sustainabledevelopment.un.org/content/documents/21252030%20Agenda%20for%20Sustainable%20Development%20web.pdf>

14 — <https://sustainabledevelopment.un.org/content/documents/733FutureWeWant.pdf>

140

141

1341 ~~defines climate change as “an inevitable and urgent global challenge with long-term~~
1342 ~~implications for the sustainable development of all countries”.~~

1343 **8. Conclusion**

1344

1345 The Earth heat inventory is a global climate indicator integrating fundamental aspects of the
1346 Earth system under global warming. Particularly, the Earth heat inventory provides the best
1347 available current estimate of the absolute value of the Earth Energy Imbalance (Cheng et al.,
1348 2017; Cheng et al., 2019; Hakuba et al., 2021; Hansen et al., 2011; Loeb et al., 2012, 2022;
1349 Trenberth et al., 2016; von Schuckmann et al., 2020). Moreover, its evaluation enables an
1350 integrated view of the effective radiative climate forcing, Earth’s surface temperature response
1351 and the climate sensitivity (Forster et al., 2022; Hansen et al., 2011; Hansen et al., 2005; Palmer
1352 & McNeall, 2014; Smith et al., 2015). Additionally, its quantification informs about the status of
1353 global warming in the Earth system as it integrates the heat ‘in the pipeline’ that will ultimately
1354 warm the deep ocean and melt ice sheets in the long term (Hansen et al., 2011; Hansen et al.,
1355 2005; IPCC, 2021). The Earth heat inventory also reveals how much and where surplus
1356 anthropogenic heat is available for melting the cryosphere and warming the ocean, land and
1357 atmosphere, which in turn allows for an evaluation of associated changes in the climate system
1358 and is essential to improve seasonal-to-decadal climate predictions and projections on century
1359 timescales to enable improved planning for and adaptation to climate change (Hansen et al.,
1360 2011; von Schuckmann et al., 2016, 2020). Regular international assessment on the Earth heat
1361 inventory enables concerted international and multidisciplinary collaboration and advancements
1362 in climate science, including to contribute to the development of recommendations for the status
1363 and evolution of the global climate observing system (GCOS, 2021; von Schuckmann et al.,
1364 2020).

1365

1366 This study builds on the first internationally and multidisciplinary driven Earth heat inventory in
1367 2020 (von Schuckmann et al., 2020) and provides an update on total Earth system heat
1368 accumulation, heat storage in all Earth system components (ocean, land, cryosphere, atmosphere)
1369 and the Earth energy imbalance up to the year 2020. Moreover, this study improved earlier
1370 estimates, and further extended and fostered international collaboration, allowing to move
1371 towards a more complete view on where and how much heat is stored in the Earth system
1372 through the addition of new estimates such as for permafrost thawing, inland freshwater (section
1373 4) and Antarctic sea ice (section 5). Results obtained reveal a total Earth system heat gain of
1374 381 ± 61 ZJ over the period 1971–2020, with an associated total heating rate of 0.48 ± 0.1 W m⁻².
1375 About 89 % of this heat stored in the ocean, about 6 % on land, about 4 % in the cryosphere and
1376 about 1 % in the atmosphere (Fig. 8, 10). The analysis additionally reconfirms an increased
1377 heating rate which amounts to 0.76 ± 0.2 W/m⁻² for the most recent era 2006-2020. Albeit the
1378 drivers for this change still need to be elucidated and most likely reflect the interplay between
1379 natural variability and anthropogenic change (Kramer et al., 2021; Liu et al., 2020; Loeb et al.,
1380 2021), their implications for changes in the Earth system are reflected in the many record levels
1381 of change in the 2000s reported elsewhere, e.g., (Cheng et al., 2022; Forster et al., 2022; Gulev et
1382 al., 2021).

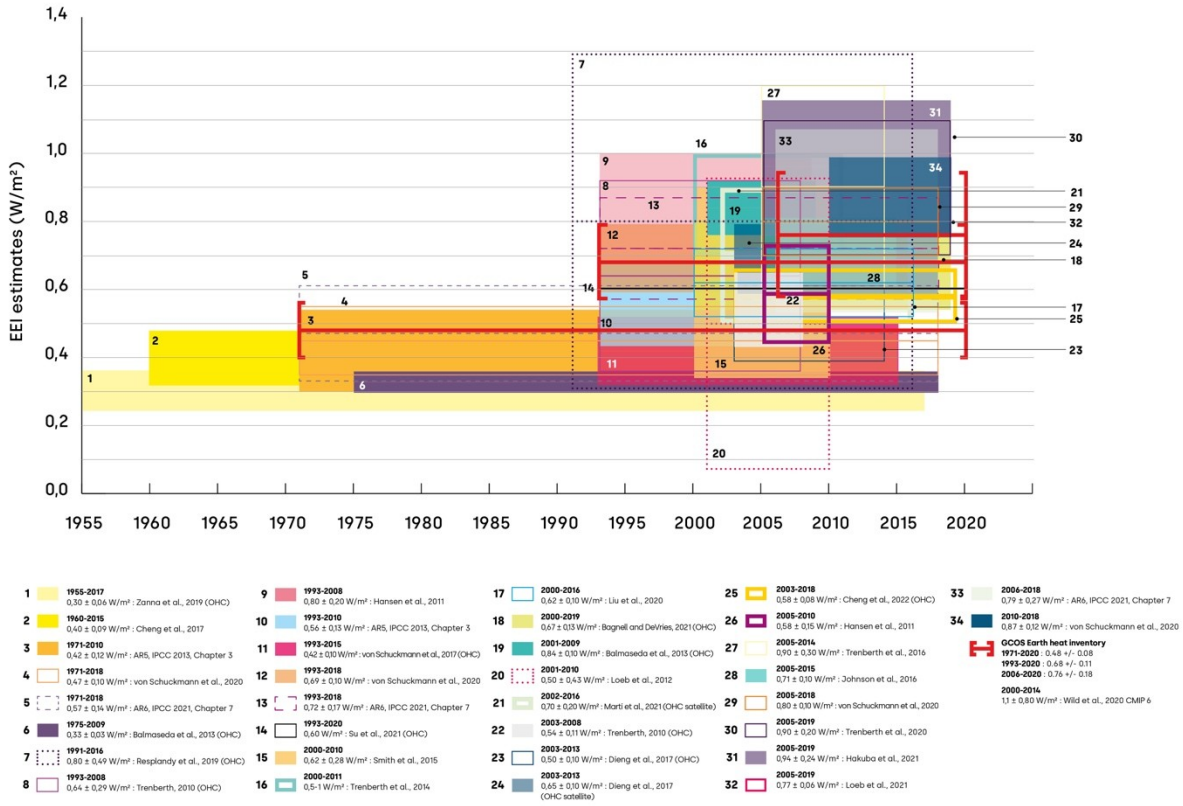
1383

1384 The Paris Agreement builds upon the United Nations Framework Convention on Climate Change
1385 and for the first time all nations agreed to undertake ambitious efforts to combat climate change,
1386 with the central aim to keep global temperature rise this century well below 2 °C above pre

1387 industrial levels and to limit the temperature increase even further to 1.5 °C. Article 14 of the
 1388 Paris Agreement requires the Conference of the Parties serving as the meeting of the Parties to
 1389 the Paris Agreement (CMA) to periodically take stock of the implementation of the Paris
 1390 Agreement and to assess collective progress towards achieving the purpose of the agreement and
 1391 its long-term goals through the so-called Global Stocktake of the Paris Agreement (GST)¹⁵ based
 1392 on best available science.

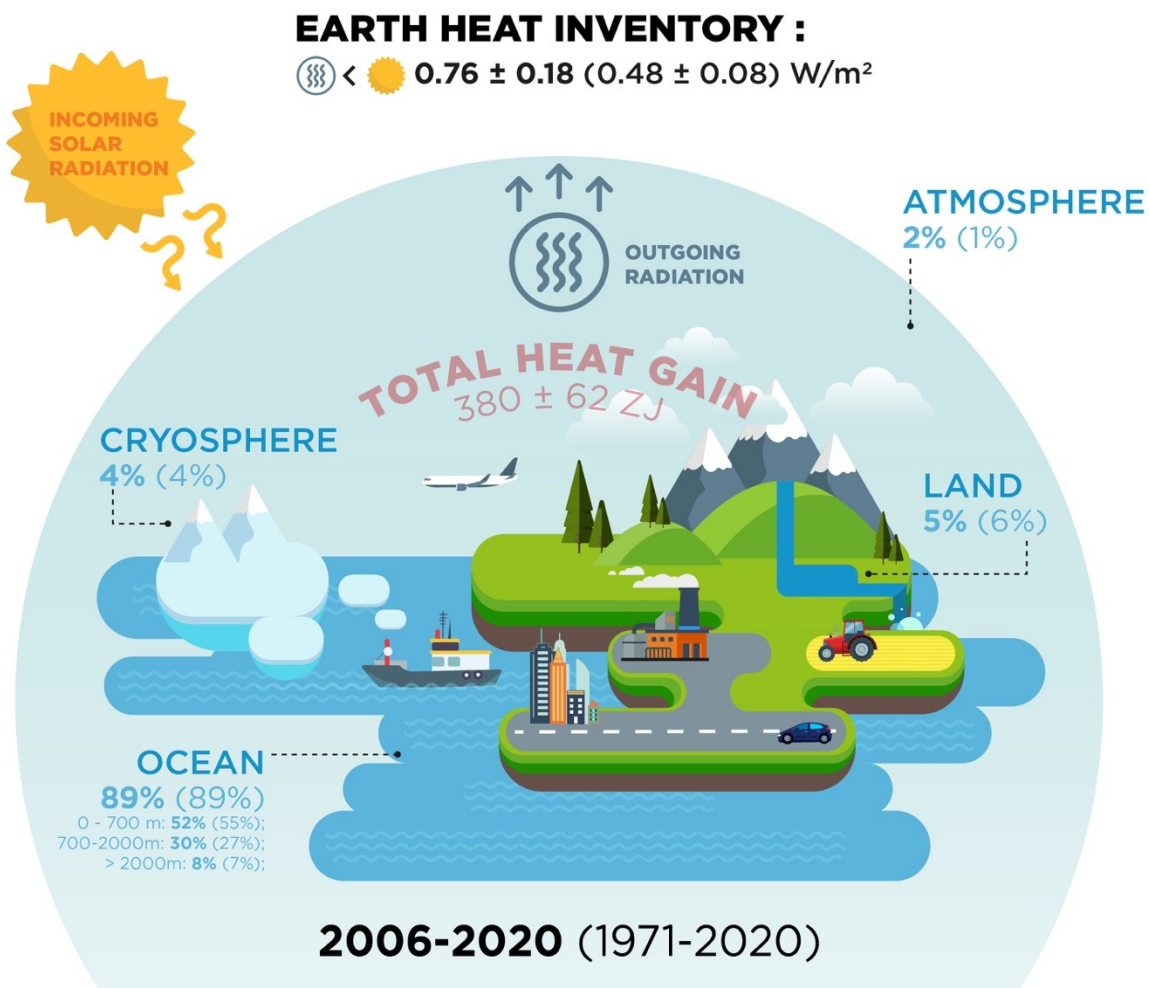
1393
 1394 The Earth heat inventory provides information on how much and where heat is accumulated and
 1395 stored in the Earth system. Moreover, it provides a measure of how much the Earth is out of
 1396 energy balance, and when combined with directly measured net flux at the top of the atmosphere,
 1397 enables also to understand the change of the EEI over time. This in turn allows for assessing the
 1398 portion of the anthropogenic forcing that the Earth's climate system has not yet responded to
 1399 (Hansen et al., 2005) and defines additional global warming that will occur without further
 1400 change in human-induced forcing (Hansen et al., 2017). ~~The Earth heat inventory is thus one of~~
 1401 ~~the key critical global climate change indicators defining the prospects for continued global~~
 1402 ~~warming and climate change (Hansen et al., 2011; von Schuckmann et al., 2016; 2020)(Hansen~~
 1403 ~~et al., 2017). The Earth heat inventory is thus one of the key critical global climate change~~
 1404 ~~indicators defining the prospects for continued global warming and climate change (Hansen et~~
 1405 ~~al., 2011; von Schuckmann et al., 2016; 2020).~~ Hence, we call for an implementation of the Earth
 1406 heat inventory into the global stocktake.

146 15 — [https://unfccc.int/topics/global-stocktake/global-stocktake#:~:text=The%20global%20stocktake%20of%20the,term%20goals%20\(Article%2014\)._https://unfccc.int/topics/global-stocktake/global-stocktake#:~:text=The%20global%20stocktake%20of%20the,term%20goals%20\(Article%2014\)._\(Last access 01.02.2023\)](https://unfccc.int/topics/global-stocktake/global-stocktake#:~:text=The%20global%20stocktake%20of%20the,term%20goals%20(Article%2014)._https://unfccc.int/topics/global-stocktake/global-stocktake#:~:text=The%20global%20stocktake%20of%20the,term%20goals%20(Article%2014)._(Last%20access%2001.02.2023))



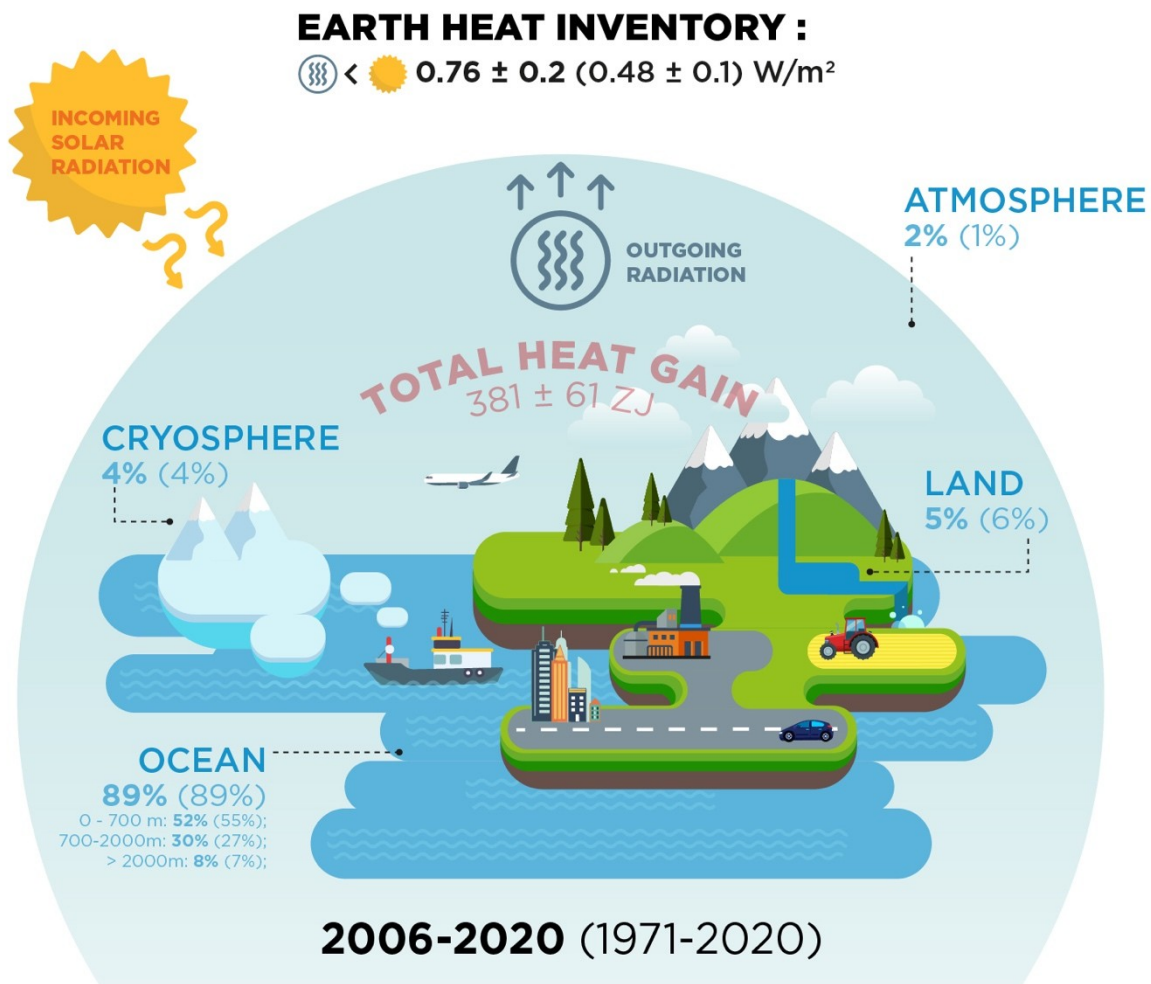
1408
1409
1410
1411
1412
1413
1414
1415

Figure 10: Overview on EEI and d(OHC)/dt (indicated with (OHC) in the legend) estimates as obtained from previous publications; references are listed in the figure legend. The color bars take into account the uncertainty ranges provided in each publication, respectively. For comparison, the estimates of our Earth heat inventory based on the results of Fig. 8 have been added (red lines) for the periods 1971–2020, 1993–2020 and 2006–2020.



1416
1417
1418
1419

Figure 11



1420

1421

1422 **Figure 10:** Schematic presentation on the Earth heat inventory for the current anthropogenically
 1423 driven positive Earth energy imbalance at the top of the atmosphere (TOA). The relative
 1424 partition (in %) of the Earth heat inventory presented in Fig. 8 for the different components is
 1425 given for the ocean (upper: 0–700 m, intermediate: 700–2000 m, deep: >2000 m), land,
 1426 cryosphere (grounded and floating ice) and atmosphere, for the periods 2006–2020 and 1971–
 1427 2020 (for the latter period values are provided in parentheses), as well as for the EEI. The total
 1428 heat gain (in red) over the period 1971–2020 is obtained from the Earth heat inventory as
 1429 presented in Fig. 8.

1430

1431 The quantifications presented in this study are the result of multidisciplinary global-scale
 1432 collaboration and demonstrate the critical importance of concerted international efforts for
 1433 climate change monitoring and community-based recommendations for the [GCOS-global climate
 1434 observing system](#). For the [GOOSocean observing system](#), the core Argo sampling needs to be
 1435 sustained – which includes the maintenance of shipboard collection of reference data for
 1436 validation - and complemented by remote sensing data. Extensions such as into the deep ocean
 1437 layer need to be further fostered, and technical developments for the measurements under ice and
 1438 in shallower areas need to be sustained and extended. Moreover, continued efforts are needed to

1439 further advance bias correction methodologies, uncertainty evaluations, data recovery and
1440 processing of the historical dataset. [Spatial geodetic observations and the closure of the sea level](#)
1441 [budget serve as a valuable constraint for the full column OHC. Although the independent](#)
1442 [estimates agree within uncertainty, the geodetic approach suggest slightly larger OHC linear](#)
1443 [trends, especially since 2016. Though efforts are under way to investigate the emerging](#)
1444 [discrepancy \(e.g., Barnoud et al., 2021\), the causes are not yet fully understood and require](#)
1445 [further investigation.](#)

1446
1447

1448 For the ground heat storage, the estimate had been hampered by a lack of subsurface temperature
1449 profiles in the southern hemisphere, as well as by the fact that most of the profiles were
1450 measured before the 2000s. Subsurface temperature data are direct and independent (not proxy)
1451 measurements of temperature yielding information on the temporal variation of the ground
1452 surface temperature and ground heat flux at the land surface. A larger spatial scale dataset of the
1453 thermal state of the subsurface from the last millennium to the present will aid in the continuing
1454 monitoring of continental heat storage, provide initial conditions for Land Surface Model (LSM)
1455 components of Earth System Models (ESMs) (Cuesta-Valero et al., 2019), and serve as a dataset
1456 for validation of climate models' simulations (Cuesta-Valero et al., 2021; Cuesta-Valero et al.,
1457 2016). Progress in understanding climate variability through the last millennium must lean on
1458 additional data acquisition as the only way to reduce uncertainty in the paleoclimatic record and
1459 on changes to the current state of the continental energy reservoir. Remote sensing data are
1460 expected to be very valuable to retrieve recent past and future changes in ground heat flux at
1461 short-time scales with near global coverage. However, collecting subsurface temperature data is
1462 urgent as we must make a record of the present thermal state of the subsurface before the
1463 subsurface climate baseline is affected by the downward propagating thermal signal from current
1464 climate heating. Furthermore, an international organization should take responsibility to gather
1465 and curate all measured subsurface temperature profiles currently available and those that will be
1466 measured in the future, as the current practices, in which individual researchers are responsible
1467 for measuring, storing and distributing the data, have led to fragmented datasets, restrictions in
1468 the use of data, and loss of the original datasets. Support from GCOS for an international data
1469 acquisition and curating efforts would be extremely important in this context.

1470

1471 For the permafrost estimates, the primary sources of uncertainty arise from lacking information
1472 about the amount and distribution of ground ice in permafrost regions, as well as measurements
1473 of liquid water content ([Nitzbon et al., 2022](#))([Nitzbon et al., 2022](#)). Permafrost heat storage is
1474 defined as the required heat to change the mass of ground ice at a certain location, thus
1475 monitoring changes in ground ice and water contents would be required to improve estimates of
1476 this component of the continental heat storage. Nevertheless, the current monitoring system for
1477 permafrost soils is focused on soil temperature, and the distribution of stations is still relatively
1478 scarce in comparison with the vast areas that need to be surveyed (Biskaborn et al., 2015). Due to
1479 the current limitations in the observational data, a permafrost model was used to estimate the
1480 heat uptake by thawing of ground ice. This approach retrieves latent heat fluxes in extensive
1481 areas and at depths relevant to analyze the long-term change in ground ice mass, but at the cost
1482 of ignoring other relevant processes, such as ground subsidence, to balance model performance
1483 with computational resources. Including permafrost heat storage in the Tibetan Plateau is a

1484 priority for the next iteration of this work, as well as to explore new methods to evaluate model
1485 simulations using the available observations in permafrost areas.

1486
1487 For inland water heat storage, a better representation of lake and reservoir volume would be
1488 possible by better accounting for lake bathymetry using the GLOBathy (Khazaei et al., 2022)
1489 dataset and results from the upcoming Surface Water and Ocean Topography (SWOT) mission.
1490 These improvements in the representation of lake volume, and an updated lake mask will be
1491 available in the upcoming ISIMIP3 simulation round, next to improved meteorological forcing
1492 data (Golub et al., 2022). In contrast to (Vanderkelen et al., 2020), the heat storage in rivers is
1493 not included in this analysis due to the high uncertainties in simulated river water volume. To
1494 reduce the uncertainty in river heat storage, the estimation of river water storage should be
1495 improved, together with an explicit representation of water temperature in the global
1496 hydrological models (Wanders et al., 2019). These improvements will be incorporated in
1497 ISIMIP3 and will lead to better estimates of inland water heat storage, thus enhancing future
1498 estimates of continental heat storage. In the long run, these model-based estimates could be
1499 supplemented or replaced by observation-based estimates, which would however require a large,
1500 global-scale effort to monitor lake and river temperatures at high spatial resolution and over long
1501 time periods. Estimates for inland water heat storage and permafrost heat storage in this analysis
1502 depend heavily on model simulations, which is of particular challenge for analyzing and adding
1503 uncertainty ranges, as the sources of uncertainty in model simulations differ from those in
1504 observational records (Cuesta-Valero et al., 2022a). Future estimates should hence focus on a
1505 hybrid approach considering in situ measurements, reanalysis, remote sensing data and model
1506 simulations, consistent with the methods employed for deriving cryosphere and atmosphere heat
1507 storage for the Earth heat inventory.

1508
1509 For the cryosphere, sustained remote sensing for all of the cryosphere components is critical in
1510 quantifying future changes over these vast and inaccessible regions; in situ observations are also
1511 needed for process understanding and in order to properly calibrate and validate them. For sea
1512 ice, observations of the albedo, the area and ice thickness are all essential - the continuation of
1513 satellite altimeter missions with high inclination, polar focused orbits is critical in our ability to
1514 monitor sea ice thickness in particular. Observations of snow thickness with multi-frequency
1515 altimeters and microwave radiometers are essential for further constraining sea ice thickness
1516 estimates. For ice sheets and glaciers, reliable gravimetric, geodetic, and ice velocity
1517 measurements, knowledge of ice thickness and extent, snow/firn thickness and density, and the
1518 continuation of the now three-decade long satellite altimeter record are essential in understanding
1519 changes in the mass balance of grounded and floating ice. The recent failure of Sentinel-1b,
1520 which in tandem with Sentinel-1a could be used to systematically measure ice speed changes
1521 every 6 days, means that images are now being acquired every 12 days and thus an earlier launch
1522 of Sentinel-1c should be encouraged to regain the ability to monitor ice speed changes over short
1523 time-scales. The estimate of glacier heat uptake is particularly affected by lacking knowledge of
1524 ice melt below sea level, and to a lesser degree, lacking knowledge of firn and ice temperatures.
1525 This lack of observations is likely related to most studies on glaciers foeussingfocusing on their
1526 contribution to sea-level rise or seasonal water availability, where melt below sea level and
1527 warming of ice do not matter much. However, it becomes obvious here that this gap introduces a
1528 systematic bias in the estimate of cryospheric energy uptake, which is presumably small
1529 compared to the other components, but unconstrained. Although the Antarctic sea ice change and

1530 the warming of Greenland and Antarctic firm are poorly constrained or have not significantly
 1531 contributed to this assessment, they may become increasingly important over the coming
 1532 decades. Similarly, there exists the possibility for rapid change associated with positive ice
 1533 dynamical feedbacks at the marine margins of the Antarctic Ice Sheet. Sustained monitoring of
 1534 each of these components will, therefore, serve the dual purpose of furthering the understanding
 1535 of the dynamics and quantifying the contribution to Earth's energy budget. In addition to data
 1536 collection, open access to the data and data synthesis products, as well as coordinated
 1537 international efforts, are key to the continued monitoring of the ice loss from the cryosphere and
 1538 its related energy uptake.

1539
 1540 For the atmosphere, there is a need to sustain and enhance a coherent operational long-term
 1541 monitoring system for the provision of climate data records of essential climate variables.
 1542 Observations from radiosonde stations within the GCOS reference upper air network (GRUAN)
 1543 and from satellite-based GNSS radio occultation deliver thermodynamic profiling observations
 1544 of benchmark quality and stability from surface to stratopause. For climate monitoring, it is of
 1545 critical importance to ensure continuity of such observations with global coverage over all local
 1546 times. This continuity of radio occultation observations in the future is not sufficiently
 1547 guaranteed as we are facing an imminent observational gap in mid- to high latitudes for most
 1548 local times(IROWG, 2021), which is a major concern. Thus, there is an urgent need for satellite
 1549 missions in high inclination orbits to provide full global and local time coverage in order to
 1550 ensure global climate monitoring. Operational radio occultation missions need to be maintained
 1551 as backbone for a global climate observing system and long-term availability and archiving of
 1552 measurement data, metadata and processing information needs to be ensured.

1553
 1554 In summary, we also call for urgently needed actions for enabling continuity, archiving, rescuing
 1555 and calibrating efforts to assure improved and long-term monitoring capacity of the [GCOSglobal](#)
 1556 [climate observing system](#) for the Earth heat inventory, [and to complement with measurements](#)
 1557 [from space for assessing the changes of EEI \(e.g., Loeb et al., -2021; von Schuckmann et al.,](#)
 1558 [2016\)](#). **Particularly, the summarized recommendations include**

- 1559
- 1560 • Need to sustain, reinforce or even to establish data repositories for historical climate data
 - 1561 (archiving)
 - 1562 • Need to reinforce efforts for recovery projects for historical data and associated meta-data
 - 1563 information (rescuing)
 - 1564 • Need to sustain and reinforce the [GCOSglobal climate observing system](#) for assuring the
 - 1565 monitoring of the Earth heat inventory targets, [such as for the polar, deep and shallow](#)
 - 1566 [ocean, and of top-of-the-atmosphere radiation fluxes](#) (continuity)
 - 1567 • Need to foster calibration measurements (in situ) for assuring quality and reliability of
 - 1568 large-scale measurement techniques (e.g., remote sensing, autonomous components (eg
 - 1569 argo) (calibrating)

1570
 1571 A continuous effort to regularly update the Earth heat inventory is important as this global
 1572 climate indicator crosses multidisciplinary boundaries and calls for the inclusion of new science
 1573 knowledge from the different disciplines involved, including the evolution of climate observing
 1574 systems and associated data products, uncertainty evaluations, and processing tools. The
 1575 outcomes have further demonstrated how we are able to evolve our estimates for the Earth heat

1576 inventory while bringing together different expertise and major climate science advancements
 1577 through a concerted international effort. All of these component estimates are at the leading edge
 1578 of climate science. Their union has provided a new and unique insight on the inventory of heat in
 1579 the Earth system, its evolution over time and the absolute values. The data product of this effort
 1580 is made available and can be thus used for ~~model validation purposes~~ climate model validation
 1581 purposes. The results also demonstrate that further efforts are needed for uncertainty evaluations,
 1582 such as for example the use of synthetic profile analyses. Indeed, improving the climate
 1583 observing system will allow for reduced uncertainties for estimating the Earth heat inventory.
 1584 However, further evaluations are needed to unravel uncertainties of the different components of
 1585 the Earth heat inventory, which rely for example on non-homogeneous data sampling and large
 1586 data gaps, the use of different measurement types and statistical approaches, instrumental bias
 1587 corrections, and their joint analysis of mode-based quantifications.
 1588

1589 This study has demonstrated the unique value of such a concerted international effort, and we
 1590 thus call for a regular evaluation of the Earth heat inventory. This updated attempt presented here
 1591 has been focused on the global area average only, and evolving into regional heat storage and
 1592 redistribution, the inclusion of various timescales (e.g., seasonal, year to year) and other climate
 1593 study tools (e.g., indirect methods, ocean reanalyses) would be an important asset of this much
 1594 needed regular international framework for the Earth heat inventory. This would also respond
 1595 directly to the request of GCOS to establish the observational requirements needed to further
 1596 monitor the Earth's cycles and the global energy budget (GCOS, 2021). The outcome of this
 1597 study will therefore directly feed into ~~GCOS~~ GCOS assessments of the status of the global
 1598 climate observing system, and the identified observation requirements will guide the
 1599 development of the next generation of in situ and satellite global climate observations as
 1600 specified by GCOS by all national meteorological services and space agencies and other oceanic
 1601 and terrestrial networks.
 1602
 1603

1604 **Acknowledgements.**

1605 Ocean: OHC estimate from the product ISAS (Gaillard et al., 2016) was provided by ‘Service National
 1606 d’Observation Argo France’ (INSU/CNRS) at OSU IUEM (<https://www.argo-france.fr/>).
 1607 Atmosphere: We acknowledge the WEGC EOPAC team for providing the OPSv5.6 RO data (available online at
 1608 <https://doi.org/10.25364/WEGC/OPS5.6:2020.1>) as well as quality-processed Vaisala RS data, UCAR/CDAAC
 1609 (Boulder, CO, USA) for access to RO phase and orbit data, ECMWF (Reading, UK) for access to operational
 1610 analysis and forecast data, ERA5 reanalysis data, and RS data from the ERA-Interim archive, JMA (Tokyo, Japan)
 1611 for provision of the JRA55 and JRA55C reanalysis data, and NASA GMAO (Greenbelt, MD, USA) for access of
 1612 the MERRA-2 reanalysis data.
 1613
 1614
 1615

1616 **Financial support.**

1617 Maximilian Gorfer was supported by WEGC atmospheric remote sensing and climate system research group young
 1618 scientist funds. Michael Mayer was supported by Austrian Science Fund project P33177.
 1619
 1620 Donata Giglio and Mikael Kuusela acknowledge support from NOAA (~~AwardAwards~~ [NA21OAR4310261](#)), and
 1621 [NA21OAR4310258](#).
 1622
 1623 L.C. acknowledges financial supports from the Strategic Priority Research Program of the Chinese Academy of
 1624 Sciences (XDB42040402), National Natural Science Foundation of China (grant number 42122046, 42076202).

1625
1626 J.C. and Y.L. were supported by the Centre for Southern Hemisphere Oceans Research (CSHOR), jointly funded by
1627 the Qingdao National Laboratory for Marine Science and Technology (QNLN, China) and the Commonwealth
1628 Scientific and Industrial Research Organisation (CSIRO, Australia), and the Australian Research Council's
1629 Discovery Project funding scheme (project DP190101173) and the [Australian Research Council Special Research
1630 Initiative, Australian Centre for Excellence in Antarctic Science \(Project Number SR200100008\)](#). TMcD and PMB
1631 gratefully acknowledge Australian Research Council support through grant FL150100090. This paper contributes to
1632 the tasks of the Joint SCOR/IAPSO/IAPWS Committee on the Thermophysical Properties of Seawater.

1633
1634 Hugo Beltrami was supported by grants from the National Sciences and Engineering Research Council of Canada
1635 Discovery Grant (NSERC DG 140576948) and the Canada Research Chairs Program (CRC 230687). Hugo Beltrami
1636 holds a Canada Research Chair in Climate Dynamics

1637
1638 Francisco José Cuesta-Valero is an Alexander von Humboldt Research Fellow at the Helmholtz Centre for
1639 Environmental Research (UFZ).

1640
1641 Richard P. Allan is funded by the National Centre for Earth Observation RCUK grant NE/RO16518/1.

1642
1643
1644 [F. W. Landerer and M. Z. Hakuba were supported by Jet Propulsion Laboratory, California Institute of Technology,
1645 under a contract with the National Aeronautics and Space Administration \(80NM0018D0004\).](#)

1646 1647 **References**

1648
1649 [Abraham, J., Cheng, L., Mann, M. E., Trenberth, K., & von Schuckmann, K. \(2022\). The ocean
1650 response to climate change guides both adaptation and mitigation efforts. *Atmospheric and
1651 Oceanic Science Letters*, *15*\(4\), 100221.
1652 <https://doi.org/https://doi.org/10.1016/j.aosl.2022.100221>](#)

1653 [Abraham, J. P., Baringer, M., Bindoff, N. L., Boyer, T., Cheng, L. J., Church, J. A.,
1654 Conroy, J. L., Domingues, C. M., Fasullo, J. T., Gilson, J., Goni, G., Good, S. A.,
1655 Gorman, J. M., Gouretski, V., Ishii, M., Johnson, G. C., Kizu, S., Lyman, J. M.,
1656 Macdonald, A. M., ... Willis, J. K. \(2013\). A review of global ocean temperature
1657 observations: Implications for ocean heat content estimates and climate change.
1658 *Reviews of Geophysics*, *51*\(3\), 450–483. <https://doi.org/10.1002/rog.20022>](#)

1659 [Abram, N., Gattuso, J.-P., Prakash, A., Cheng, L., Chidichimo, M. P., Croteau, S., Enomoto, H.,
1660 Garschagen, M., Gruber, N., Harper, S., Holland, E., Kudela, R. M., Rice, J., Steffen, K., &
1661 von Schuckmann, K. \(2019\). Framing and Context of the Report. In H. O. Pörtner, D. C.
1662 Roberts, V. Masson-Delmotte, P. Zhai, M. Tignor, E. Poloczanska, K. Mintenbeck, A.
1663 Alegria, M. Nicolai, A. Okem, J. Petzold, B. Rama, & N. M. Weyer \(Eds.\), *IPCC Special
1664 Report on the Ocean and Cryosphere in a Changing Climate* \(pp. 73–129\). in press.
1665 <https://www.ipcc.ch/srocc/>](#)

1666 [Adusumilli, S., Fricker, H. A., Medley, B., Padman, L., & Siegfried, M. R. \(2020\). Interannual
1667 variations in meltwater input to the Southern Ocean from Antarctic ice shelves. *Nature
1668 Geoscience*, *13*\(9\), 616–620. <https://doi.org/10.1038/s41561-020-0616-z>](#)

1669 [Allison, L. C., Roberts, C. D., Palmer, M. D., Hermanson, L., Killick, R. E., Rayner, N. A.,
1670 Smith, D. M., & Andrews, M. B. \(2019\). Towards quantifying uncertainty in ocean heat
1671 content changes using synthetic profiles. *Environmental Research Letters*, *14*\(8\), 084037.
1672 <https://doi.org/10.1088/1748-9326/ab2b0b>](#)

1673 [Angerer, B., Ladstädter, F., Scherllin-Pirscher, B., Schwärz, M., Steiner, A. K., Foelsche, U., &
1674 Kirchengast, G. \(2017\). Quality aspects of the Wegener Center multi-satellite GPS radio](#)

- 1675 [occultation record OPSv5.6. *Atmospheric Measurement Techniques*, 10\(12\), 4845–4863.](#)
 1676 <https://doi.org/10.5194/amt-10-4845-2017>
- 1677 [Barker, P. M., & McDougall, T. J. \(2020\). Two Interpolation Methods Using Multiply-Rotated
 1678 Piecewise Cubic Hermite Interpolating Polynomials. *Journal of Atmospheric and Oceanic
 1679 Technology*, 37\(4\), 605–619. <https://doi.org/10.1175/JTECH-D-19-0211.1>](#)
- 1680 [Barnoud, A., Pfeffer, J., Guérou, A., Frery, M.-L., Siméon, M., Cazenave, A., Chen, J., Llovel,
 1681 W., Thierry, V., Legeais, J.-F., & Ablain, M. \(2021\). Contributions of Altimetry and Argo
 1682 to Non-Closure of the Global Mean Sea Level Budget Since 2016. *Geophysical Research
 1683 Letters*, 48\(14\), e2021GL092824. <https://doi.org/https://doi.org/10.1029/2021GL092824>](#)
- 1684 [Bell, B., Hersbach, H., Simmons, A., Berrisford, P., Dahlgren, P., Horányi, A., Muñoz-Sabater,
 1685 J., Nicolas, J., Radu, R., Schepers, D., Soci, C., Villaume, S., Bidlot, J.-R., Haimberger, L.,
 1686 Woollen, J., Buontempo, C., & Thépaut, J.-N. \(2021\). The ERA5 global reanalysis:
 1687 Preliminary extension to 1950. *Quarterly Journal of the Royal Meteorological Society*,
 1688 147\(741\), 4186–4227. <https://doi.org/https://doi.org/10.1002/qj.4174>](#)
- 1689 [Beltrami, H., & Mareschal, J.-C. \(1992\). Ground temperature histories for central and eastern
 1690 Canada from geothermal measurements: Little Ice Age signature. *Geophysical Research
 1691 Letters*, 19\(7\), 689–692. <https://doi.org/10.1029/92GL00671>](#)
- 1692 [Beltrami, H., Smerdon, J. E., Pollack, H. N., & Huang, S. \(2002\). Continental heat gain in the
 1693 global climate system. *Geophysical Research Letters*, 29\(8\), 8-1-8–3.
 1694 <https://doi.org/10.1029/2001GL014310>](#)
- 1695 [Berrisford, P., Kållberg, P., Kobayashi, S., Dee, D., Uppala, S., Simmons, A. J., Poli, P., & Sato,
 1696 H. \(2011\). Atmospheric conservation properties in ERA-Interim. *Quarterly Journal of the
 1697 Royal Meteorological Society*, 137\(659\), 1381–1399. <https://doi.org/10.1002/qj.864>](#)
- 1698 [Biskaborn, B. K., Lanckman, J.-P., Lantuit, H., Elger, K., Streletskiy, D. A., Cable, W. L., &
 1699 Romanovsky, V. E. \(2015\). The new database of the Global Terrestrial Network for
 1700 Permafrost \(GTN-P\). *Earth Syst. Sci. Data*, 7\(2\), 245–259. \[https://doi.org/10.5194/essd-7-
 1701 245-2015\]\(https://doi.org/10.5194/essd-7-245-2015\)](#)
- 1702 [Boyer, T., Domingues, C. M., Good, S. A., Johnson, G. C., Lyman, J. M., Ishii, M., Gouretski,
 1703 V., Willis, J. K., Antonov, J., Wijffels, S., Church, J. A., Cowley, R., & Bindoff, N. L.
 1704 \(2016\). Sensitivity of Global Upper-Ocean Heat Content Estimates to Mapping Methods,
 1705 XBT Bias Corrections, and Baseline Climatologies. *Journal of Climate*, 29\(13\), 4817–4842.
 1706 <https://doi.org/10.1175/JCLI-D-15-0801.1>](#)
- 1707 [Brown, J., Ferrians Jr., O. J., Heginbottom, J. A., & Melnikov, E. S. \(1997\). Circum-Arctic map
 1708 of permafrost and ground-ice conditions. In *Circum-Pacific Map*.
 1709 <https://doi.org/10.3133/cp45>](#)
- 1710 [Carr, J. R., Stokes, C. R., & Vieli, A. \(2017\). Threefold increase in marine-terminating outlet
 1711 glacier retreat rates across the Atlantic Arctic: 1992–2010. *Annals of Glaciology*, 58\(74\),
 1712 72–91. <https://doi.org/DOI: 10.1017/aog.2017.3>](#)
- 1713 [Cheng, L., Abraham, J., Goni, G., Boyer, T., Wijffels, S., Cowley, R., Gouretski, V., Reseghetti,
 1714 F., Kizu, S., Dong, S., Bringas, F., Goes, M., Houpert, L., Sprintall, J., & Zhu, J. \(2015\).
 1715 XBT Science: Assessment of Instrumental Biases and Errors. *Bulletin of the American
 1716 Meteorological Society*, 97\(6\), 924–933. <https://doi.org/10.1175/BAMS-D-15-00031.1>](#)
- 1717 [Cheng, L., Abraham, J., Hausfather, Z., & Trenberth, K. E. \(2019\). How fast are the oceans
 1718 warming? *Science*, 363\(6423\), 128. <https://doi.org/10.1126/science.aav7619>](#)
- 1719 [Cheng, L., Foster, G., Hausfather, Z., Trenberth, K. E., & Abraham, J. \(2022\). Improved
 1720 Quantification of the Rate of Ocean Warming. *Journal of Climate*, 35\(14\), 4827–4840.](#)

- 1721 <https://doi.org/10.1175/JCLI-D-21-0895.1>
- 1722 Cheng, L., Luo, H., Boyer, T., Cowley, R., Abraham, J., Gouretski, V., Reseghetti, F., & Zhu, J.
- 1723 (2018). How Well Can We Correct Systematic Errors in Historical XBT Data? *Journal of*
- 1724 *Atmospheric and Oceanic Technology*, 35(5), 1103–1125. [https://doi.org/10.1175/JTECH-](https://doi.org/10.1175/JTECH-D-17-0122.1)
- 1725 [D-17-0122.1](https://doi.org/10.1175/JTECH-D-17-0122.1)
- 1726 Cheng, L., Schuckmann, K. von, Abraham, J., Trenberth, K., Mann, M., Zanna, L., England, M.
- 1727 H., Zika, J. D., Fasullo, J., Yu, Y., Pan, Y., Zhu, J., Newsom, E., Bronselaer, B., & Lin, X.
- 1728 (2022). Past and future ocean warming. *Nature, under review*.
- 1729 Cheng, L., Trenberth, K. E., Fasullo, J., Boyer, T., Abraham, J., & Zhu, J. (2017). Improved
- 1730 estimates of ocean heat content from 1960 to 2015. *Science Advances*, 3(3), e1601545.
- 1731 <https://doi.org/10.1126/sciadv.1601545>
- 1732 Cheng, L., Trenberth, K., Fasullo, J., Abraham, J., Boyer, T., von Schuckmann, K., & Zhu, J.
- 1733 (2017). Taking the Pulse of the Planet. *Eos*. <https://doi.org/10.1029/2017EO081839>
- 1734 Cheng, L., Zhu, J., Cowley, R., Boyer, T., & Wijffels, S. (2014). Time, Probe Type, and
- 1735 Temperature Variable Bias Corrections to Historical Expendable Bathythermograph
- 1736 Observations. *Journal of Atmospheric and Oceanic Technology*, 31(8), 1793–1825.
- 1737 <https://doi.org/10.1175/JTECH-D-13-00197.1>
- 1738 Chiodo, G., & Haimberger, L. (2010). Interannual changes in mass consistent energy budgets
- 1739 from ERA-Interim and satellite data. *Journal of Geophysical Research: Atmospheres*,
- 1740 115(D2). <https://doi.org/10.1029/2009JD012049>
- 1741 Church, J. A., White, N. J., Konikow, L. F., Domingues, C. M., Cogley, J. G., Rignot, E.,
- 1742 Gregory, J. M., van den Broeke, M. R., Monaghan, A. J., & Velicogna, I. (2011). Revisiting
- 1743 the Earth's sea-level and energy budgets from 1961 to 2008. *Geophysical Research Letters*,
- 1744 38(18). <https://doi.org/10.1029/2011GL048794>
- 1745 Ciais, P., Sabine, C., Bala, G., Bopp, L., Brovkin, V., Canadell, J., Chhabra, A., DeFries, R.,
- 1746 Galloway, J., Heimann, M., Jones, C., Le Quéré, C., Myneni, R. B., Piao, S., & Thornton, P.
- 1747 (2014). *Carbon and Other Biogeochemical Cycles*. In *Climate Change 2013 – The Physical*
- 1748 *Science Basis: Working Group I Contribution to the Fifth Assessment Report of the*
- 1749 *Intergovernmental Panel on Climate Change*. Cambridge University Press.
- 1750 <https://doi.org/https://doi.org/DOI:10.1017/CBO9781107415324.015>
- 1751 Cleveland, W. S. (1979). Robust Locally Weighted Regression and Smoothing Scatterplots. *J.*
- 1752 *Am.Stat.Assoc.*, 74, 829–836.
- 1753 Clough, W. J., & Hansen, L. B. (1979). The Ross Ice Shelf Project. *Science*, 203(4379), 433–
- 1754 434. <https://doi.org/10.1126/science.203.4379.433>
- 1755 CMEMS. (2022). *Copernicus Marine Ocean Monitoring Indicator: Global ocean heat content*.
- 1756 [https://marine.copernicus.eu/access-data/ocean-monitoring-indicators/global-ocean-heat-](https://marine.copernicus.eu/access-data/ocean-monitoring-indicators/global-ocean-heat-content-0-2000m-time-series-and-trend)
- 1757 [content-0-2000m-time-series-and-trend](https://marine.copernicus.eu/access-data/ocean-monitoring-indicators/global-ocean-heat-content-0-2000m-time-series-and-trend)
- 1758 Cohen, J., Zhang, X., Francis, J., Jung, T., Kwok, R., Overland, J., Ballinger, T., Bhatt, U. S.,
- 1759 Chen, H. W., Coumou, D., Feldstein, S., Handorf, D., Henderson, G., Ionita, M.,
- 1760 Kretschmer, M., Laliberte, F., Lee, S., Linderholm, H. W., Maslowski, W., ... Yoon, J.
- 1761 (2020). Divergent consensus on Arctic amplification influence on midlatitude severe
- 1762 winter weather. *Nature Climate Change*, 10, 20–29. [https://doi.org/10.1038/s41558-019-](https://doi.org/10.1038/s41558-019-0662-y)
- 1763 [0662-y](https://doi.org/10.1038/s41558-019-0662-y)
- 1764 Cook, A. J., & Vaughan, D. G. (2010). Overview of areal changes of the ice shelves on the
- 1765 Antarctic Peninsula over the past 50 years. *The Cryosphere*, 4(1), 77–98.
- 1766 <https://doi.org/10.5194/tc-4-77-2010>

- 1767 [Crisp, D., Dolman, H., Tanhua, T., McKinley, G. A., Hauck, J., Bastos, A., Sitch, S., Eggleston,](#)
1768 [S., & Aich, V. \(2022\). How Well Do We Understand the Land-Ocean-Atmosphere Carbon](#)
1769 [Cycle? *Reviews of Geophysics*, 60\(2\), e2021RG000736.](#)
1770 <https://doi.org/https://doi.org/10.1029/2021RG000736>
- 1771 [Cuesta-Valero, F. J., Beltrami, H., Gruber, S., García-García, A., & González-Rouco, J. F.](#)
1772 [\(2022b\). A new bootstrap technique to quantify uncertainty in estimates of ground surface](#)
1773 [temperature and ground heat flux histories from geothermal data. Submitted. *Geoscientific*](#)
1774 [Model Development](#), 15, 7913–7932. [https://doi.org/https://doi.org/10.5194/gmd-15-7913-](https://doi.org/https://doi.org/10.5194/gmd-15-7913-2022)
1775 [2022](#)
- 1776 [Cuesta-Valero, F. J., García-García, A., Beltrami, H., & Finnis, J. \(2021\). First assessment of the](#)
1777 [earth heat inventory within CMIP5 historical simulations. *Earth Syst. Dynam.*, 12\(2\), 581–](#)
1778 [600. <https://doi.org/10.5194/esd-12-581-2021>](#)
- 1779 [Cuesta-Valero, F. J., García-García, A., Beltrami, H., González-Rouco, J. F., & García-](#)
1780 [Bustamante, E. \(2021\). Long-Term Global Ground Heat Flux and Continental Heat Storage](#)
1781 [from Geothermal Data. *Climate of the Past*, 17\(1\), 451–468. \[https://doi.org/10.5194/cp-17-\]\(https://doi.org/10.5194/cp-17-451-2021\)](#)
1782 [451-2021](#)
- 1783 [Cuesta-Valero, F. J., García-García, A., Beltrami, H., Zorita, E., & Jaume-Santero, F. \(2019\).](#)
1784 [Long-term Surface Temperature \(LoST\) database as a complement for GCM preindustrial](#)
1785 [simulations. *Clim. Past*, 15\(3\), 1099–1111. <https://doi.org/10.5194/cp-15-1099-2019>](#)
- 1786 [Cuesta-Valero, Francisco José, Beltrami, H., García-García, A., Krinner, G., Langer, M.,](#)
1787 [MacDougall, A., Nitzbon, J., Peng, J., von Schuckmann, K., Seneviratne, S. I., Thiery, W.,](#)
1788 [Vanderkelen, I., & Wu, T. \(2023\). *GCOS EHI 1960-2020 Continental Heat Content*](#)
1789 [\(Version 2\). World Data Center for Climate \(WDCC\) at DKRZ.](#)
1790 https://doi.org/https://doi.org/10.26050/WDCC/GCOS_EHI_1960-2020_CoHC_v2
- 1791 [Cuesta-Valero, Francisco José, Beltrami, H., Burke, E., García-García, A., MacDougall, A.,](#)
1792 [Peng, J., Schuckmann, K. von, Seneviratne, S. I., Smith, N., Thiery, W., Vanderkelen, I., &](#)
1793 [Wu, T. \(2022a\). Continental Heat Storage: Contributions from the Ground, Inland Waters,](#)
1794 [and Permafrost Thawing. *Earth System Dynamics Discussions*, 1–33.](#)
1795 <https://doi.org/https://doi.org/10.5194/esd-2022-32>
- 1796 [Cuesta-Valero, Francisco José, García-García, A., Beltrami, H., & Smerdon, J. E. \(2016\). First](#)
1797 [assessment of continental energy storage in CMIP5 simulations. *Geophysical Research*](#)
1798 [Letters](#), 43(10), 5326–5335. <https://doi.org/10.1002/2016GL068496>
- 1799 [de Vrese, P., Stacke, T., Caves Rugenstein, J., Goodman, J., & Brovkin, V. \(2021\). Snowfall-](#)
1800 [albedo feedbacks could have led to deglaciation of snowball Earth starting from mid-](#)
1801 [latitudes. *Communications Earth & Environment*, 2\(1\), 91. \[https://doi.org/10.1038/s43247-\]\(https://doi.org/10.1038/s43247-021-00160-4\)](#)
1802 [021-00160-4](#)
- 1803 [Demezhko, D. Y., & Gornostaeva, A. A. \(2015\). Late Pleistocene–Holocene ground surface heat](#)
1804 [flux changes reconstructed from borehole temperature data. *Climate of the Past*, 11\(4\), 647–](#)
1805 [652. <https://doi.org/10.5194/cp-11-647-2015>](#)
- 1806 [Denning, A. S. \(2022\). Where Has All the Carbon Gone? *Annual Review of Earth and Planetary*](#)
1807 [Sciences](#), 50(1), 55–78. <https://doi.org/10.1146/annurev-earth-032320-092010>
- 1808 [Desbruyères, D. G., Purkey, S. G., McDonagh, E. L., Johnson, G. C., & King, B. A. \(2016\).](#)
1809 [Deep and abyssal ocean warming from 35 years of repeat hydrography. *Geophysical*](#)
1810 [Research Letters](#), 43(19), 10, 310–356, 365. <https://doi.org/10.1002/2016GL070413>
- 1811 [Desbruyères, D., McDonagh, E. L., King, B. A., & Thierry, V. \(2017\). Global and Full-Depth](#)
1812 [Ocean Temperature Trends during the Early Twenty-First Century from Argo and Repeat](#)

- 1813 [Hydrography. *Journal of Climate*, 30\(6\), 1985–1997. https://doi.org/10.1175/JCLI-D-16-](https://doi.org/10.1175/JCLI-D-16-0396.1)
 1814 [0396.1](https://doi.org/10.1175/JCLI-D-16-0396.1)
- 1815 [Dieng, H. B., Cazenave, A., Meyssignac, B., & Ablain, M. \(2017\). New estimate of the current](https://doi.org/10.1002/2017GL073308)
 1816 [rate of sea level rise from a sea level budget approach. *Geophysical Research Letters*, 44\(8\),](https://doi.org/10.1002/2017GL073308)
 1817 [3744–3751. https://doi.org/10.1002/2017GL073308](https://doi.org/10.1002/2017GL073308)
- 1818 [Domingues, C. M., Church, J. A., White, N. J., Gleckler, P. J., Wijffels, S. E., Barker, P. M., &](https://doi.org/10.1038/nature07080)
 1819 [Dunn, J. R. \(2008\). Improved estimates of upper-ocean warming and multi-decadal sea-](https://doi.org/10.1038/nature07080)
 1820 [level rise. *Nature*, 453\(7198\), 1090–1093. https://doi.org/10.1038/nature07080](https://doi.org/10.1038/nature07080)
- 1821 [Dorigo, W., Dietrich, S., Aires, F., Brocca, L., Carter, S., Cretaux, J.-F., Dunkerley, D.,](https://doi.org/10.1175/BAMS-D-19-0316.1)
 1822 [Enomoto, H., Forsberg, R., Güntner, A., Hegglin, M. I., Hollmann, R., Hurst, D. F.,](https://doi.org/10.1175/BAMS-D-19-0316.1)
 1823 [Johannessen, J. A., Kummerow, C., Lee, T., Luoju, K., Looser, U., Miralles, D. G., ...](https://doi.org/10.1175/BAMS-D-19-0316.1)
 1824 [Aich, V. \(2021\). Closing the Water Cycle from Observations across Scales: Where Do We](https://doi.org/10.1175/BAMS-D-19-0316.1)
 1825 [Stand? *Bulletin of the American Meteorological Society*, 102\(10\), E1897–E1935.](https://doi.org/10.1175/BAMS-D-19-0316.1)
 1826 <https://doi.org/10.1175/BAMS-D-19-0316.1>
- 1827 [ECMWF-IFS. \(2015\). *ECMWF-IFS: Part IV: Physical processes. IFS documentation–Cy41r1.*](https://www.ecmwf.int/en/elibrary/9211-partiv-physical-processes)
 1828 <https://www.ecmwf.int/en/elibrary/9211-partiv-physical-processes>
- 1829 [Eicken, H., Fischer, H., & Lemke, P. \(1995\). Effects of the snow cover on Antarctic sea ice and](https://doi.org/10.3189/S0260305500016086)
 1830 [potential modulation of its response to climate change. *Annals of Glaciology*, 21, 369–376.](https://doi.org/10.3189/S0260305500016086)
 1831 [https://doi.org/DOI: 10.3189/S0260305500016086](https://doi.org/10.3189/S0260305500016086)
- 1832 [Farinotti, D., Huss, M., Fürst, J. J., Landmann, J., Machguth, H., Maussion, F., & Pandit, A.](https://doi.org/10.1038/s41561-019-0300-3)
 1833 [\(2019\). A consensus estimate for the ice thickness distribution of all glaciers on Earth.](https://doi.org/10.1038/s41561-019-0300-3)
 1834 [*Nature Geoscience*, 12, 168–173. https://doi.org/10.1038/s41561-019-0300-3](https://doi.org/10.1038/s41561-019-0300-3)
- 1835 [Faroux, S., Kaptué Tchuenté, A. T., Roujean, J.-L., Masson, V., Martin, E., & Le Moigne, P.](https://doi.org/10.5194/gmd-6-563-2013)
 1836 [\(2013\). ECOCLIMAP-II/Europe: a twofold database of ecosystems and surface parameters](https://doi.org/10.5194/gmd-6-563-2013)
 1837 [at 1 km resolution based on satellite information for use in land surface, meteorological and](https://doi.org/10.5194/gmd-6-563-2013)
 1838 [climate models. *Geosci. Model Dev.*, 6\(2\), 563–582. https://doi.org/10.5194/gmd-6-563-](https://doi.org/10.5194/gmd-6-563-2013)
 1839 [2013](https://doi.org/10.5194/gmd-6-563-2013)
- 1840 [Fischer, E. M., Sippel, S., & Knutti, R. \(2021\). Increasing probability of record-shattering](https://doi.org/10.1038/s41558-021-01092-9)
 1841 [climate extremes. *Nature Climate Change*, 11\(8\), 689–695. https://doi.org/10.1038/s41558-](https://doi.org/10.1038/s41558-021-01092-9)
 1842 [021-01092-9](https://doi.org/10.1038/s41558-021-01092-9)
- 1843 [Forster, P., Storelvmo, T., Armour, K., Collins, W., Dufresne, J.-L., Frame, D., Lunt, D. J.,](https://doi.org/10.1017/9781009157896.009)
 1844 [Mauritsen, T., Palmer, M. D., Watanabe, M., Wild, M., & Zhang, H. \(2022\). *The Earth's*](https://doi.org/10.1017/9781009157896.009)
 1845 [*Energy Budget, Climate Feedbacks, and Climate Sensitivity. In Climate Change 2021: The*](https://doi.org/10.1017/9781009157896.009)
 1846 [*Physical Science Basis. Contribution of Working Group I to the Sixth Assessment Report of*](https://doi.org/10.1017/9781009157896.009)
 1847 [*the Intergovernmental Panel on Climate Change \(V. Masson-Delmotte, P. Zhai, A. Pirani,*](https://doi.org/10.1017/9781009157896.009)
 1848 [*S. L. Connors, C. Péan, S. Berger, N. Caud, Y. Chen, L. Goldfarb, M. I. Gomis, M. Huang,*](https://doi.org/10.1017/9781009157896.009)
 1849 [*K. Leitzell, E. Lonnoy, J. B. R. Matthews, T. K. Maycock, T. Waterfield, O. Yelekçi, R.*](https://doi.org/10.1017/9781009157896.009)
 1850 [*Yu, & B. Zhou \(eds.\)\). Cambridge University Press, Cambridge, United Kingdom and New*](https://doi.org/10.1017/9781009157896.009)
 1851 [*York, NY, USA. https://doi.org/10.1017/9781009157896.009*](https://doi.org/10.1017/9781009157896.009)
- 1852 [Friedlingstein, P., Jones, M. W., O'Sullivan, M., Andrew, R. M., Bakker, D. C. E., Hauck, J., Le](https://doi.org/10.5194/essd-14-1917-2022)
 1853 [Quéré, C., Peters, G. P., Peters, W., Pongratz, J., Sitch, S., Canadell, J. G., Ciais, P.,](https://doi.org/10.5194/essd-14-1917-2022)
 1854 [Jackson, R. B., Alin, S. R., Anthoni, P., Bates, N. R., Becker, M., Bellouin, N., ... Zeng, J.](https://doi.org/10.5194/essd-14-1917-2022)
 1855 [\(2022\). Global Carbon Budget 2021. *Earth Syst. Sci. Data*, 14\(4\), 1917–2005.](https://doi.org/10.5194/essd-14-1917-2022)
 1856 <https://doi.org/10.5194/essd-14-1917-2022>
- 1857 [Frieler, K., Lange, S., Piontek, F., Reyer, C., Schewe, J., Warszawski, L., Zhao, F., Chini, L.,](https://doi.org/10.1002/2017GL073308)
 1858 [Denvil, S., Emanuel, K., Geiger, T., Halladay, K., Hurtt, G., Mengel, M., Murakami, D.,](https://doi.org/10.1002/2017GL073308)

- 1859 [Ostberg, S., Popp, A., Riva, R., Stevanovic, M., & Yamagata, Y. \(2017\). Assessing the](#)
 1860 [impacts of 1.5°C global warming - Simulation protocol of the Inter-Sectoral Impact Model](#)
 1861 [Intercomparison Project \(ISIMIP2b\). *Geoscientific Model Development*, 10, 4321–4345.](#)
 1862 <https://doi.org/10.5194/gmd-10-4321-2017>
- 1863 [Fu, Q., Solomon, S., Pahlavan, H. A., & Lin, P. \(2019\). Observed changes in Brewer–Dobson](#)
 1864 [circulation for 1980–2018. *Environmental Research Letters*, 14\(11\), 114026.](#)
 1865 <https://doi.org/10.1088/1748-9326/ab4de7>
- 1866 [Gädeke, A., Langer, M., Boike, J., Burke, E. J., Chang, J., Head, M., Reyer, C. P. O., Schaphoff,](#)
 1867 [S., Thiery, W., & Thonicke, K. \(2021\). Climate change reduces winter overland travel](#)
 1868 [across the Pan-Arctic even under low-end global warming scenarios. *Environmental*](#)
 1869 [Research Letters](#), 16(2), 24049. <https://doi.org/10.1088/1748-9326/abdcd2>
- 1870 [Gaillard, F., Reynaud, T., Thierry, V., Kolodziejczyk, N., & von Schuckmann, K. \(2016\). In](#)
 1871 [Situ–Based Reanalysis of the Global Ocean Temperature and Salinity with ISAS:](#)
 1872 [Variability of the Heat Content and Steric Height. *Journal of Climate*, 29\(4\), 1305–1323.](#)
 1873 <https://doi.org/10.1175/JCLI-D-15-0028.1>
- 1874 [GCOS. \(2021\). *The Status of the Global Climate Observing System 2021: Executive Summary.*](#)
 1875 [\(GCOS-239\).](#)
- 1876 [Gelaro, R., McCarty, W., Suárez, M. J., Todling, R., Molod, A., Takacs, L., Randles, C. A.,](#)
 1877 [Darmenov, A., Bosilovich, M. G., Reichle, R., Wargan, K., Coy, L., Cullather, R., Draper,](#)
 1878 [C., Akella, S., Buchard, V., Conaty, A., da Silva, A. M., Gu, W., ... Zhao, B. \(2017\). The](#)
 1879 [Modern-Era Retrospective Analysis for Research and Applications, Version 2 \(MERRA-2\)](#)
 1880 [\(I200, Trans.\). *Journal of Climate*, 30\(14\), 5419–5454. https://doi.org/10.1175/JCLI-D-16-](#)
 1881 [0758.1](#)
- 1882 [Golub, M., Thiery, W., Marcé, R., Pierson, D., Vanderkelen, I., Mercado-Bettín, D., Woolway,](#)
 1883 [R., Grant, L., Jennings, E., Kraemer, B., Schewe, J., Zhao, F., Frieler, K., Mengel, M.,](#)
 1884 [Bogomolov, V., Bouffard, D., Côté, M., Couture, R.-M., Debolskiy, A., & Zdorovenova,](#)
 1885 [G. \(2022\). A framework for ensemble modelling of climate change impacts on lakes](#)
 1886 [worldwide: the ISIMIP Lake Sector. *Geoscientific Model Development*, 15, 4597–4623.](#)
 1887 <https://doi.org/10.5194/gmd-15-4597-2022>
- 1888 [Good, S. A. \(2017\). The impact of observational sampling on time series of global 0–700 m](#)
 1889 [ocean average temperature: a case study. *International Journal of Climatology*, 37\(5\),](#)
 1890 [2260–2268. https://doi.org/10.1002/joc.4654](#)
- 1891 [Good, S. A., Martin, M. J., & Rayner, N. A. \(2013a\). EN4: Quality controlled ocean temperature](#)
 1892 [and salinity profiles and monthly objective analyses with uncertainty estimates \(I5197,](#)
 1893 [Trans.\). *Journal of Geophysical Research: Oceans*, 118\(12\), 6704–6716.](#)
 1894 <https://doi.org/10.1002/2013JC009067>
- 1895 [Good, S. A., Martin, M. J., & Rayner, N. A. \(2013b\). EN4: Quality controlled ocean temperature](#)
 1896 [and salinity profiles and monthly objective analyses with uncertainty estimates. *Journal of*](#)
 1897 [Geophysical Research: Oceans](#), 118(12), 6704–6716.
 1898 <https://doi.org/10.1002/2013JC009067>
- 1899 [Gorfer, M. \(2022\). *Monitoring of climate change and variability in atmospheric heat content*](#)
 1900 [based on climate records and reanalyses. *Sci. Rep. 94-2022*. Wegener Center Verlag.](#)
 1901 <https://wegcenter.uni-graz.at/wegener-center-verlag/2022>
- 1902 [Gould, J., Sloyan, B., & Visbeck, M. \(2013\). Chapter 3 - In Situ Ocean Observations: A Brief](#)
 1903 [History, Present Status, and Future Directions. In G. Siedler, S. M. Griffies, J. Gould, & J.](#)
 1904 [A. Church \(Eds.\), *Ocean Circulation and Climate* \(Vol. 103, pp. 59–81\). Academic Press.](#)

- 1905 <https://doi.org/https://doi.org/10.1016/B978-0-12-391851-2.00003-9>
- 1906 [Gouretski, V., & Cheng, L. \(2020\). Correction for Systematic Errors in the Global Dataset of](#)
- 1907 [Temperature Profiles from Mechanical Bathythermographs. *Journal of Atmospheric and*](#)
- 1908 [Oceanic Technology, 37\(5\), 841–855. <https://doi.org/10.1175/JTECH-D-19-0205.1>](#)
- 1909 [Grant, L., Vanderkelen, I., Gudmundsson, L., Tan, Z., Perroud, M., Stepanenko, V. M.,](#)
- 1910 [Debolskiy, A. V., Droppers, B., Janssen, A. B. G., Woolway, R. I., Choulga, M., Balsamo,](#)
- 1911 [G., Kirillin, G., Schewe, J., Zhao, F., del Valle, I. V., Golub, M., Pierson, D., Marcé, R., ...](#)
- 1912 [Thiery, W. \(2021\). Attribution of global lake systems change to anthropogenic forcing.](#)
- 1913 [Nature Geoscience, 14\(11\), 849–854. <https://doi.org/10.1038/s41561-021-00833-x>](#)
- 1914 [Gregory, J. M., & Andrews, T. \(2016\). Variation in climate sensitivity and feedback parameters](#)
- 1915 [during the historical period. *Geophysical Research Letters, 43\(8\), 3911–3920.*](#)
- 1916 [https://doi.org/10.1002/2016GL068406](#)
- 1917 [Grise, K. M., Davis, S. M., Simpson, I. R., Waugh, D. W., Fu, Q., Allen, R. J., Rosenlof, K. H.,](#)
- 1918 [Ummenhofer, C. C., Karnauskas, K. B., Maycock, A. C., Quan, X. W., Birner, T., & Staten,](#)
- 1919 [P. W. \(2019\). Recent tropical expansion: Natural variability or forced response? *Journal of*](#)
- 1920 [Climate, 32\(5\), 1551–1571. <https://doi.org/10.1175/JCLI-D-18-0444.1>](#)
- 1921 [Gulev, S. K., Thorne, P. W., Ahn, J., Dentener, F. J., Domingues, C. M., Gerland, S., Gong, D.,](#)
- 1922 [Kaufman, D. S., Nnamchi, H. C., Quaas, J., Rivera, J. A., Sathyendranath, S., Smith, S. L.,](#)
- 1923 [Trewin, B., Schuckmann, K. von, & Vose, R. S. \(2021\). *Changing State of the Climate*](#)
- 1924 [System Supplementary Material. In *Climate Change 2021: The Physical Science Basis.*](#)
- 1925 [Contribution of Working Group I to the Sixth Assessment Report of the Intergovernmental](#)
- 1926 [Panel on Climate Change \(V. Masson-Delmotte, P. Zhai, A. Pirani, S. L. Connors, C. Péan,](#)
- 1927 [S. Berger, N. Caud, Y. Chen, L. Goldfarb, M. I. Gomis, M. Huang, K. Leitzell, E. Lonnoy,](#)
- 1928 [J. B. R. Matthews, T. K. Maycock, T. Waterfield, O. Yelekçi, R. Yu, & B. Zhou \(eds.\)\).](#)
- 1929 [Cambridge University Press., <https://doi.org/10.1017/9781009157896.004>](#)
- 1930 [Hakuba, M. Z., Frederikse, T., & Landerer, F. W. \(2021\). Earth’s Energy Imbalance From the](#)
- 1931 [Ocean Perspective \(2005–2019\). *Geophysical Research Letters, 48\(16\), e2021GL093624.*](#)
- 1932 [https://doi.org/https://doi.org/10.1029/2021GL093624](#)
- 1933 [Hansen, J., Sato, M., Kharecha, P., & von Schuckmann, K. \(2011\). Earth’s energy imbalance and](#)
- 1934 [implications. *Atmos. Chem. Phys., 11\(24\), 13421–13449. \[https://doi.org/10.5194/acp-11-\]\(https://doi.org/10.5194/acp-11-13421-2011\)*](#)
- 1935 [13421-2011](#)
- 1936 [Hansen, J., Sato, M., Kharecha, P., von Schuckmann, K., Beerling, D. J., Cao, J., Marcott, S.,](#)
- 1937 [Masson-Delmotte, V., Prather, M. J., Rohling, E. J., Shakun, J., Smith, P., Lacic, A.,](#)
- 1938 [Russell, G., & Ruedy, R. \(2017\). Young people’s burden: requirement of negative CO₂](#)
- 1939 [emissions. *Earth Syst. Dynam., 8\(3\), 577–616. <https://doi.org/10.5194/esd-8-577-2017>*](#)
- 1940 [Hansen, James, Nazarenko, L., Ruedy, R., Sato, M., Willis, J., Del Genio, A., Koch, D., Lacic,](#)
- 1941 [A., Lo, K., Menon, S., Novakov, T., Perlwitz, J., Russell, G., Gavin A., S., & Tausnev, N.](#)
- 1942 [\(2005\). Earth’s Energy Imbalance: Confirmation and Implications. *Science, 308\(5727\),*](#)
- 1943 [1431–1435. <https://doi.org/10.1126/science.1110252>](#)
- 1944 [Hartmann, A., & Rath, V. \(2005\). Uncertainties and shortcomings of ground surface temperature](#)
- 1945 [histories derived from inversion of temperature logs. *Journal of Geophysics and*](#)
- 1946 [Engineering, 2\(4\), 299–311. <https://doi.org/10.1088/1742-2132/2/4/S02>](#)
- 1947 [Hersbach, H., de Rosnay, P., Bell, B., Schepers, D., Simmons, A., Soci, C., Abdalla, S., Alonso-](#)
- 1948 [Balmaseda, M., Balsamo, G., Bechtold, P., Berrisford, P., Bidlot, J.-R., de Boissésou, E.,](#)
- 1949 [Bonavita, M., Browne, P., Buizza, R., Dahlgren, P., Dee, D., Dragani, R., ... Zuo, H.](#)
- 1950 [\(2018\). *Operational global reanalysis: progress, future directions and synergies with NWP.*](#)

- 1951 <https://www.ecmwf.int/node/18765>
- 1952 [Hersbach, Hans, Bell, B., Berrisford, P., Hirahara, S., Horányi, A., Muñoz-Sabater, J., Nicolas,](#)
- 1953 [J., Peubey, C., Radu, R., Schepers, D., Simmons, A., Soci, C., Abdalla, S., Abellan, X.,](#)
- 1954 [Balsamo, G., Bechtold, P., Biavati, G., Bidlot, J., Bonavita, M., ... Thépaut, J. N. \(2020\).](#)
- 1955 [The ERA5 global reanalysis. *Quarterly Journal of the Royal Meteorological Society*, 146,](#)
- 1956 [1999–2049. <https://doi.org/10.1002/qj.3803>](#)
- 1957 [Hopcroft, P. O., Gallagher, K., & Pain, C. C. \(2007\). Inference of past climate from borehole](#)
- 1958 [temperature data using Bayesian Reversible Jump Markov chain Monte Carlo. *Geophysical*](#)
- 1959 [Journal International](#), 171(3), 1430–1439. <https://doi.org/10.1111/j.1365->
- 1960 [246X.2007.03596.x](#)
- 1961 [Hosoda, S., Ohira, T., & Nakamura, T. \(2008\). *A monthly mean dataset of global oceanic*](#)
- 1962 [temperature and salinity derived from Argo float observations.](#)
- 1963 [http://www.jamstec.go.jp/ARGO/argo_web/ancient/MapQ/Hosoda_et al_MOAA_GPV.pdf](#)
- 1964 [Hugelius, G., Bockheim, J. G., Camill, P., Elberling, B., Grosse, G., Harden, J. W., Johnson, K.,](#)
- 1965 [Jorgenson, T., Koven, C. D., Kuhry, P., Michaelson, G., Mishra, U., Palmtag, J., Ping, C.-](#)
- 1966 [L., O'Donnell, J., Schirrmeister, L., Schuur, E. A. G., Sheng, Y., Smith, L. C., ... Yu, Z.](#)
- 1967 [\(2013\). A new data set for estimating organic carbon storage to 3 m depth in soils of the](#)
- 1968 [northern circumpolar permafrost region. *Earth Syst. Sci. Data*, 5\(2\), 393–402.](#)
- 1969 [https://doi.org/10.5194/essd-5-393-2013](#)
- 1970 [IPCC. \(2019\). *IPCC Special Report on the Ocean and Cryosphere in a Changing Climate* \(H.-O.](#)
- 1971 [Pörtner, D. C. Roberts, V. Masson-Delmotte, P. Zhai, M. Tignor, E. Poloczanska, K.](#)
- 1972 [Mintenbeck, A. Alegría, M. Nicolai, A. Okem, J. Petzold, B. Rama, & N. M. Weyer \(eds.\)\).](#)
- 1973 [Cambridge University Press. <https://doi.org/https://doi.org/10.1017/9781009157964>](#)
- 1974 [IPCC. \(2021a\). *Climate Change 2021: The Physical Science Basis. Contribution of Working*](#)
- 1975 [Group I to the Sixth Assessment Report of the Intergovernmental Panel on Climate Change](#)
- 1976 [\(V. Masson-Delmotte, P. Zhai, A. Pirani, S. L. Connors, C. Péan, S. Berger, N. Caud, Y.](#)
- 1977 [Chen, L. Goldfarb, M. I. Gomis, M. Huang, K. Leitzell, E. Lonnoy, J. B. R. Matthews, T.](#)
- 1978 [K. Maycock, T. Waterfield, O. Yelekçi, R. Yu, & B. Zhou \(eds.\)\). Cambridge University](#)
- 1979 [Press, Cambridge, United Kingdom and New York, NY, USA.](#)
- 1980 [https://doi.org/10.1017/9781009157896](#)
- 1981 [IPCC. \(2021b\). *Summary for Policymakers. In: Climate Change 2021: The Physical Science*](#)
- 1982 [Basis. Contribution of Working Group I to the Sixth Assessment Report of the](#)
- 1983 [Intergovernmental Panel on Climate Change \(V. Masson-Delmotte, P. Zhai, A. Pirani, S. L.](#)
- 1984 [Connors, C. Péan, S. Berger, N. Caud, Y. Chen, L. Goldfarb, M. I. Gomis, M. Huang, K.](#)
- 1985 [Leitzell, E. Lonnoy, J. B. R. Matthews, T. K. Maycock, T. Waterfield, O. Yelekçi, R. Yu, &](#)
- 1986 [B. Zhou \(eds.\)\). Cambridge University Press. <https://doi.org/10.1017/9781009157896.001>](#)
- 1987 [IPCC. \(2022a\). *Climate Change 2022: Mitigation of Climate Change. Contribution of Working*](#)
- 1988 [Group III to the Sixth Assessment Report of the Intergovernmental Panel on Climate](#)
- 1989 [Change \(P. R. Shukla, J. Skea, R. Slade, A. Al Khourdajie, R. van Diemen, D. McCollum,](#)
- 1990 [M. Pathak, S. Some, P. Vyas, R. Fradera, M. Belkacemi, A. Hasija, G. Lisboa, S. Luz, & J.](#)
- 1991 [Malley \(eds.\)\). Cambridge University Press, Cambridge, UK and New York, NY, USA.](#)
- 1992 [https://doi.org/10.1017/9781009157926](#)
- 1993 [IPCC. \(2022b\). *Summary for Policymakers, In: Climate Change 2022: Impacts, Adaptation, and*](#)
- 1994 [Vulnerability. Contribution of Working Group II to the Sixth Assessment Report of the](#)
- 1995 [Intergovernmental Panel on Climate Change \(H.-O. Pörtner, D. C. Roberts, M. Tignor, E.](#)
- 1996 [S. Poloczanska, K. Mintenbeck, A. Alegría, M. Craig, S. Langsdorf, S. Lösschke, V. Möller,](#)

- 1997 [A. Okem, & B. Rama \(eds.\)\). Cambridge University Press. https://doi.org/in_press](https://doi.org/in_press)
- 1998 [IROWG. \(2021\). Report of IROWG activities: Outcome and recommendations from the IROWG-](https://doi.org/10.1029/2020GL091585)
- 1999 [8 Workshop, CGMS-49 IROWG-WP-01 V3, 28 April 2021, International Radio Occultation](https://doi.org/10.1029/2020GL091585)
- 2000 [Working Group. https://irowg.org/wpcms/wp-content/uploads/2021/07/CGMS-49-IROWG-](https://doi.org/10.1029/2020GL091585)
- 2001 [WP-01.pdf](https://doi.org/10.1029/2020GL091585)
- 2002 [Ishii, M., Fukuda, Y., Hirahara, S., Yasui, S., Suzuki, T., & Sato, K. \(2017\). Accuracy of Global](https://doi.org/10.1029/2017-030)
- 2003 [Upper Ocean Heat Content Estimation Expected from Present Observational Data Sets.](https://doi.org/10.1029/2017-030)
- 2004 [SOLA, 13, 163–167. https://doi.org/10.2151/sola.2017-030](https://doi.org/10.1029/2017-030)
- 2005 [Jan, A., & Painter, S. L. \(2020\). Permafrost thermal conditions are sensitive to shifts in snow](https://doi.org/10.1088/1748-9326/ab8ec4)
- 2006 [timing. Environmental Research Letters, 15\(8\), 084026. https://doi.org/10.1088/1748-](https://doi.org/10.1088/1748-9326/ab8ec4)
- 2007 [9326/ab8ec4](https://doi.org/10.1088/1748-9326/ab8ec4)
- 2008 [Jaume-Santero, F., Pickler, C., Beltrami, H., & Mareschal, J.-C. \(2016\). North American](https://doi.org/10.5194/cp-12-2181-2016)
- 2009 [regional climate reconstruction from ground surface temperature histories. Clim. Past,](https://doi.org/10.5194/cp-12-2181-2016)
- 2010 [12\(12\), 2181–2194. https://doi.org/10.5194/cp-12-2181-2016](https://doi.org/10.5194/cp-12-2181-2016)
- 2011 [Johnson, G. C., Lumpkin, R., Boyer, T., Bringas, F., Cetinić, I., Chambers, D. P., Cheng, L.,](https://doi.org/10.1175/BAMS-D-22-0072.1)
- 2012 [Dong, S., Feely, R. A., Fox-Kemper, B., Frajka-Williams, E., Franz, B. A., Fu, Y., Gao, M.,](https://doi.org/10.1175/BAMS-D-22-0072.1)
- 2013 [Garg, J., Gilson, J., Goni, G., Hamlington, B. D., Hewitt, H. T., ... Zhang, H.-M. \(2022\).](https://doi.org/10.1175/BAMS-D-22-0072.1)
- 2014 [Global Oceans. Bulletin of the American Meteorological Society, 103\(8\), S143–S192.](https://doi.org/10.1175/BAMS-D-22-0072.1)
- 2015 <https://doi.org/10.1175/BAMS-D-22-0072.1>
- 2016 [Johnson, G. C., Purkey, S. G., Zilberman, N. V., & Roemmich, D. \(2019\). Deep Argo Quantifies](https://doi.org/10.1029/2018GL081685)
- 2017 [Bottom Water Warming Rates in the Southwest Pacific Basin. Geophysical Research](https://doi.org/10.1029/2018GL081685)
- 2018 [Letters, 46\(5\), 2662–2669. https://doi.org/10.1029/2018GL081685](https://doi.org/10.1029/2018GL081685)
- 2019 [Kashiwase, H., Ohshima, K. I., Nihashi, S., & Eicken, H. \(2017\). Evidence for ice-ocean albedo](https://doi.org/10.1038/s41598-017-08467-z)
- 2020 [feedback in the Arctic Ocean shifting to a seasonal ice zone. Scientific Reports, 7\(1\), 8170.](https://doi.org/10.1038/s41598-017-08467-z)
- 2021 <https://doi.org/10.1038/s41598-017-08467-z>
- 2022 [Kern, S., Lavergne, T., Notz, D., Pedersen, L. T., Tonboe, R. T., Saldo, R., & Sørensen, A. M.](https://doi.org/10.5194/tc-13-3261-2019)
- 2023 [\(2019\). Satellite passive microwave sea-ice concentration data set intercomparison: closed](https://doi.org/10.5194/tc-13-3261-2019)
- 2024 [ice and ship-based observations. The Cryosphere, 13\(12\), 3261–3307.](https://doi.org/10.5194/tc-13-3261-2019)
- 2025 <https://doi.org/10.5194/tc-13-3261-2019>
- 2026 [Khazaei, B., Read, L. K., Casali, M., Sampson, K. M., & Yates, D. N. \(2022\). GLOBathy, the](https://doi.org/10.1038/s41597-022-01132-9)
- 2027 [global lakes bathymetry dataset. Scientific Data, 9\(1\), 36. https://doi.org/10.1038/s41597-](https://doi.org/10.1038/s41597-022-01132-9)
- 2028 [022-01132-9](https://doi.org/10.1038/s41597-022-01132-9)
- 2029 [Kobayashi, S., Ota, Y., Harada, Y., Ebata, A., Moriya, M., Onoda, H., Onogi, K., Kamahori, H.,](https://doi.org/10.2151/jmsj.2015-001)
- 2030 [Kobayashi, C., Endo, H., Miyaoka, K., & Takahashi, K. \(2015\). The JRA-55 Reanalysis:](https://doi.org/10.2151/jmsj.2015-001)
- 2031 [General Specifications and Basic Characteristics. Journal of the Meteorological Society of](https://doi.org/10.2151/jmsj.2015-001)
- 2032 [Japan. Ser. II, 93\(1\), 5–48. https://doi.org/10.2151/jmsj.2015-001](https://doi.org/10.2151/jmsj.2015-001)
- 2033 [Kramer, R. J., He, H., Soden, B. J., Oreopoulos, L., Myhre, G., Forster, P. M., & Smith, C. J.](https://doi.org/10.1029/2020GL091585)
- 2034 [\(2021\). Observational Evidence of Increasing Global Radiative Forcing. Geophysical](https://doi.org/10.1029/2020GL091585)
- 2035 [Research Letters, 48\(7\), e2020GL091585.](https://doi.org/10.1029/2020GL091585)
- 2036 [https://doi.org/https://doi.org/10.1029/2020GL091585](https://doi.org/10.1029/2020GL091585)
- 2037 [Kuhlbrodt, T., & Gregory, J. M. \(2012\). Ocean heat uptake and its consequences for the](https://doi.org/10.1029/2012GL052952)
- 2038 [magnitude of sea level rise and climate change. Geophysical Research Letters, 39\(18\).](https://doi.org/10.1029/2012GL052952)
- 2039 <https://doi.org/10.1029/2012GL052952>
- 2040 [Kuusela, M., & Giglio, D. \(2022\). Global Ocean Heat Content Anomalies based on Argo data.](https://doi.org/10.5281/ZENODO.6131625)
- 2041 [https://doi.org/https://doi.org/10.5281/ZENODO.6131625](https://doi.org/10.5281/ZENODO.6131625)
- 2042 [Labe, Z., Magnusdottir, G., & Stern, H. \(2018\). Variability of Arctic Sea Ice Thickness Using](https://doi.org/10.5281/ZENODO.6131625)

- 2043 [PIOMAS and the CESM Large Ensemble. *Journal of Climate*, 31\(8\), 3233–3247.](#)
2044 <https://doi.org/10.1175/JCLI-D-17-0436.1>
- 2045 [Ladstädter, F., Steiner, A. K., Schwärz, M., & Kirchengast, G. \(2015\). Climate intercomparison
2046 of GPS radio occultation, RS90/92 radiosondes and GRUAN from 2002 to 2013.
2047 *Atmospheric Measurement Techniques*, 8\(4\), 1819–1834. \[https://doi.org/10.5194/amt-8-
2048 1819-2015\]\(https://doi.org/10.5194/amt-8-1819-2015\)](#)
- 2049 [Ladstädter, Florian, Steiner, A. K., & Gleisner, H. \(2023\). Resolving the 21st century
2050 temperature trends of the upper troposphere–lower stratosphere with satellite observations.
2051 *Scientific Reports*, 13\(1\), 1306. <https://doi.org/10.1038/s41598-023-28222-x>](#)
- 2052 [Lane, A. C. \(1923\). Geotherms of Lake Superior Copper Country. *GSA Bulletin*, 34\(4\), 703–720.
2053 <https://doi.org/10.1130/GSAB-34-703>](#)
- 2054 [Lavergne, T., Macdonald Sørensen, A., Kern, S., Tonboe, R., Notz, D., Aaboe, S., Bell, L.,
2055 Dybkjær, G., Eastwood, S., Gabarro, C., Heygster, G., Anne Killie, M., Brandt Kreiner, M.,
2056 Lavelle, J., Saldo, R., Sandven, S., & Pedersen, L. T. \(2019\). Version 2 of the EUMETSAT
2057 OSI SAF and ESA CCI sea-ice concentration climate data records. *Cryosphere*, 13\(1\), 49–
2058 78. <https://doi.org/10.5194/tc-13-49-2019>](#)
- 2059 [Laxon, S. W., Giles, K. A., Ridout, A. L., Wingham, D. J., Willatt, R., Cullen, R., Kwok, R.,
2060 Schweiger, A., Zhang, J., Haas, C., Hendricks, S., Krishfield, R., Kurtz, N., Farrell, S., &
2061 Davidson, M. \(2013\). CryoSat-2 estimates of Arctic sea ice thickness and volume \(I326,
2062 *Trans.*\) *Geophysical Research Letters*. <https://doi.org/10.1002/grl.50193>](#)
- 2063 [Levitus, S., Antonov, J. I., Boyer, T. P., Baranova, O. K., Garcia, H. E., Locarnini, R. A.,
2064 Mishonov, A. V., Reagan, J. R., Seidov, D., Yarosh, E. S., & Zweng, M. M. \(2012\). World
2065 ocean heat content and thermosteric sea level change \(0–2000 m\), 1955–2010. *Geophysical
2066 Research Letters*, 39\(10\). <https://doi.org/10.1029/2012GL051106>](#)
- 2067 [Li, H., Xu, F., Zhou, W., Wang, D., Wright, J. S., Liu, Z., & Lin, Y. \(2017\). Development of a
2068 global gridded Argo data set with Barnes successive corrections. *Journal of Geophysical
2069 Research: Oceans*, 122\(2\), 866–889. <https://doi.org/https://doi.org/10.1002/2016JC012285>](#)
- 2070 [Li, Y., Church, J. A., McDougall, T. J., & Barker, P. M. \(2022\). Sensitivity of Observationally
2071 Based Estimates of Ocean Heat Content and Thermal Expansion to Vertical Interpolation
2072 Schemes. *Geophysical Research Letters*, 49, e2022G.
2073 <https://doi.org/https://doi.org/10.1029/2022GL101079>](#)
- 2074 [Liao, S., Luo, H., Wang, J., Shi, Q., Zhang, J., & Yang, Q. \(2022\). An evaluation of Antarctic
2075 sea-ice thickness from the Global Ice-Ocean Modeling and Assimilation System based on in
2076 situ and satellite observations. *The Cryosphere*, 16\(5\), 1807–1819.
2077 <https://doi.org/10.5194/tc-16-1807-2022>](#)
- 2078 [Ligtenberg, S. R. M., Kuipers Munneke, P., Noël, B. P. Y., & van den Broeke, M. R. \(2018\).
2079 Brief communication: Improved simulation of the present-day Greenland firn layer \(1960–
2080 2016\). *The Cryosphere*, 12\(5\), 1643–1649. <https://doi.org/10.5194/tc-12-1643-2018>](#)
- 2081 [Liu, C., Allan, R. P., Mayer, M., Hyder, P., Desbruyères, D., Cheng, L., Xu, J., Xu, F., & Zhang,
2082 Y. \(2020\). Variability in the global energy budget and transports 1985–2017. *Climate
2083 Dynamics*, 55\(11\), 3381–3396. <https://doi.org/10.1007/s00382-020-05451-8>](#)
- 2084 [Llovel, W., Willis, J. K., Landerer, F. W., & Fukumori, I. \(2014\). Deep-ocean contribution to sea
2085 level and energy budget not detectable over the past decade. *Nature Climate Change*, 4\(11\),
2086 1031–1035. <https://doi.org/10.1038/nclimate2387>](#)
- 2087 [Loeb, N. G., Johnson, G. C., Thorsen, T. J., Lyman, J. M., Rose, F. G., & Kato, S. \(2021\).
2088 Satellite and Ocean Data Reveal Marked Increase in Earth's Heating Rate. *Geophysical*](#)

- 2089 [Research Letters, 48\(13\), e2021GL093047.](#)
 2090 <https://doi.org/https://doi.org/10.1029/2021GL093047>
- 2091 [Loeb, N. G., Lyman, J. M., Johnson, G. C., Allan, R. P., Doelling, D. R., Wong, T., Soden, B. J.,](#)
 2092 [& Stephens, G. L. \(2012\). Observed changes in top-of-the-atmosphere radiation and upper-](#)
 2093 [ocean heating consistent within uncertainty. *Nature Geoscience*, 5\(2\), 110–113.](#)
 2094 <https://doi.org/10.1038/ngeo1375>
- 2095 [Loeb, N. G., Mayer, M., Kato, S., Fasullo, J. T., Zuo, H., Senan, R., Lyman, J. M., Johnson, G.](#)
 2096 [C., & Balmaseda, M. \(2022\). Evaluating Twenty-Year Trends in Earth’s Energy Flows](#)
 2097 [From Observations and Reanalyses. *Journal of Geophysical Research: Atmospheres*,](#)
 2098 [127\(12\), e2022JD036686. <https://doi.org/https://doi.org/10.1029/2022JD036686>](#)
- 2099 [Loeb, N. G., Thorsen, T. J., Norris, J. R., Wang, H., & Su, W. \(2018\). Changes in Earth’s energy](#)
 2100 [budget during and after the “Pause” in global warming: An observational perspective](#)
 2101 [\(15948, Trans.\). *Climate*, 6\(3\), 62. <https://doi.org/10.3390/cli6030062>](#)
- 2102 [Lyman, J. M., & Johnson, G. C. \(2014\). Estimating Global Ocean Heat Content Changes in the](#)
 2103 [Upper 1800 m since 1950 and the Influence of Climatology Choice. *Journal of Climate*,](#)
 2104 [27\(5\), 1945–1957. <https://doi.org/10.1175/JCLI-D-12-00752.1>](#)
- 2105 [MacIntosh, C. R., Merchant, C. J., & von Schuckmann, K. \(2017\). Uncertainties in Steric Sea](#)
 2106 [Level Change Estimation During the Satellite Altimeter Era: Concepts and Practices.](#)
 2107 [*Surveys in Geophysics*, 38\(1\), 59–87. <https://doi.org/10.1007/s10712-016-9387-x>](#)
- 2108 [Mankoff, K. D., Colgan, W., Solgaard, A., Karlsson, N. B., Ahlström, A. P., van As, D., Box, J.](#)
 2109 [E., Khan, S. A., Kjeldsen, K. K., Mougnot, J., & Fausto, R. S. \(2019\). Greenland Ice Sheet](#)
 2110 [solid ice discharge from 1986 through 2017. *Earth Syst. Sci. Data*, 11\(2\), 769–786.](#)
 2111 <https://doi.org/10.5194/essd-11-769-2019>
- 2112 [Marti, F., Blazquez, A., Meyssignac, B., Ablain, M., Barnoud, A., Fraudeau, R., Jugier, R.,](#)
 2113 [Chenal, J., Larnicol, G., Pfeffer, J., Restano, M., & Benveniste, J. \(2022\). Monitoring the](#)
 2114 [ocean heat content change and the Earth energy imbalance from space altimetry and space](#)
 2115 [gravimetry. *Earth Syst. Sci. Data*, 14\(1\), 229–249. \[https://doi.org/10.5194/essd-14-229-\]\(https://doi.org/10.5194/essd-14-229-2022\)](#)
 2116 [2022](#)
- 2117 [Masson, V., Champeaux, J.-L., Chauvin, F., Meriguet, C., & Lacaze, R. \(2003\). A Global](#)
 2118 [Database of Land Surface Parameters at 1-km Resolution in Meteorological and Climate](#)
 2119 [Models. *Journal of Climate*, 16\(9\), 1261–1282. \[https://doi.org/10.1175/1520-\]\(https://doi.org/10.1175/1520-0442\(2003\)16<1261:AGDOLS>2.0.CO;2\)](#)
 2120 [0442\(2003\)16<1261:AGDOLS>2.0.CO;2](#)
- 2121 [Matthews, T., Byrne, M., Horton, R., Murphy, C., Pielke Sr, R., Raymond, C., Thorne, P., &](#)
 2122 [Wilby, R. L. \(2022\). Latent heat must be visible in climate communications. *WIREs Climate*](#)
 2123 [Change, 13\(4\), e779. <https://doi.org/https://doi.org/10.1002/wcc.779>](#)
- 2124 [Mayer, J., Mayer, M., & Haimberger, L. \(2021b\). Consistency and Homogeneity of Atmospheric](#)
 2125 [Energy, Moisture, and Mass Budgets in ERA5. *Journal of Climate*, 34\(10\), 3955–3974.](#)
 2126 <https://doi.org/10.1175/JCLI-D-20-0676.1>
- 2127 [Mayer, M., Lien, V. S., Mork, K. A., von Schuckmann, K., Monier, M., & Greiner, E. \(2021a\).](#)
 2128 [Ocean heat content in the High North, in Copernicus Marine Service Ocean State Report,](#)
 2129 [Issue 5. *Journal of Operational Oceanography*, 14:sup1, 17–23.](#)
 2130 <https://doi.org/10.1080/1755876X.2021.1946240>
- 2131 [Mayer, Michael, Haimberger, L., Edwards, J. M., & Hyder, P. \(2017\). Toward Consistent](#)
 2132 [Diagnostics of the Coupled Atmosphere and Ocean Energy Budgets. *Journal of Climate*,](#)
 2133 [30\(22\), 9225–9246. <https://doi.org/10.1175/JCLI-D-17-0137.1>](#)
- 2134 [Meng, L., Liu, J., Tarasick, D. W., Randel, W. J., Steiner, A. K., Wilhelmsen, H., Wang, L., &](#)

- 2135 [Haimberger, L. \(2022\). Continuous rise of the tropopause in the Northern Hemisphere over](#)
 2136 [1980–2020. *Science Advances*, 7\(45\), eabi8065. <https://doi.org/10.1126/sciadv.abi8065>](#)
 2137 [Meyssignac, B., Boyer, T., Zhao, Z., Hakuba, M. Z., Landerer, F. W., Stammer, D., Köhl, A.,](#)
 2138 [Kato, S., L'Ecuyer, T., Ablain, M., Abraham, J. P., Blazquez, A., Cazenave, A., Church, J.](#)
 2139 [A., Cowley, R., Cheng, L., Domingues, C. M., Giglio, D., Gouretski, V., ... Zilberman, N.](#)
 2140 [\(2019\). Measuring Global Ocean Heat Content to Estimate the Earth Energy Imbalance.](#)
 2141 [Frontiers in Marine Science, 6, 432.](#)
 2142 <https://www.frontiersin.org/article/10.3389/fmars.2019.00432>
 2143 [Millan, R., Mouginit, J., Rabatel, A., & Morlighem, M. \(2022\). Ice velocity and thickness of the](#)
 2144 [world's glaciers. *Nature Geoscience*, 15\(2\), 124–129. \[https://doi.org/10.1038/s41561-021-\]\(https://doi.org/10.1038/s41561-021-00885-z\)](#)
 2145 [00885-z](#)
 2146 [Moltmann, T., Turton, J., Zhang, H.-M., Nolan, G., Gouldman, C., Griesbauer, L., Willis, Z.,](#)
 2147 [Piniella, Á. M., Barrell, S., Andersson, E., Gallage, C., Charpentier, E., Belbeoch, M., Poli,](#)
 2148 [P., Rea, A., Burger, E. F., Legler, D. M., Lumpkin, R., Meinig, C., ... Zhang, Y. \(2019\). A](#)
 2149 [Global Ocean Observing System \(GOOS\), Delivered Through Enhanced Collaboration](#)
 2150 [Across Regions, Communities, and New Technologies . In *Frontiers in Marine Science*](#)
 2151 [\(Vol. 6, p. 291\). <https://www.frontiersin.org/article/10.3389/fmars.2019.00291>](#)
 2152 [Moon, T., & Joughin, I. \(2008\). Changes in ice front position on Greenland's outlet glaciers from](#)
 2153 [1992 to 2007. *Journal of Geophysical Research: Earth Surface*, 113\(F2\).](#)
 2154 <https://doi.org/https://doi.org/10.1029/2007JF000927>
 2155 [Moore, G. W. K., Våge, K., Renfrew, I. A., & Pickart, R. S. \(2022\). Sea-ice retreat suggests re-](#)
 2156 [organization of water mass transformation in the Nordic and Barents Seas. *Nature*](#)
 2157 [Communications, 13\(1\), 67. <https://doi.org/10.1038/s41467-021-27641-6>](#)
 2158 [Motyka, R. J., Truffer, M., Fahnestock, M., Mortensen, J., Rysgaard, S., & Howat, I. \(2011\).](#)
 2159 [Submarine melting of the 1985 Jakobshavn Isbræ floating tongue and the triggering of the](#)
 2160 [current retreat. *Journal of Geophysical Research: Earth Surface*, 116\(F1\).](#)
 2161 <https://doi.org/https://doi.org/10.1029/2009JF001632>
 2162 [Mouginit, J., Rignot, E., Bjørk, A., van den Broeke, M., Millan, R., Morlighem, M., Noël, B.,](#)
 2163 [Scheuchl, B., & Wood, M. \(2019\). Forty-six years of Greenland Ice Sheet mass balance](#)
 2164 [from 1972 to 2018. *Proceedings of the National Academy of Sciences*, 116\(19\), 9239–9244.](#)
 2165 <https://doi.org/10.1073/pnas.1904242116>
 2166 [Mouginit, J., Rignot, E., Scheuchl, B., Fenty, I., Khazendar, A., Morlighem, M., Buzzi, A., &](#)
 2167 [Paden, J. \(2015\). Fast retreat of Zachariæ Isstrøm, northeast Greenland. *Science*, 350\(6266\),](#)
 2168 [1357–1361. <https://doi.org/10.1126/science.aac7111>](#)
 2169 [Münchow, A., Padman, L., & Fricker, H. A. \(2014\). Interannual changes of the floating ice shelf](#)
 2170 [of Petermann Gletscher, North Greenland, from 2000 to 2012. *Journal of Glaciology*,](#)
 2171 [60\(221\), 489–499. \[https://doi.org/DOI: 10.3189/2014JoG13J135\]\(https://doi.org/DOI:10.3189/2014JoG13J135\)](#)
 2172 [Nauels, A., Meinshausen, M., Mengel, M., Lorbacher, K., & Wigley, T. M. L. \(2017\).](#)
 2173 [Synthesizing long-term sea level rise projections – the MAGICC sea level model v2.0.](#)
 2174 [Geosci. Model Dev., 10\(6\), 2495–2524. <https://doi.org/10.5194/gmd-10-2495-2017>](#)
 2175 [Nicolaus, M., Hoppmann, M., Arndt, S., Hendricks, S., Katlein, C., Nicolaus, A., Rossmann, L.,](#)
 2176 [Schiller, M., & Schwegmann, S. \(2021\). Snow Depth and Air Temperature Seasonality on](#)
 2177 [Sea Ice Derived From Snow Buoy Measurements . In *Frontiers in Marine Science* \(Vol.](#)
 2178 [8\). <https://www.frontiersin.org/article/10.3389/fmars.2021.655446>](#)
 2179 [Nitzbon, J., Krinner, G., Schneider von Deimling, T., Werner, M., & Langer, M. \(2022\).](#)
 2180 [Quantifying the Permafrost Heat Sink in Earth's Climate System. Submitted. *Geophysical*](#)

- 2181 [Research Letters, under revi. https://doi.org/DOI: 10.1002/essoar.10511600.1](https://doi.org/DOI: 10.1002/essoar.10511600.1)
- 2182 Palmer, M D, Haines, K., Tett, S. F. B., & Ansell, T. J. (2007). Isolating the signal of ocean
- 2183 global warming. *Geophysical Research Letters*, *34*(23).
- 2184 <https://doi.org/https://doi.org/10.1029/2007GL031712>
- 2185 Palmer, M D, & McNeall, D. J. (2014). Internal variability of Earth's energy budget simulated
- 2186 by CMIP5 climate models. *Environmental Research Letters*, *9*(3), 034016.
- 2187 <https://doi.org/10.1088/1748-9326/9/3/034016>
- 2188 Palmer, M D, Roberts, C. D., Balmaseda, M., Chang, Y.-S., Chepurin, G., Ferry, N., Fujii, Y.,
- 2189 Good, S. A., Guinehut, S., Haines, K., Hernandez, F., Köhl, A., Lee, T., Martin, M. J.,
- 2190 Masina, S., Masuda, S., Peterson, K. A., Storto, A., Toyoda, T., ... Xue, Y. (2017). Ocean
- 2191 heat content variability and change in an ensemble of ocean reanalyses. *Climate Dynamics*,
- 2192 *49*(3), 909–930. <https://doi.org/10.1007/s00382-015-2801-0>
- 2193 Palmer, Matthew D, Domingues, C. M., Slangen, A. B. A., & Boeira Dias, F. (2021). An
- 2194 ensemble approach to quantify global mean sea-level rise over the 20th century from tide
- 2195 gauge reconstructions (I3507, Trans.). *Environmental Research Letters*, *16*(4), 044043.
- 2196 <https://doi.org/10.1088/1748-9326/abdaec>
- 2197 Park, H., Fedorov, A. N., Zheleznyak, M. N., Konstantinov, P. Y., & Walsh, J. E. (2015). Effect
- 2198 of snow cover on pan-Arctic permafrost thermal regimes. *Climate Dynamics*, *44*(9), 2873–
- 2199 2895. <https://doi.org/10.1007/s00382-014-2356-5>
- 2200 Perovich, D., Polashenski, C., Arntsen, A., & Stwertka, C. (2017). Anatomy of a late spring
- 2201 snowfall on sea ice. *Geophysical Research Letters*, *44*(6), 2802–2809.
- 2202 <https://doi.org/https://doi.org/10.1002/2016GL071470>
- 2203 Pickler, C., Beltrami, H., & Mareschal, jean-claude. (2016). Laurentide Ice Sheet basal
- 2204 temperatures during the last glacial cycle as inferred from borehole data. *Climate of the*
- 2205 *Past*, *12*, 115–127. <https://doi.org/10.5194/cp-12-115-2016>
- 2206 Pisoft, P., Sacha, P., Polvani, L. M., Añel, J. A., de la Torre, L., Eichinger, R., Foelsche, U.,
- 2207 Huszar, P., Jacobi, C., Karlicky, J., Kuchar, A., Miksovsky, J., Zak, M., & Rieder, H. E.
- 2208 (2021). Stratospheric contraction caused by increasing greenhouse gases. *Environmental*
- 2209 *Research Letters*, *16*(6), 64038. <https://doi.org/10.1088/1748-9326/abfe2b>
- 2210 Purkey, S. G., & Johnson, G. C. (2010). Warming of Global Abyssal and Deep Southern Ocean
- 2211 Waters between the 1990s and 2000s: Contributions to Global Heat and Sea Level Rise
- 2212 Budgets. *Journal of Climate*, *23*(23), 6336–6351. <https://doi.org/10.1175/2010JCLI3682.1>
- 2213 Qu, X., & Hall, A. (2007). What Controls the Strength of Snow-Albedo Feedback? *Journal of*
- 2214 *Climate*, *20*(15), 3971–3981. <https://doi.org/10.1175/JCLI4186.1>
- 2215 Rhein, M., Rintoul S., Aoki, S., Campos, E., Chambers, D., ` , Feely, R., Gulev, S., Johnson, G.,
- 2216 Josey, S., Kostianoy, A., Mauritzen, C., Roemmich, D., Talley, L., & Wang, F. (2013).
- 2217 *Chapter 3: Observations: Ocean. In: Climate Change 2013: The Physical Science Basis.*
- 2218 *Contribution of Working Group I to the Fifth Assessment Report of the Intergovernmental*
- 2219 *Panel on Climate Change.* (T. Stocker, D. Qin, G.-K. Plattner, M. Tignor, S. Allen, J.
- 2220 Boschung, A. Nauels, Y. Xia, V. Bex, & P. Midgley (eds.)). Cambridge University Press.
- 2221 Rignot, E., Mouginot, J., Scheuchl, B., van den Broeke, M., van Wessem, M. J., & Morlighem,
- 2222 M. (2019). Four decades of Antarctic Ice Sheet mass balance from 1979–2017. *Proceedings*
- 2223 *of the National Academy of Sciences*, *116*(4), 1095.
- 2224 <https://doi.org/10.1073/pnas.1812883116>
- 2225 Roemmich, D., Church, J., Gilson, J., Monselesan, D., Sutton, P., & Wijffels, S. (2015).
- 2226 Unabated planetary warming and its ocean structure since 2006 (I3631, Trans.). *Nature*

- 2227 [Climate Change](https://doi.org/10.1038/nclimate2513), 5, 240. <https://doi.org/10.1038/nclimate2513>
- 2228 Roemmich, D., & Gilson, J. (2009). The 2004–2008 mean and annual cycle of temperature,
2229 salinity, and steric height in the global ocean from the Argo Program. *Progress in*
2230 *Oceanography*, 82(2), 81–100. <https://doi.org/https://doi.org/10.1016/j.pocean.2009.03.004>
- 2231 Santer, B D, Wigley, T. M. L., Doutriaux, C., Boyle, J. S., Hansen, J. E., Jones, P. D., Meehl, G.
2232 A., Roeckner, E., Sengupta, S., & Taylor, K. E. (2001). Accounting for the effects of
2233 volcanoes and ENSO in comparisons of modeled and observed temperature trends. *Journal*
2234 *of Geophysical Research: Atmospheres*, 106(D22), 28033–28059.
2235 <https://doi.org/https://doi.org/10.1029/2000JD000189>
- 2236 Santer, Benjamin D, Po-Chedley, S., Feldl, N., Fyfe, J. C., Fu, Q., Solomon, S., England, M.,
2237 Rodgers, K. B., Stuecker, M. F., Mears, C., Zou, C.-Z., Bonfils, C. J. W., Pallotta, G.,
2238 Zelinka, M. D., Rosenbloom, N., & Edwards, J. (2022). Robust anthropogenic signal
2239 identified in the seasonal cycle of tropospheric temperature. *Journal of Climate*, 1–51.
2240 <https://doi.org/10.1175/JCLI-D-21-0766.1>
- 2241 Santer, Benjamin D, Po-Chedley, S., Mears, C., Fyfe, J. C., Gillett, N., Fu, Q., Painter, J. F.,
2242 Solomon, S., Steiner, A. K., Wentz, F. J., Zelinka, M. D., & Zou, C.-Z. (2021). Using
2243 Climate Model Simulations to Constrain Observations. *Journal of Climate*, 34(15), 6281–
2244 6301. <https://doi.org/10.1175/JCLI-D-20-0768.1>
- 2245 Savita, A., Domingues, C. M., Boyer, T., Gouretski, V., Ishii, M., Johnson, G. C., Lyman, J. M.,
2246 Willis, J. K., Marsland, S. J., Hobbs, W., Church, J. A., Monselesan, D. P., Dobrohotoff, P.,
2247 Cowley, R., & Wijffels, S. E. (2022). Quantifying Spread in Spatiotemporal Changes of
2248 Upper-Ocean Heat Content Estimates: An Internationally Coordinated Comparison. *Journal*
2249 *of Climate*, 35(2), 851–875. <https://doi.org/10.1175/JCLI-D-20-0603.1>
- 2250 Schweiger, A. J., Wood, K. R., & Zhang, J. (2019). Arctic Sea Ice Volume Variability over
2251 1901–2010: A Model-Based Reconstruction. *Journal of Climate*, 32(15), 4731–4752.
2252 <https://doi.org/10.1175/JCLI-D-19-0008.1>
- 2253 Schweiger, A., Lindsay, R., Zhang, J., Steele, M., Stern, H., & Kwok, R. (2011). Uncertainty in
2254 modeled Arctic sea ice volume. *Journal of Geophysical Research: Oceans*, 116(C8).
2255 <https://doi.org/10.1029/2011JC007084>
- 2256 Shen, P. Y., Wang, K., Beltrami, H., & Mareschal, J.-C. (1992). A comparative study of inverse
2257 methods for estimating climatic history from borehole temperature data. *Palaeogeography,*
2258 *Palaeoclimatology, Palaeoecology*, 98(2), 113–127.
2259 [https://doi.org/https://doi.org/10.1016/0031-0182\(92\)90192-8](https://doi.org/https://doi.org/10.1016/0031-0182(92)90192-8)
- 2260 Shen, X., Ke, C.-Q., & Li, H. (2022). Snow depth product over Antarctic sea ice from 2002 to
2261 2020 using multisource passive microwave radiometers. *Earth Syst. Sci. Data*, 14(2), 619–
2262 636. <https://doi.org/10.5194/essd-14-619-2022>
- 2263 Shepherd, A., Fricker, H. A., & Farrell, S. L. (2018). Trends and connections across the
2264 Antarctic cryosphere. *Nature*, 558(7709), 223–232. [https://doi.org/10.1038/s41586-018-](https://doi.org/10.1038/s41586-018-0171-6)
2265 [0171-6](https://doi.org/10.1038/s41586-018-0171-6)
- 2266 Shepherd, A., Ivins, E., Rignot, E., Smith, B., van den Broeke, M., Velicogna, I., Whitehouse, P.,
2267 Briggs, K., Joughin, I., Krinner, G., Nowicki, S., Payne, T., Scambos, T., Schlegel, N.,
2268 Geruo, A., Agosta, C., Ahlström, A., Babonis, G., Barletta, V. R., ... Team, T. I. (2019).
2269 Mass balance of the Greenland Ice Sheet from 1992 to 2018. *Nature*.
2270 <https://doi.org/10.1038/s41586-019-1855-2>
- 2271 Slater, T., Lawrence, I. R., Ootosaka, I. N., Shepherd, A., Gourmelen, N., Jakob, L., Tepes, P.,
2272 Gilbert, L., & Nienow, P. (2021). Review article: Earth’s ice imbalance. *The Cryosphere*,

- 2273 [15\(1\), 233–246. https://doi.org/10.5194/tc-15-233-2021](https://doi.org/10.5194/tc-15-233-2021)
- 2274 [Smith, B., Fricker, A. H., Gardner, S. A., Medley, B., Nilsson, J., Paolo, S. F., Holschuh, N.,](#)
- 2275 [Adusumilli, S., Brunt, K., Csatho, B., Harbeck, K., Markus, T., Neumann, T., Siegfried, M.,](#)
- 2276 [& Zwally, J. H. \(2020\). Pervasive ice sheet mass loss reflects competing ocean and](#)
- 2277 [atmosphere processes. *Science*, 368\(6496\), 1239–1242.](#)
- 2278 <https://doi.org/10.1126/science.aaz5845>
- 2279 [Smith, D. M., Allan, R. P., Coward, A. C., Eade, R., Hyder, P., Liu, C., Loeb, N. G., Palmer, M.](#)
- 2280 [D., Roberts, C. D., & Scaife, A. A. \(2015\). Earth’s energy imbalance since 1960 in](#)
- 2281 [observations and CMIP5 models. *Geophysical Research Letters*, 42\(4\), 1205–1213.](#)
- 2282 <https://doi.org/10.1002/2014GL062669>
- 2283 [Staten, P. W., Grise, K. M., Davis, S. M., Karnauskas, K. B., Waugh, D. W., Maycock, A. C.,](#)
- 2284 [Fu, Q., Cook, K., Adam, O., Simpson, I. R., Allen, R. J., Rosenlof, K., Chen, G.,](#)
- 2285 [Ummenhofer, C. C., Quan, X.-W., Kossin, J. P., Davis, N. A., & Son, S.-W. \(2020\).](#)
- 2286 [Tropical Widening: From Global Variations to Regional Impacts. *Bulletin of the American*](#)
- 2287 [Meteorological Society](#), 101(6), E897–E904. <https://doi.org/10.1175/bams-d-19-0047.1>
- 2288 [Steiner, A. K., Ladstädter, F., Ao, C. O., Gleisner, H., Ho, S.-P., Hunt, D., Schmidt, T., Foelsche,](#)
- 2289 [U., Kirchengast, G., Kuo, Y.-H., Lauritsen, K. B., Mannucci, A. J., Nielsen, J. K.,](#)
- 2290 [Schreiner, W., Schwärz, M., Sokolovskiy, S., Syndergaard, S., & Wickert, J. \(2020b\).](#)
- 2291 [Consistency and structural uncertainty of multi-mission GPS radio occultation records](#)
- 2292 [\(I1695, Trans.\). *Atmospheric Measurement Techniques*, 13\(5\), 2547–2575.](#)
- 2293 <https://doi.org/10.5194/amt-13-2547-2020>
- 2294 [Steiner, A. K., Ladstädter, F., Randel, W. J., Maycock, A. C., Fu, Q., Claud, C., Gleisner, H.,](#)
- 2295 [Haimberger, L., Ho, S.-P., Keckhut, P., Leblanc, T., Mears, C., Polvani, L. M., Santer, B.](#)
- 2296 [D., Schmidt, T., Sofieva, V., Wing, R., & Zou, C.-Z. \(2020a\). Observed Temperature](#)
- 2297 [Changes in the Troposphere and Stratosphere from 1979 to 2018 \(I3342, Trans.\). *Journal of*](#)
- 2298 [Climate](#), 33(19), 8165–8194. <https://doi.org/10.1175/JCLI-D-19-0998.1>
- 2299 [Storto, A., Alvera-Azcárate, A., Balmaseda, M. A., Barth, A., Chevallier, M., Counillon, F.,](#)
- 2300 [Domingues, C. M., Drevillon, M., Drillet, Y., Forget, G., Garric, G., Haines, K., Hernandez,](#)
- 2301 [F., Iovino, D., Jackson, L. C., Lellouche, J.-M., Masina, S., Mayer, M., Oke, P. R., ... Zuo,](#)
- 2302 [H. \(2019\). Ocean Reanalyses: Recent Advances and Unsolved Challenges. *Frontiers in*](#)
- 2303 [Marine Science](#), 6, 418. <https://doi.org/10.3389/fmars.2019.00418>
- 2304 [Storto, A., Masina, S., Simoncelli, S., Iovino, D., Cipollone, A., Drevillon, M., Drillet, Y.,](#)
- 2305 [Schuckman, K., Parent, L., Garric, G., Greiner, E., Desportes, C., Zuo, H., Balmaseda, M.,](#)
- 2306 [& Peterson, K. \(2018\). The added value of the multi-system spread information for ocean](#)
- 2307 [heat content and steric sea level investigations in the CMEMS GREP ensemble reanalysis](#)
- 2308 [product. *Climate Dynamics*. https://doi.org/10.1007/s00382-018-4585-5](#)
- 2309 [Tilling, R. L., Ridout, A., & Shepherd, A. \(2018\). Estimating Arctic sea ice thickness and](#)
- 2310 [volume using CryoSat-2 radar altimeter data. *Advances in Space Research*, 62\(6\), 1203–](#)
- 2311 [1225. https://doi.org/https://doi.org/10.1016/j.asr.2017.10.051](#)
- 2312 [Trenberth, K. E., Fasullo, J. T., von Schuckmann, K., & Cheng, L. \(2016\). Insights into Earth’s](#)
- 2313 [Energy Imbalance from Multiple Sources. *Journal of Climate*, 29\(20\), 7495–7505.](#)
- 2314 <https://doi.org/10.1175/JCLI-D-16-0339.1>
- 2315 [Vanderkelen, I., van Lipzig, N. P. M., Lawrence, D. M., Droppers, B., Golub, M., Gosling, S. N.,](#)
- 2316 [Janssen, A. B. G., Marcé, R., Schmied, H. M., Perroud, M., Pierson, D., Pokhrel, Y., Satoh,](#)
- 2317 [Y., Schewe, J., Seneviratne, S. I., Stepanenko, V. M., Tan, Z., Woolway, R. I., & Thiery,](#)
- 2318 [W. \(2020\). Global Heat Uptake by Inland Waters. *Geophysical Research Letters*, 47\(12\).](#)

- 2319 [e2020GL087867](https://doi.org/https://doi.org/10.1029/2020GL087867). <https://doi.org/https://doi.org/10.1029/2020GL087867>
- 2320 Verver, G., Fujiwara, M., Dolmans, P., Becker, C., Fortuin, P., & Miloshevich, L. (2006).
- 2321 Performance of the Vaisala RS80A/H and RS90 Humicap Sensors and the Meteorolabor
- 2322 “Snow White” Chilled-Mirror Hygrometer in Paramaribo, Suriname. *Journal of*
- 2323 *Atmospheric and Oceanic Technology*, 23(11), 1506–1518.
- 2324 <https://doi.org/10.1175/JTECH1941.1>
- 2325 Vömel, H., Selkirk, H., Miloshevich, L., Valverde-Canossa, J., Valdés, J., Kyrö, E., Kivi, R.,
- 2326 Stolz, W., Peng, G., & Diaz, J. A. (2007). Radiation Dry Bias of the Vaisala RS92 Humidity
- 2327 Sensor. *Journal of Atmospheric and Oceanic Technology*, 24(6), 953–963.
- 2328 <https://doi.org/10.1175/JTECH2019.1>
- 2329 von Schuckmann, K., Palmer, M. D., Trenberth, K. E., Cazenave, A., Chambers, D.,
- 2330 Champollion, N., Hansen, J., Josey, S. A., Loeb, N., Mathieu, P.-P., Meyssignac, B., &
- 2331 Wild, M. (2016). An imperative to monitor Earth’s energy imbalance. *Nature Climate*
- 2332 *Change*, 6(2), 138–144. <https://doi.org/10.1038/nclimate2876>
- 2333 von Schuckmann, K., Cheng, L., Palmer, M. D., Hansen, J., Tassone, C., Aich, V., Adusumilli,
- 2334 S., Beltrami, H., Boyer, T., Cuesta-Valero, F. J., Desbruyères, D., Domingues, C., García-
- 2335 García, A., Gentine, P., Gilson, J., Gorfer, M., Haimberger, L., Ishii, M., Johnson, G. C., ...
- 2336 Wijffels, S. E. (2020). Heat stored in the Earth system: where does the energy go? *Earth*
- 2337 *Syst. Sci. Data*, 12(3), 2013–2041. <https://doi.org/10.5194/essd-12-2013-2020>
- 2338 von Schuckmann, K., & Le Traon, P.-Y. (2011). How well can we derive Global Ocean
- 2339 Indicators from Argo data? *Ocean Sci.*, 7(6), 783–791. [https://doi.org/10.5194/os-7-783-](https://doi.org/10.5194/os-7-783-2011)
- 2340 [2011](https://doi.org/10.5194/os-7-783-2011)
- 2341 von Schuckmann, Karina; Minière, A., Gues, F., Cuesta-Valero, F. J., Kirchengast, G.,
- 2342 Adusumilli, S., Straneo, F., Allan, R., Barker, P. M., Beltrami, H., Boyer, T., Cheng, L.,
- 2343 Church, J., Desbruyeres, D., Dolman, H., Domingues, C. M., García-García, A., Gilson, J.,
- 2344 Gorfer, M., ... Zemp, M. (2023). *GCOS EHI 1960-2020 Earth Heat Inventory Ocean Heat*
- 2345 *Content (Version 2)*. World Data Center for Climate (WDCC) at DKRZ.
- 2346 https://doi.org/https://doi.org/10.26050/WDCC/GCOS_EHI_1960-2020_OHC_v2
- 2347 von Schuckmann, Karina, Le Traon, P.-Y., Smith, N., Pascual, A., Brasseur, P., Fennel, K.,
- 2348 Djavidnia, S., Aaboe, S., Fanjul, E. A., Autret, E., Axell, L., Aznar, R., Benincasa, M.,
- 2349 Bentamy, A., Boberg, F., Bourdallé-Badie, R., Nardelli, B. B., Brando, V. E., Bricaud, C.,
- 2350 ... Zuo, H. (2018). Copernicus Marine Service Ocean State Report. *Journal of Operational*
- 2351 *Oceanography*, 11(sup1), S1–S142. <https://doi.org/10.1080/1755876X.2018.1489208>
- 2352 Wanders, N., Thober, S., Kumar, R., Pan, M., Sheffield, J., Samaniego, L., & Wood, E. F.
- 2353 (2019). Development and Evaluation of a Pan-European Multimodel Seasonal Hydrological
- 2354 Forecasting System. *Journal of Hydrometeorology*, 20(1), 99–115.
- 2355 <https://doi.org/10.1175/JHM-D-18-0040.1>
- 2356 Wang, X., Key, J., Kwok, R., & Zhang, J. (2016). Comparison of Arctic Sea Ice Thickness from
- 2357 Satellites, Aircraft, and PIOMAS Data. In *Remote Sensing* (Vol. 8, Issue 9).
- 2358 <https://doi.org/10.3390/rs8090713>
- 2359 WCRP Global Sea Level Budget Group. (2018). Global sea-level budget 1993–present. *Earth*
- 2360 *Syst. Sci. Data*, 10(3), 1551–1590. <https://doi.org/10.5194/essd-10-1551-2018>
- 2361 Webster, M. A., DuVivier, A. K., Holland, M. M., & Bailey, D. A. (2021). Snow on Arctic Sea
- 2362 Ice in a Warming Climate as Simulated in CESM. *Journal of Geophysical Research:*
- 2363 *Oceans*, 126(1), e2020JC016308. <https://doi.org/https://doi.org/10.1029/2020JC016308>
- 2364 Weihs, P., Laimighofer, J., Formayer, H., & Olefs, M. (2021). Influence of snow making on

- 2365 [albedo and local radiative forcing in an alpine area. *Atmospheric Research*, 255, 105448.](#)
 2366 <https://doi.org/https://doi.org/10.1016/j.atmosres.2020.105448>
- 2367 [WGMS. \(2021\). *Fluctuations of Glaciers Database*. World Glacier Monitoring Service, Zurich,](#)
 2368 [Switzerland. <https://doi.org/DOI:10.5904/wgms-fog-2021-05>](#)
- 2369 [Wijffels, S., Roemmich, D., Monselesan, D., Church, J., & Gilson, J. \(2016\). Ocean temperatures](#)
 2370 [chronicle the ongoing warming of Earth. *Nature Climate Change*, 6\(2\), 116–118.](#)
 2371 <https://doi.org/10.1038/nclimate2924>
- 2372 [Wilson, N., Straneo, F., & Heimbach, P. \(2017\). Satellite-derived submarine melt rates and mass](#)
 2373 [balance \(2011–2015\) for Greenland’s largest remaining ice tongues. *The Cryosphere*, 11,](#)
 2374 [2773–2782. <https://doi.org/10.5194/tc-11-2773-2017>](#)
- 2375 [WMO. \(2022\). *The State of the Global Climate 2021*. <https://library.wmo.int/index.php?>
 2376 \[lvl=notice_display&id=22080\]\(#\)](#)
- 2377 [Wunsch, C. \(2020\). Is the Ocean Speeding Up? Ocean Surface Energy Trends. *Journal of*
 2378 \[Physical Oceanography\]\(#\), 50, 3205–3217. <https://doi.org/10.1175/JPO-D-20-0082.1>](#)
- 2379 [Zanna, L., Khatiwala, S., Gregory, J. M., Ison, J., & Heimbach, P. \(2019\). Global reconstruction](#)
 2380 [of historical ocean heat storage and transport. *Proceedings of the National Academy of*](#)
 2381 [Sciences](#), 116(4), 1126. <https://doi.org/10.1073/pnas.1808838115>
- 2382 [Zemp, M., Huss, M., Thibert, E., Eckert, N., McNabb, R., Huber, J., Barandun, M., Machguth,](#)
 2383 [H., Nussbaumer, S. U., Gärtner-Roer, I., Thomson, L., Paul, F., Maussion, F., Kutuzov, S.,](#)
 2384 [& Cogley, J. G. \(2019\). *Global and regional glacier mass changes from 1961 to 2016*.](#)
 2385 <https://doi.org/10.5281/ZENODO.3557199>
- 2386 [Zemp, Michael, Huss, M., Eckert, N., Thibert, E., Paul, F., Nussbaumer, U. S., & Gärtner-Roer,](#)
 2387 [I. \(2020\). Brief communication: Ad hoc estimation of glacier contributions to sea-level rise](#)
 2388 [from the latest glaciological observations \(I5946, Trans.\). *Cryosphere*, 14\(3\).](#)
 2389 <https://doi.org/10.5194/tc-14-1043-2020>
- 2390 [Zhang, J., & Rothrock, D. A. \(2003\). Modeling Global Sea Ice with a Thickness and Enthalpy](#)
 2391 [Distribution Model in Generalized Curvilinear Coordinates. *Monthly Weather Review*,](#)
 2392 [131\(5\), 845–861. \[https://doi.org/10.1175/1520-0493\\(2003\\)131<0845:MGSIWA>2.0.CO;2\]\(https://doi.org/10.1175/1520-0493\(2003\)131<0845:MGSIWA>2.0.CO;2\)](#)
- 2393 [Zhang, R., Wang, H., Fu, Q., Rasch, J. P., & Wang, X. \(2019\). Unraveling driving forces](#)
 2394 [explaining significant reduction in satellite-inferred Arctic surface albedo since the 1980s.](#)
 2395 [*Proceedings of the National Academy of Sciences*, 116\(48\), 23947–23953.](#)
 2396 <https://doi.org/10.1073/pnas.1915258116>
- 2397 [Zou, C.-Z., Xu, H., Hao, X., & Fu, Q. \(2021\). Post-Millennium Atmospheric Temperature](#)
 2398 [Trends Observed From Satellites in Stable Orbits. *Geophysical Research Letters*, 48\(13\),](#)
 2399 [e2021GL093291. <https://doi.org/https://doi.org/10.1029/2021GL093291>](#)
- 2400
- 2401 [Abram, N., Gattuso, J.-P., Prakash, A., Cheng, L., Chidichimo, M. P., Crate, S., Enomoto, H.,](#)
 2402 [Garsehagen, M., Gruber, N., Harper, S., Holland, E., Kudela, R. M., Riee, J., Steffen, K., &](#)
 2403 [von Schuekmann, K. \(2019\). Framing and Context of the Report. In H. O. Pörtner, D. C.](#)
 2404 [Roberts, V. Masson-Delmotte, P. Zhai, M. Tignor, E. Poloezanska, K. Mintenbeck, A.](#)
 2405 [Alegría, M. Nicolai, A. Okem, J. Petzold, B. Rama, & N. M. Weyer \(Eds.\), *IPCC Special*](#)
 2406 [Report on the Ocean and Cryosphere in a Changing Climate \(pp. 73–129\). in press.](#)
 2407 <https://www.ipee.ch/sroee/>
- 2408 [Adusumilli, Susheel; Hendrieks, Stefan; Korosov, Anton; Straneo, Fiammetta; Lavergne,](#)
 2409 [Thomas; Lawrence, Isobel; Marzeion, Ben; Otosaka, Inès; Schweiger, Axel; Shepherd,](#)
 2410 [Andrew; Slater, Donald; Slater, Thomas; Timmermanns, Mary-Louise; Zemp, Michael](#)

- 2411 (2022). Heat stored in the Earth system 1960–2020: Where does the energy go?, submitted
 2412 to Earth System Science Data. (2022). World Data Center for Climate (WDCC) at DKRZ.
 2413 https://www.wde-climate.de/ui/entry?aeronym=GCOS_EHI_1960-2020_CrHC
 2414 Adusumilli, S., Frieker, H. A., Medley, B., Padman, L., & Siegfried, M. R. (2020). Interannual
 2415 variations in meltwater input to the Southern Ocean from Antarctic ice shelves. *Nature*
 2416 *Geoscience*, *13*(9), 616–620. <https://doi.org/10.1038/s41561-020-0616-z>
 2417 Allison, L. C., Roberts, C. D., Palmer, M. D., Hermanson, L., Killick, R. E., Rayner, N. A.,
 2418 Smith, D. M., & Andrews, M. B. (2019). Towards quantifying uncertainty in ocean heat
 2419 content changes using synthetic profiles. *Environmental Research Letters*, *14*(8), 084037.
 2420 <https://doi.org/10.1088/1748-9326/ab2b0b>
 2421 Angerer, B., Ladstädter, F., Scherllin-Pirscher, B., Schwärz, M., Steiner, A. K., Foelsehe, U., &
 2422 Kirchongast, G. (2017). Quality aspects of the Wegener Center multi-satellite GPS radio-
 2423 occultation record OPSv5.6. *Atmospheric Measurement Techniques*, *10*(12), 4845–4863.
 2424 <https://doi.org/10.5194/amt-10-4845-2017>
 2425 Bell, B., Hersbach, H., Simmons, A., Berrisford, P., Dahlgren, P., Horányi, A., Muñoz-Sabater,
 2426 J., Nicolas, J., Radu, R., Schepers, D., Soci, C., Villaume, S., Bidlot, J.-R., Haimberger, L.,
 2427 Woollen, J., Buontempo, C., & Thépaut, J.-N. (2021). The ERA5 global reanalysis:
 2428 Preliminary extension to 1950. *Quarterly Journal of the Royal Meteorological Society*,
 2429 *147*(741), 4186–4227. <https://doi.org/https://doi.org/10.1002/qj.4174>
 2430 Beltrami, H., & Marechal, J.-C. (1992). Ground temperature histories for central and eastern
 2431 Canada from geothermal measurements: Little Ice Age signature. *Geophysical Research*
 2432 *Letters*, *19*(7), 689–692. <https://doi.org/10.1029/92GL00671>
 2433 Beltrami, H., Smerdon, J. E., Pollack, H. N., & Huang, S. (2002). Continental heat gain in the
 2434 global climate system. *Geophysical Research Letters*, *29*(8), 8-1-8-3.
 2435 <https://doi.org/10.1029/2001GL014310>
 2436 Berrisford, P., Källberg, P., Kobayashi, S., Dee, D., Uppala, S., Simmons, A. J., Poli, P., & Sato,
 2437 H. (2011). Atmospheric conservation properties in ERA-Interim. *Quarterly Journal of the*
 2438 *Royal Meteorological Society*, *137*(659), 1381–1399. <https://doi.org/10.1002/qj.864>
 2439 Biskaborn, B. K., Lanckman, J.-P., Lantuit, H., Elger, K., Streletskiy, D. A., Cable, W. L., &
 2440 Romanovsky, V. E. (2015). The new database of the Global Terrestrial Network for
 2441 Permafrost (GTN-P). *Earth Syst. Sci. Data*, *7*(2), 245–259. [https://doi.org/10.5194/essd-7-](https://doi.org/10.5194/essd-7-245-2015)
 2442 [245-2015](https://doi.org/10.5194/essd-7-245-2015)
 2443 Boyer, T., Domingues, C. M., Good, S. A., Johnson, G. C., Lyman, J. M., Ishii, M., Gouretski,
 2444 V., Willis, J. K., Antonov, J., Wijffels, S., Church, J. A., Cowley, R., & Bindoff, N. L.
 2445 (2016). Sensitivity of Global Upper-Ocean Heat Content Estimates to Mapping Methods,
 2446 XBT Bias Corrections, and Baseline Climatologies. *Journal of Climate*, *29*(13), 4817–4842.
 2447 <https://doi.org/10.1175/JCLI-D-15-0801.1>
 2448 Cabanes, C., Grouazel, A., von Schuckmann, K., Hamon, M., Turpin, V., Coatanoean, C., Paris,
 2449 F., Guinehut, S., Boone, C., Ferry, N., de Boyer Montégut, C., Carval, T., Reverdin, G.,
 2450 Pouliquen, S., & Le Traon, P.-Y. (2013). The CORA dataset: validation and diagnostics of
 2451 in-situ ocean temperature and salinity measurements. *Ocean Sci.*, *9*(1), 1–18.
 2452 <https://doi.org/10.5194/os-9-1-2013>
 2453 Castelao, G. P. (2020). A Framework to Quality Control Oceanographic Data. *Journal of Open*
 2454 *Source Software*. *Journal of Open Source Software*, *5*(48), 2063.
 2455 <https://doi.org/https://doi.org/10.21105/joss.02063>
 2456 Castelão, G. P. (2021). A machine learning approach to quality control oceanographic data.

- 2457 *Computers & Geosciences*, 155, 104803.
 2458 <https://doi.org/https://doi.org/10.1016/j.cageo.2021.104803>
- 2459 Cheng, L., Abraham, J., Hausfather, Z., & Trenberth, K. E. (2019). How fast are the oceans
 2460 warming? *Science*, 363(6423), 128. <https://doi.org/10.1126/science.aav7619>
- 2461 Cheng, L., Foster, G., Hausfather, Z., Trenberth, K. E., & Abraham, J. (2022). Improved
 2462 Quantification of the Rate of Ocean Warming. *Journal of Climate*, 35(14), 4827–4840.
 2463 <https://doi.org/10.1175/JCLI-D-21-0895.1>
- 2464 Cheng, L., Luo, H., Boyer, T., Cowley, R., Abraham, J., Gouretski, V., Reseghetti, F., & Zhu, J.
 2465 (2018). How Well Can We Correct Systematic Errors in Historical XBT Data? *Journal of*
 2466 *Atmospheric and Oceanic Technology*, 35(5), 1103–1125. <https://doi.org/10.1175/JTECH-D-17-0122.1>
- 2468 Cheng, L., Schuckmann, K. von, Abraham, J., Trenberth, K., Mann, M., Zanna, L., England, M.
 2469 H., Zika, J. D., Fasullo, J., Yu, Y., Pan, Y., Zhu, J., Newsom, E., Bronselaer, B., & Lin, X.
 2470 (2022). Past and future ocean warming. *Nature*, under review.
- 2471 Cheng, L., Trenberth, K. E., Fasullo, J., Boyer, T., Abraham, J., & Zhu, J. (2017). Improved
 2472 estimates of ocean heat content from 1960 to 2015. *Science Advances*, 3(3), e1601545.
 2473 <https://doi.org/10.1126/sciadv.1601545>
- 2474 Cheng, L., Trenberth, K., Fasullo, J., Abraham, J., Boyer, T., von Schuckmann, K., & Zhu, J.
 2475 (2017). Taking the Pulse of the Planet. *Eos*. <https://doi.org/10.1029/2017EO081839>
- 2476 Chiodo, G., & Haimberger, L. (2010). Interannual changes in mass consistent energy budgets
 2477 from ERA-Interim and satellite data. *Journal of Geophysical Research: Atmospheres*,
 2478 115(D2). <https://doi.org/10.1029/2009JD012049>
- 2479 Church, J. A., White, N. J., Konikow, L. F., Domingues, C. M., Cogley, J. G., Rignot, E.,
 2480 Gregory, J. M., van den Broeke, M. R., Monaghan, A. J., & Velicogna, I. (2011). Revisiting
 2481 the Earth's sea-level and energy budgets from 1961 to 2008. *Geophysical Research Letters*,
 2482 38(18). <https://doi.org/10.1029/2011GL048794>
- 2483 Ciais, P., Sabine, C., Bala, G., Bopp, L., Brovkin, V., Canadell, J., Chhabra, A., DeFries, R.,
 2484 Galloway, J., Heimann, M., Jones, C., Le Quéré, C., Myneni, R. B., Piao, S., & Thornton, P.
 2485 (2014). *Carbon and Other Biogeochemical Cycles*. In *Climate Change 2013—The Physical*
 2486 *Science Basis: Working Group I Contribution to the Fifth Assessment Report of the*
 2487 *Intergovernmental Panel on Climate Change*. Cambridge University Press.
 2488 <https://doi.org/https://doi.org/DOI: 10.1017/CBO9781107415324.015>
- 2489 Cleveland, W. S. (1979). Robust Locally Weighted Regression and Smoothing Scatterplots. *J.*
 2490 *Am. Stat. Assoc.*, 74, 829–836.
- 2491 Clough, W. J., & Hansen, L. B. (1979). The Ross Ice Shelf Project. *Science*, 203(4379), 433–
 2492 434. <https://doi.org/10.1126/science.203.4379.433>
- 2493 Cohen, J., Zhang, X., Francis, J., Jung, T., Kwok, R., Overland, J., Ballinger, T., Bhatt, U. S.,
 2494 Chen, H. W., Coumou, D., Feldstein, S., Handorf, D., Henderson, G., Ionita, M.,
 2495 Kretschmer, M., Laliberte, F., Lee, S., Linderholm, H. W., Maslowski, W., ... Yoon, J.
 2496 (2020). Divergent consensus on Arctic amplification influence on midlatitude severe
 2497 winter weather. *Nature Climate Change*, 10, 20–29. <https://doi.org/10.1038/s41558-019-0662-y>
- 2498
 2499 Cook, A. J., & Vaughan, D. G. (2010). Overview of areal changes of the ice shelves on the
 2500 Antarctic Peninsula over the past 50 years. *The Cryosphere*, 4(1), 77–98.
 2501 <https://doi.org/10.5194/te-4-77-2010>
- 2502 Cowley, R., Killiek, R. E., Boyer, T., Gouretski, V., Reseghetti, F., Kizu, S., Palmer, M. D.,

- 2503 Cheng, L., Storto, A., Le Menn, M., Simonecelli, S., Macdonald, A. M., & Domingues, C.
 2504 M. (2021). International Quality-Controlled Ocean Database (IQuOD) v0.1: The
 2505 Temperature Uncertainty Specification. In *Frontiers in Marine Science* (Vol. 8).
 2506 <https://www.frontiersin.org/articles/10.3389/fmars.2021.689695>
- 2507 Crisp, D., Dolman, H., Tanhua, T., McKinley, G. A., Hauck, J., Bastos, A., Sitch, S., Eggleston,
 2508 S., & Aich, V. (2022). How Well Do We Understand the Land-Ocean-Atmosphere Carbon
 2509 Cycle? *Reviews of Geophysics*, 60(2), e2021RG000736.
 2510 <https://doi.org/https://doi.org/10.1029/2021RG000736>
- 2511 Cuesta-Valero, F. J., Beltrami, H., García-García, A., Krinner, G., Langer, M., MacDougall, A.,
 2512 Nitzbon, J., Peng, J., von Schueckmann, K., Seneviratne, S. I., Smith, N., Thiery, W.,
 2513 Vanderkelen, I., & Wu, T. (2022). Continental Heat Storage: Contributions from Ground,
 2514 Inland Waters, and Permafrost Thawing, submitted. *Earth System Dynamics*, submitted.
- 2515 Cuesta-Valero, F. J., Beltrami, H., Gruber, S., García-García, A., & González-Rouco, J. F.
 2516 (2022). A new bootstrap technique to quantify uncertainty in estimates of ground surface
 2517 temperature and ground heat flux histories from geothermal data. Submitted. *Geoscientific
 2518 Model Development*, submitted.
- 2519 Cuesta-Valero, Francisco; Beltrami, Hugo; García-García, Almudena; Krinner, Gerhard; Langer,
 2520 Moritz; MacDougall, Andrew; Nitzbon, Jean; Peng, Jian; von Schueckmann, Karina;
 2521 Seneviratne, Sonia; Smith, Noah; Thiery, Wim; Vanderkelen, Inne; Wu, Tonghua (2022).
 2522 Continental heat storage: Contributions from the ground, inland waters, and permafrost
 2523 thawing, submitted to Earth System Dynamics (2022c). World Data Center for Climate
 2524 (WDCC) at DKRZ. [https://www.wdc-climate.de/ui/entry?acronym=GCOS_EHI_1960-
 2525 2020_CoHC](https://www.wdc-climate.de/ui/entry?acronym=GCOS_EHI_1960-2020_CoHC)
- 2526 Cuesta-Valero, F. J., García-García, A., Beltrami, H., & Finnis, J. (2021). First assessment of the
 2527 earth heat inventory within CMIP5 historical simulations. *Earth Syst. Dynam.*, 12(2), 581–
 2528 600. <https://doi.org/10.5194/esd-12-581-2021>
- 2529 Cuesta-Valero, F. J., García-García, A., Beltrami, H., González-Rouco, J. F., & García-
 2530 Bustamante, E. (2021). Long-Term Global Ground Heat Flux and Continental Heat Storage
 2531 from Geothermal Data. *Climate of the Past*, 17(1), 451–468. [https://doi.org/10.5194/ep-17-
 2532 451-2021](https://doi.org/10.5194/ep-17-451-2021)
- 2533 Cuesta-Valero, F. J., García-García, A., Beltrami, H., Zorita, E., & Jaime-Santero, F. (2019).
 2534 Long-term Surface Temperature (LoST) database as a complement for GCM preindustrial
 2535 simulations. *Clim. Past*, 15(3), 1099–1111. <https://doi.org/10.5194/ep-15-1099-2019>
- 2536 Cuesta-Valero, Francisco José, Beltrami, H., Burke, E., García-García, A., MacDougall, A.,
 2537 Peng, J., Schueckmann, K. von, Seneviratne, S. I., Smith, N., Thiery, W., Vanderkelen, I., &
 2538 Wu, T. (2022). Continental Heat Storage: Contributions from the Ground, Inland Waters,
 2539 and Permafrost Thawing. *Submitted to Earth System Data*.
- 2540 Cuesta-Valero, Francisco José, García-García, A., Beltrami, H., & Smerdon, J. E. (2016). First
 2541 assessment of continental energy storage in CMIP5 simulations. *Geophysical Research
 2542 Letters*, 43(10), 5326–5335. <https://doi.org/10.1002/2016GL068496>
- 2543 de Vrese, P., Staacke, T., Caves Rügenstein, J., Goodman, J., & Brovkin, V. (2021). Snowfall-
 2544 albedo feedbacks could have led to deglaciation of snowball Earth starting from mid-
 2545 latitudes. *Communications Earth & Environment*, 2(1), 91. [https://doi.org/10.1038/s43247-
 2546 021-00160-4](https://doi.org/10.1038/s43247-021-00160-4)
- 2547 Demezhko, D. Y., & Gornostaeva, A. A. (2015). Late Pleistocene–Holocene ground surface heat
 2548 flux changes reconstructed from borehole temperature data. *Climate of the Past*, 11(4), 647–

- 2549 652. <https://doi.org/DOI:10.5194/cp-11-647-2015>
- 2550 Denning, A. S. (2022). Where Has All the Carbon Gone? *Annual Review of Earth and Planetary*
2551 *Sciences*, 50(1), 55–78. <https://doi.org/10.1146/annurev-earth-032320-092010>
- 2552 Desbruyères, D. G., Purkey, S. G., McDonagh, E. L., Johnson, G. C., & King, B. A. (2016).
2553 Deep and abyssal ocean warming from 35 years of repeat hydrography. *Geophysical*
2554 *Research Letters*, 43(19), 10, 310–356, 365. <https://doi.org/10.1002/2016GL070413>
- 2555 Desbruyères, D., McDonagh, E. L., King, B. A., & Thierry, V. (2017). Global and Full-Depth
2556 Ocean Temperature Trends during the Early Twenty-First Century from Argo and Repeat
2557 Hydrography. *Journal of Climate*, 30(6), 1985–1997. <https://doi.org/10.1175/JCLI-D-16-0396.1>
- 2559 Dieng, H. B., Cazenave, A., Meyssignac, B., & Ablain, M. (2017). New estimate of the current
2560 rate of sea level rise from a sea level budget approach. *Geophysical Research Letters*, 44(8),
2561 3744–3751. <https://doi.org/10.1002/2017GL073308>
- 2562 Domingues, C. M., Church, J. A., White, N. J., Gleckler, P. J., Wijffels, S. E., Barker, P. M., &
2563 Dunn, J. R. (2008). Improved estimates of upper-ocean warming and multi-decadal sea-
2564 level rise. *Nature*, 453(7198), 1090–1093. <https://doi.org/10.1038/nature07080>
- 2565 Dorigo, W., Dietrich, S., Aires, F., Brocca, L., Carter, S., Cretaux, J.-F., Dunkerley, D.,
2566 Enomoto, H., Forsberg, R., Güntner, A., Hegglin, M. I., Hollmann, R., Hurst, D. F.,
2567 Johannessen, J. A., Kummerow, C., Lee, T., Luoju, K., Looser, U., Miralles, D. G., ...
2568 Aich, V. (2021). Closing the Water Cycle from Observations across Scales: Where Do We
2569 Stand? *Bulletin of the American Meteorological Society*, 102(10), E1897–E1935.
2570 <https://doi.org/10.1175/BAMS-D-19-0316.1>
- 2571 Eicken, H., Fischer, H., & Lemke, P. (1995). Effects of the snow cover on Antarctic sea ice and
2572 potential modulation of its response to climate change. *Annals of Glaciology*, 21, 369–376.
2573 <https://doi.org/DOI:10.3189/S0260305500016086>
- 2574 Farinotti, D., Huss, M., Fürst, J. J., Landmann, J., Machguth, H., Maussion, F., & Pandit, A.
2575 (2019). A consensus estimate for the ice thickness distribution of all glaciers on Earth.
2576 *Nature Geoscience*, 12, 168–173. <https://doi.org/10.1038/s41561-019-0300-3>
- 2577 Fischer, E. M., Sippel, S., & Knutti, R. (2021). Increasing probability of record-shattering
2578 climate extremes. *Nature Climate Change*, 11(8), 689–695. <https://doi.org/10.1038/s41558-021-01092-9>
- 2580 Forster, P., Storelvmo, T., Armour, K., Collins, W., Dufresne, J.-L., Frame, D., Lunt, D. J.,
2581 Mauritsen, T., Palmer, M. D., Watanabe, M., Wild, M., & Zhang, H. (2022). *The Earth's*
2582 *Energy Budget, Climate Feedbacks, and Climate Sensitivity*. In *Climate Change 2021: The*
2583 *Physical Science Basis. Contribution of Working Group I to the Sixth Assessment Report of*
2584 *the Intergovernmental Panel on Climate Change* (V. Masson-Delmotte, P. Zhai, A. Pirani,
2585 S. L. Connors, C. Péan, S. Berger, N. Caud, Y. Chen, L. Goldfarb, M. I. Gomis, M. Huang,
2586 K. Leitzell, E. Lonnoy, J. B. R. Matthews, T. K. Maycock, T. Waterfield, O. Yelekçi, R.
2587 Yu, & B. Zhou (eds.)). Cambridge University Press, Cambridge, United Kingdom and New
2588 York, NY, USA. <https://doi.org/10.1017/9781009157896.009>
- 2589 Friedlingstein, P., Jones, M. W., O'Sullivan, M., Andrew, R. M., Bakker, D. C. E., Hauck, J., Le
2590 Quéré, C., Peters, G. P., Peters, W., Pongratz, J., Sitch, S., Canadell, J. G., Ciais, P.,
2591 Jackson, R. B., Alin, S. R., Anthoni, P., Bates, N. R., Becker, M., Bellouin, N., ... Zeng, J.
2592 (2022). Global Carbon Budget 2021. *Earth Syst. Sci. Data*, 14(4), 1917–2005.
2593 <https://doi.org/10.5194/essd-14-1917-2022>
- 2594 Frieler, K., Lange, S., Piontek, F., Reyer, C., Schewe, J., Warszawski, L., Zhao, F., Chini, L.,

- 2595 Denvil, S., Emanuel, K., Geiger, T., Halladay, K., Hurtt, G., Mengel, M., Murakami, D.,
 2596 Ostberg, S., Popp, A., Riva, R., Stevanovic, M., & Yamagata, Y. (2017). Assessing the
 2597 impacts of 1.5°C global warming – Simulation protocol of the Inter-Sectoral Impact Model
 2598 Interecomparison Project (ISIMIP2b). *Geoscientific Model Development*, *10*, 4321–4345.
 2599 <https://doi.org/10.5194/gmd-10-4321-2017>
- 2600 Fu, Q., Solomon, S., Pahlavan, H. A., & Lin, P. (2019). Observed changes in Brewer–Dobson
 2601 circulation for 1980–2018. *Environmental Research Letters*, *14*(11), 114026.
 2602 <https://doi.org/10.1088/1748-9326/ab4de7>
- 2603 Gädeke, A., Langer, M., Boike, J., Burke, E. J., Chang, J., Head, M., Reyer, C. P. O., Schaphoff,
 2604 S., Thiery, W., & Thonicke, K. (2021). Climate change reduces winter overland travel
 2605 across the Pan-Arctic even under low-end global warming scenarios. *Environmental*
 2606 *Research Letters*, *16*(2), 24049. <https://doi.org/10.1088/1748-9326/abdef2>
- 2607 Gaillard, F., Reynaud, T., Thierry, V., Kolodziejczyk, N., & von Schuckmann, K. (2016). In
 2608 Situ–Based Reanalysis of the Global Ocean Temperature and Salinity with ISAS:–
 2609 Variability of the Heat Content and Steric Height. *Journal of Climate*, *29*(4), 1305–1323.
 2610 <https://doi.org/10.1175/JCLI-D-15-0028.1>
- 2611 GCOS. (2016). *The Global Observing System for Climate: Implementation needs*, World
 2612 *Meteorological Organization, Geneva, Switzerland.*
- 2613 GCOS. (2021). *The Status of the Global Climate Observing System 2021: Executive Summary.*
 2614 *(GCOS-239).*
- 2615 Gelaro, R., McCarty, W., Suárez, M. J., Todling, R., Molod, A., Takacs, L., Randles, C. A.,
 2616 Darmenov, A., Bosilovich, M. G., Reichle, R., Wargan, K., Coy, L., Cullather, R., Draper,
 2617 C., Akella, S., Buchard, V., Conaty, A., da Silva, A. M., Gu, W., ... Zhao, B. (2017). The
 2618 Modern-Era Retrospective Analysis for Research and Applications, Version 2 (MERRA-2)
 2619 (1200, trans.). *Journal of Climate*, *30*(14), 5419–5454. <https://doi.org/10.1175/JCLI-D-16-0758.1>
- 2620
- 2621 Golub, M., Thiery, W., Marec, R., Pierson, D., Vanderkelen, I., Mereado-Bettin, D., Woolway,
 2622 R., Grant, L., Jennings, E., Kraemer, B., Schewe, J., Zhao, F., Frieler, K., Mengel, M.,
 2623 Bogomolov, V., Bouffard, D., Côté, M., Couture, R.-M., Debolskiy, A., & Zdrovennova,
 2624 G. (2022). A framework for ensemble modelling of climate change impacts on lakes
 2625 worldwide: the ISIMIP Lake Sector. *Geoscientific Model Development*, *15*, 4597–4623.
 2626 <https://doi.org/10.5194/gmd-15-4597-2022>
- 2627 Goni, G. J., Sprintall, J., Bringas, F., Cheng, L., Cirano, M., Dong, S., Domingues, R., Goes, M.,
 2628 Lopez, H., Morrow, R., Rivero, U., Rossby, T., Todd, R. E., Trinanes, J., Zilberman, N.,
 2629 Baringer, M., Boyer, T., Cowley, R., Domingues, C. M., ... Volkov, D. (2019). More Than
 2630 50 Years of Successful Continuous Temperature Section Measurements by the Global
 2631 Expendable Bathythermograph Network, Its Integrability, Societal Benefits, and Future.
 2632 *Frontiers in Marine Science*, *6*, 452.
 2633 <https://www.frontiersin.org/article/10.3389/fmars.2019.00452>
- 2634 Good, S. A. (2017). The impact of observational sampling on time series of global 0–700 m
 2635 ocean average temperature: a case study. *International Journal of Climatology*, *37*(5),
 2636 2260–2268. <https://doi.org/10.1002/joc.4654>
- 2637 Good, S. A., Martin, M. J., & Rayner, N. A. (2013). EN4: Quality controlled ocean temperature
 2638 and salinity profiles and monthly objective analyses with uncertainty estimates (15197,
 2639 trans.). *Journal of Geophysical Research: Oceans*, *118*(12), 6704–6716.
 2640 <https://doi.org/10.1002/2013JC009067>

- 2641 GOOS. (2019). *The Global Ocean Observing System Strategy. GOOS Report No. 239, IOC*
 2642 *Brochure 2019-5 (IOC/Bro/2019/5 rev.2)*. [https://www.goosocean.org/index.php?](https://www.goosocean.org/index.php?option=com_oe&task=viewDocumentRecord&docID=24590)
 2643 [option=com_oe&task=viewDocumentRecord&docID=24590](https://www.goosocean.org/index.php?option=com_oe&task=viewDocumentRecord&docID=24590)
- 2644 Gorfer, M. (2022). *Monitoring of climate change and variability in atmospheric heat content*
 2645 *based on climate records and reanalyses, Sci. Rep. 94-2022*. Wegener Center Verlag.
 2646 <https://wegecenter.uni-graz.at/wegener-center-verlag/2022>
- 2647 Gould, J., Sloyan, B., & Visbeck, M. (2013). Chapter 3—In Situ Ocean Observations: A Brief
 2648 History, Present Status, and Future Directions. In G. Siedler, S. M. Griffies, J. Gould, & J.
 2649 A. Church (Eds.), *Ocean Circulation and Climate* (Vol. 103, pp. 59–81). Academic Press.
 2650 <https://doi.org/https://doi.org/10.1016/B978-0-12-391851-2.00003-9>
- 2651 Gouretski, V., & Cheng, L. (2020). Correction for Systematic Errors in the Global Dataset of
 2652 Temperature Profiles from Mechanical Bathythermographs. *Journal of Atmospheric and*
 2653 *Oceanic Technology*, 37(5), 841–855. <https://doi.org/10.1175/JTECH-D-19-0205.1>
- 2654 Grant, L., Vanderkelen, I., Gudmundsson, L., Tan, Z., Perroud, M., Stepanenko, V. M.,
 2655 Debolskiy, A. V., Droppers, B., Janssen, A. B. G., Woolway, R. I., Choulga, M., Balsamo,
 2656 G., Kirillin, G., Schewe, J., Zhao, F., del Valle, I. V., Golub, M., Pierson, D., Marec, R., ...
 2657 Thierry, W. (2021). Attribution of global lake systems change to anthropogenic forcing.
 2658 *Nature Geoscience*, 14(11), 849–854. <https://doi.org/10.1038/s41561-021-00833-x>
- 2659 Gregory, J. M., & Andrews, T. (2016). Variation in climate sensitivity and feedback parameters
 2660 during the historical period. *Geophysical Research Letters*, 43(8), 3911–3920.
 2661 <https://doi.org/10.1002/2016GL068406>
- 2662 Grise, K. M., Davis, S. M., Simpson, I. R., Waugh, D. W., Fu, Q., Allen, R. J., Rosenlof, K. H.,
 2663 Ummenhofer, C. C., Karnauskas, K. B., Mayeock, A. C., Quan, X. W., Birner, T., & Staten,
 2664 P. W. (2019). Recent tropical expansion: Natural variability or forced response? *Journal of*
 2665 *Climate*, 32(5), 1551–1571. <https://doi.org/10.1175/JCLI-D-18-0444.1>
- 2666 Guinehut, S., Dhomps, A.-L., Larnicol, G., & Le Traon, P.-Y. (2012). High resolution 3-D
 2667 temperature and salinity fields derived from in-situ and satellite observations. *Ocean Sci.*,
 2668 8(5), 845–857. <https://doi.org/10.5194/os-8-845-2012>
- 2669 Gulev, S. K., Thorne, P. W., Ahn, J., Dentener, F. J., Domingues, C. M., Gerland, S., Gong, D.,
 2670 Kaufman, D. S., Nnamechi, H. C., Quaas, J., Rivera, J. A., Sathyendranath, S., Smith, S. L.,
 2671 Trewin, B., Schuckmann, K. von, & Vose, R. S. (2021). *Changing State of the Climate*
 2672 *System Supplementary Material. In Climate Change 2021: The Physical Science Basis.*
 2673 *Contribution of Working Group I to the Sixth Assessment Report of the Intergovernmental*
 2674 *Panel on Climate Change* (V. Masson-Delmotte, P. Zhai, A. Pirani, S. L. Connors, C. Péan,
 2675 S. Berger, N. Caud, Y. Chen, L. Goldfarb, M. I. Gomis, M. Huang, K. Leitzell, E. Lonnoy,
 2676 J. B. R. Matthews, T. K. Mayeock, T. Waterfield, O. Yelekçi, R. Yu, & B. Zhou (eds.)).
 2677 Cambridge University Press. <https://doi.org/10.1017/9781009157896.004>
- 2678 Hakuba, M. Z., Frederikse, T., & Landerer, F. W. (2021). Earth's Energy Imbalance From the
 2679 Ocean Perspective (2005–2019). *Geophysical Research Letters*, 48(16), e2021GL093624.
 2680 <https://doi.org/https://doi.org/10.1029/2021GL093624>
- 2681 Hansen, J., Sato, M., Kharecha, P., & von Schuckmann, K. (2011). Earth's energy imbalance and
 2682 implications. *Atmos. Chem. Phys.*, 11(24), 13421–13449. [https://doi.org/10.5194/acp-11-](https://doi.org/10.5194/acp-11-13421-2011)
 2683 [13421-2011](https://doi.org/10.5194/acp-11-13421-2011)
- 2684 Hansen, J., Sato, M., Kharecha, P., von Schuckmann, K., Beerling, D. J., Cao, J., Marcott, S.,
 2685 Masson-Delmotte, V., Prather, M. J., Rohling, E. J., Shakun, J., Smith, P., Laisis, A.,
 2686 Russell, G., & Ruedy, R. (2017). Young people's burden: requirement of negative CO₂

- emissions. *Earth Syst. Dynam.*, 8(3), 577–616. <https://doi.org/10.5194/esd-8-577-2017>
- 2688 Hansen, James, Nazarenko, L., Ruedy, R., Sato, M., Willis, J., Del Genio, A., Koch, D., Lacis,
2689 A., Lo, K., Menon, S., Novakov, T., Perlwitz, J., Russell, G., Gavin A., S., & Tausnev, N.
2690 (2005). Earth's Energy Imbalance: Confirmation and Implications. *Science*, 308(5727),
2691 1431–1435. <https://doi.org/10.1126/science.1110252>
- 2692 Hartmann, A., & Rath, V. (2005). Uncertainties and shortcomings of ground surface temperature
2693 histories derived from inversion of temperature logs. *Journal of Geophysics and*
2694 *Engineering*, 2(4), 299–311. <https://doi.org/10.1088/1742-2132/2/4/S02>
- 2695 Hersbach, H., de Rosnay, P., Bell, B., Shepeters, D., Simmons, A., Soci, C., Abdalla, S., Alonso-
2696 Balmaseda, M., Balsamo, G., Bechtold, P., Berrisford, P., Bidlot, J.-R., de Boissésou, E.,
2697 Bonavita, M., Browne, P., Buizza, R., Dahlgren, P., Dee, D., Dragani, R., ... Zuo, H.
2698 (2018). *Operational global reanalysis: progress, future directions and synergies with NWP*.
2699 <https://www.ecmwf.int/node/18765>
- 2700 Hersbach, Hans, Bell, B., Berrisford, P., Hirahara, S., Horányi, A., Muñoz-Sabater, J., Nicolas,
2701 J., Peubey, C., Radu, R., Shepeters, D., Simmons, A., Soci, C., Abdalla, S., Abellan, X.,
2702 Balsamo, G., Bechtold, P., Biavati, G., Bidlot, J., Bonavita, M., ... Thépaut, J. N. (2020).
2703 The ERA5 global reanalysis. *Quarterly Journal of the Royal Meteorological Society*, 146,
2704 1999–2049. <https://doi.org/10.1002/qj.3803>
- 2705 Høperoft, P. O., Gallagher, K., & Pain, C. C. (2007). Inference of past climate from borehole
2706 temperature data using Bayesian Reversible Jump Markov chain Monte Carlo. *Geophysical*
2707 *Journal International*, 171(3), 1430–1439. [https://doi.org/10.1111/j.1365-](https://doi.org/10.1111/j.1365-246X.2007.03596.x)
2708 [246X.2007.03596.x](https://doi.org/10.1111/j.1365-246X.2007.03596.x)
- 2709 Hosoda, S., Ohira, T., & Nakamura, T. (2008). *A monthly mean dataset of global oceanic*
2710 *temperature and salinity derived from Argo float observations*.
2711 http://www.jamstec.go.jp/ARGO/argo_web/ancient/MapQ/Hosoda_etal_MOAA_GPV.pdf
- 2712 IPCC. (2019). *IPCC Special Report on the Ocean and Cryosphere in a Changing Climate* (H.-O.
2713 Pörtner, D. C. Roberts, V. Masson-Delmotte, P. Zhai, M. Tignor, E. Poloczanska, K.
2714 Mintenbeck, A. Alegria, M. Nicolai, A. Okem, J. Petzold, B. Rama, & N. M. Weyer (eds.)).
2715 Cambridge University Press. <https://doi.org/10.1017/9781009157964>
- 2716 IPCC. (2021). *Summary for Policymakers. In: Climate Change 2021: The Physical Science*
2717 *Basis. Contribution of Working Group I to the Sixth Assessment Report of the*
2718 *Intergovernmental Panel on Climate Change* (V. Masson-Delmotte, P. Zhai, A. Pirani, S. L.
2719 Connors, C. Péan, S. Berger, N. Caud, Y. Chen, L. Goldfarb, M. I. Gomis, M. Huang, K.
2720 Leitzell, E. Lonnoy, J. B. R. Matthews, T. K. Maycock, T. Waterfield, O. Yelekçi, R. Yu, &
2721 B. Zhou (eds.)). Cambridge University Press. <https://doi.org/10.1017/9781009157896.001>
- 2722 IPCC. (2022a). *Climate Change 2022: Impacts, Adaptation, and Vulnerability. Contribution of*
2723 *Working Group II to the Sixth Assessment Report of the Intergovernmental Panel on*
2724 *Climate Change* (H.-O. Pörtner, D. C. Roberts, M. Tignor, E. S. Poloczanska, K.
2725 Mintenbeck, A. Alegria, M. Craig, S. Langsdorf, S. Löschke, V. Möller, A. Okem, & B.
2726 Rama (eds.)). Cambridge University Press, Cambridge, UK and New York, NY, USA.
2727 <https://doi.org/inpress>
- 2728 IPCC. (2022b). *Climate Change 2022: Mitigation of Climate Change. Contribution of Working*
2729 *Group III to the Sixth Assessment Report of the Intergovernmental Panel on Climate*
2730 *Change* (P. R. Shukla, J. Skea, R. Slade, A. Al Khourdajie, R. van Diemen, D. McCollum,
2731 M. Pathak, S. Some, P. Vyas, R. Fradera, M. Belkacemi, A. Hasija, G. Lisboa, S. Luz, & J.
2732 Malley (eds.)). Cambridge University Press, Cambridge, UK and New York, NY, USA.

- 2733 <https://doi.org/10.1017/9781009157926>
- 2734 IPCC. (2022c). *Summary for Policymakers, In: Climate Change 2022: Impacts, Adaptation, and*
- 2735 *Vulnerability. Contribution of Working Group II to the Sixth Assessment Report of the*
- 2736 *Intergovernmental Panel on Climate Change* (H.-O. Pörtner, D. C. Roberts, M. Tignor, E.
- 2737 S. Poloczanska, K. Mintenbeck, A. Alegría, M. Craig, S. Langsdorf, S. Löschke, V. Möller,
- 2738 A. Okem, & B. Rama (eds.)). Cambridge University Press. https://doi.org/in_press
- 2739 IROWG. (2021). *Report of IROWG activities: Outcome and recommendations from the IROWG-*
- 2740 *8 Workshop, CGMS-49 IROWG-WP-01 V3, 28 April 2021, International Radio Occultation*
- 2741 *Working Group*. [https://irowg.org/wpems/wp-content/uploads/2021/07/CGMS-49-IROWG-](https://irowg.org/wpems/wp-content/uploads/2021/07/CGMS-49-IROWG-WP-01.pdf)
- 2742 [WP-01.pdf](https://irowg.org/wpems/wp-content/uploads/2021/07/CGMS-49-IROWG-WP-01.pdf)
- 2743 Ishii, M., Fukuda, Y., Hirahara, S., Yasui, S., Suzuki, T., & Sato, K. (2017). Accuracy of Global
- 2744 Upper Ocean Heat Content Estimation Expected from Present Observational Data Sets.
- 2745 *SOLA*, *13*, 163–167. <https://doi.org/10.2151/sola.2017-030>
- 2746 Jan, A., & Painter, S. L. (2020). Permafrost thermal conditions are sensitive to shifts in snow
- 2747 timing. *Environmental Research Letters*, *15*(8), 084026. [https://doi.org/10.1088/1748-](https://doi.org/10.1088/1748-9326/ab8ee4)
- 2748 [9326/ab8ee4](https://doi.org/10.1088/1748-9326/ab8ee4)
- 2749 Jaume-Santero, F., Pickler, C., Beltrami, H., & Mareschal, J.-C. (2016). North American-
- 2750 regional climate reconstruction from ground surface temperature histories. *Clim. Past*,
- 2751 *12*(12), 2181–2194. <https://doi.org/10.5194/ep-12-2181-2016>
- 2752 Johnson, G. C., Lyman, J. M., & Loeb, N. G. (2016). Improving estimates of Earth's energy
- 2753 imbalance. *Nature Climate Change*, *6*(7), 639–640. <https://doi.org/10.1038/nclimate3043>
- 2754 Johnson, G. C., Purkey, S. G., Zilberman, N. V., & Roemmich, D. (2019). Deep Argo Quantifies
- 2755 Bottom Water Warming Rates in the Southwest Pacific Basin. *Geophysical Research*
- 2756 *Letters*, *46*(5), 2662–2669. <https://doi.org/10.1029/2018GL081685>
- 2757 Kashiwase, H., Ohshima, K. I., Nihashi, S., & Eicken, H. (2017). Evidence for ice-ocean albedo
- 2758 feedback in the Arctic Ocean shifting to a seasonal ice zone. *Scientific Reports*, *7*(1), 8170.
- 2759 <https://doi.org/10.1038/s41598-017-08467-z>
- 2760 Khazaei, B., Read, L. K., Casali, M., Sampson, K. M., & Yates, D. N. (2022). GLOBathy, the
- 2761 global lakes bathymetry dataset. *Scientific Data*, *9*(1), 36. [https://doi.org/10.1038/s41597-](https://doi.org/10.1038/s41597-022-01132-9)
- 2762 [022-01132-9](https://doi.org/10.1038/s41597-022-01132-9)
- 2763 King, B. A., Firing, E., & Joyce, T. (2001). Chapter 3.1 Shipboard observations during WOCE-
- 2764 *Int. Geophys.*, *77*, 99–122. [https://doi.org/https://doi.org/10.1016/S0074-6142\(01\)80114-5](https://doi.org/https://doi.org/10.1016/S0074-6142(01)80114-5)
- 2765 Kirchengast, Gottfried; Gorfer, Maximilian; Haimberger, Leopold; Mayer, Michael; Steiner,
- 2766 Andrea; Allan, Richard (2022). Heat stored in the Earth system 1960-2020: Where does the
- 2767 energy go?, submitted to Earth System Science Data. (2022). World Data Center for
- 2768 Climate (WDCC) at DKRZ. [https://www.wde-climate.de/ui/entry?](https://www.wde-climate.de/ui/entry?acronym=GCOS_EHI_1960-2020_AHC)
- 2769 [acronym=GCOS_EHI_1960-2020_AHC](https://www.wde-climate.de/ui/entry?acronym=GCOS_EHI_1960-2020_AHC)
- 2770 Kobayashi, S., Ota, Y., Harada, Y., Ebata, A., Moriya, M., Onoda, H., Onogi, K., Kamahori, H.,
- 2771 Kobayashi, C., Endo, H., Miyaoka, K., & Takahashi, K. (2015). The JRA-55 Reanalysis:
- 2772 General Specifications and Basic Characteristics. *Journal of the Meteorological Society of*
- 2773 *Japan. Ser. II*, *93*(1), 5–48. <https://doi.org/10.2151/jmsj.2015-001>
- 2774 Kramer, R. J., He, H., Soden, B. J., Oreopoulos, L., Myhre, G., Forster, P. M., & Smith, C. J.
- 2775 (2021). Observational Evidence of Increasing Global Radiative Forcing. *Geophysical*
- 2776 *Research Letters*, *48*(7), e2020GL091585.
- 2777 <https://doi.org/https://doi.org/10.1029/2020GL091585>
- 2778 Kuhlbrodt, T., & Gregory, J. M. (2012). Ocean heat uptake and its consequences for the

- 2779 magnitude of sea level rise and climate change. *Geophysical Research Letters*, 39(18).
 2780 <https://doi.org/10.1029/2012GL052952>
- 2781 Kuusela, M., & Giglio, D. (2022). *Global Ocean Heat Content Anomalies based on Argo data*.
 2782 <https://doi.org/10.5281/ZENODO.6131625>
- 2783 Labe, Z., Magnusdottir, G., & Stern, H. (2018). Variability of Arctic Sea Ice Thickness Using
 2784 PIOMAS and the CESM Large Ensemble. *Journal of Climate*, 31(8), 3233–3247.
 2785 <https://doi.org/10.1175/JCLI-D-17-0436.1>
- 2786 Ladstädter, F., Steiner, A. K., Schwärz, M., & Kirehngast, G. (2015). Climate intercomparison
 2787 of GPS radio occultation, RS90/92 radiosondes and GRUAN from 2002 to 2013.
 2788 *Atmospheric Measurement Techniques*, 8(4), 1819–1834. [https://doi.org/10.5194/amt-8-](https://doi.org/10.5194/amt-8-1819-2015)
 2789 [1819-2015](https://doi.org/10.5194/amt-8-1819-2015)
- 2790 Lane, A. C. (1923). Geotherms of Lake Superior Copper Country. *GSA Bulletin*, 34(4), 703–720.
 2791 <https://doi.org/10.1130/GSAB-34-703>
- 2792 Lavergne, T., Macdonald Sørensen, A., Kern, S., Tonboe, R., Notz, D., Aaboe, S., Bell, L.,
 2793 Dybkjaer, G., Eastwood, S., Gabarro, C., Heygster, G., Anne Killie, M., Brandt Kreiner, M.,
 2794 Lavelle, J., Saldo, R., Sandven, S., & Pedersen, L. T. (2019). Version 2 of the EUMETSAT-
 2795 OSI SAF and ESA CCI sea-ice concentration climate data records. *Cryosphere*, 13(1), 49–
 2796 78. <https://doi.org/10.5194/te-13-49-2019>
- 2797 Laxon, S. W., Giles, K. A., Ridout, A. L., Wingham, D. J., Willatt, R., Cullen, R., Kwok, R.,
 2798 Schweiger, A., Zhang, J., Haas, C., Hendriks, S., Krishfield, R., Kurtz, N., Farrell, S., &
 2799 Davidson, M. (2013). CryoSat-2 estimates of Arctic sea ice thickness and volume (I326-
 2800 trans.). *Geophysical Research Letters*. <https://doi.org/10.1002/grl.50193>
- 2801 Leahy, T. P., Llopis, F. P., Palmer, M. D., & Robinson, N. H. (2018). Using Neural Networks to
 2802 Correct Historical Climate Observations (I6042, trans.). *Journal of Atmospheric and*
 2803 *Oceanic Technology*, 35(10), 2053–2059. <https://doi.org/10.1175/JTECH-D-18-0012.1>
- 2804 Levitus, S., Antonov, J. I., Boyer, T. P., Baranova, O. K., Garcia, H. E., Locarnini, R. A.,
 2805 Mishonov, A. V., Reagan, J. R., Seidov, D., Yarosh, E. S., & Zweng, M. M. (2012). World
 2806 ocean heat content and thermosteric sea level change (0–2000 m), 1955–2010. *Geophysical*
 2807 *Research Letters*, 39(10). <https://doi.org/10.1029/2012GL051106>
- 2808 Li, H., Xu, F., Zhou, W., Wang, D., Wright, J. S., Liu, Z., & Lin, Y. (2017). Development of a
 2809 global gridded Argo data set with Barnes successive corrections. *Journal of Geophysical*
 2810 *Research: Oceans*, 122(2), 866–889. <https://doi.org/10.1002/2016JC012285>
- 2811 Liao, S., Luo, H., Wang, J., Shi, Q., Zhang, J., & Yang, Q. (2022). An evaluation of Antarctic
 2812 sea-ice thickness from the Global Ice-Ocean Modeling and Assimilation System based on in
 2813 situ and satellite observations. *The Cryosphere*, 16(5), 1807–1819.
 2814 <https://doi.org/10.5194/te-16-1807-2022>
- 2815 Ligtenberg, S. R. M., Kuipers Munneke, P., Noël, B. P. Y., & van den Broeke, M. R. (2018).
 2816 Brief communication: Improved simulation of the present-day Greenland firn layer (1960–
 2817 2016). *The Cryosphere*, 12(5), 1643–1649. <https://doi.org/10.5194/te-12-1643-2018>
- 2818 Liu, C., Allan, R. P., Mayer, M., Hyder, P., Desbruyères, D., Cheng, L., Xu, J., Xu, F., & Zhang,
 2819 Y. (2020). Variability in the global energy budget and transports 1985–2017. *Climate*
 2820 *Dynamics*, 55(11), 3381–3396. <https://doi.org/10.1007/s00382-020-05451-8>
- 2821 Llovel, W., Willis, J. K., Landerer, F. W., & Fukumori, I. (2014). Deep-ocean contribution to sea
 2822 level and energy budget not detectable over the past decade. *Nature Climate Change*, 4(11),
 2823 1031–1035. <https://doi.org/10.1038/nclimate2387>
- 2824 Loeb, N. G., Johnson, G. C., Thorsen, T. J., Lyman, J. M., Rose, F. G., & Kato, S. (2021).

- 2825 Satellite and Ocean Data Reveal Marked Increase in Earth's Heating Rate. *Geophysical*
 2826 *Research Letters*, 48(13), e2021GL093047.
 2827 <https://doi.org/https://doi.org/10.1029/2021GL093047>
- 2828 Loeb, N. G., Lyman, J. M., Johnson, G. C., Allan, R. P., Doelling, D. R., Wong, T., Soden, B. J.,
 2829 & Stephens, G. L. (2012). Observed changes in top-of-the-atmosphere radiation and upper-
 2830 ocean heating consistent within uncertainty. *Nature Geoscience*, 5(2), 110–113.
 2831 <https://doi.org/10.1038/ngeo1375>
- 2832 Loeb, N. G., Mayer, M., Kato, S., Fasullo, J. T., Zuo, H., Senan, R., Lyman, J. M., Johnson, G.
 2833 C., & Balmaseda, M. (2022). Evaluating Twenty-Year Trends in Earth's Energy Flows
 2834 From Observations and Reanalyses. *Journal of Geophysical Research: Atmospheres*,
 2835 127(12), e2022JD036686. <https://doi.org/https://doi.org/10.1029/2022JD036686>
- 2836 Lyman, J. M., & Johnson, G. C. (2014). Estimating Global Ocean Heat Content Changes in the
 2837 Upper 1800 m since 1950 and the Influence of Climatology Choice. *Journal of Climate*,
 2838 27(5), 1945–1957. <https://doi.org/10.1175/JCLI-D-12-00752.1>
- 2839 MacIntosh, C. R., Merchant, C. J., & von Schuckmann, K. (2017). Uncertainties in Steric Sea
 2840 Level Change Estimation During the Satellite Altimeter Era: Concepts and Practices.
 2841 *Surveys in Geophysics*, 38(1), 59–87. <https://doi.org/10.1007/s10712-016-9387-x>
- 2842 Mankoff, K. D., Colgan, W., Solgaard, A., Karlsson, N. B., Ahlström, A. P., van As, D., Box, J.
 2843 E., Khan, S. A., Kjeldsen, K. K., Mouginot, J., & Fausto, R. S. (2019). Greenland Ice Sheet
 2844 solid ice discharge from 1986 through 2017. *Earth Syst. Sci. Data*, 11(2), 769–786.
 2845 <https://doi.org/10.5194/essd-11-769-2019>
- 2846 Marti, F., Blazquez, A., Meyssignac, B., Ablain, M., Barnoud, A., Fraudeau, R., Jugier, R.,
 2847 Chenal, J., Larnicol, G., Pfeffer, J., Restano, M., & Benveniste, J. (2022). Monitoring the
 2848 ocean heat content change and the Earth energy imbalance from space altimetry and space
 2849 gravimetry. *Earth Syst. Sci. Data*, 14(1), 229–249. <https://doi.org/10.5194/essd-14-229-2022>
- 2850
- 2851 Matthews, T., Byrne, M., Horton, R., Murphy, C., Pielke Sr, R., Raymond, C., Thorne, P., &
 2852 Wilby, R. L. (2022). Latent heat must be visible in climate communications. *WIREs Climate*
 2853 *Change*, 13(4), e779. <https://doi.org/https://doi.org/10.1002/wcc.779>
- 2854 Mayer, J., Mayer, M., & Haimberger, L. (2021). Consistency and Homogeneity of Atmospheric
 2855 Energy, Moisture, and Mass Budgets in ERA5. *Journal of Climate*, 34(10), 3955–3974.
 2856 <https://doi.org/10.1175/JCLI-D-20-0676.1>
- 2857 Mayer, M., Lien, V. S., Mork, K. A., von Schuckmann, K., Monier, M., & Greiner, E. (2021).
 2858 Ocean heat content in the High North, in Copernicus Marine Service Ocean State Report,
 2859 Issue 5. *Journal of Operational Oceanography*, 14:sup1, 17–23.
 2860 <https://doi.org/10.1080/1755876X.2021.1946240>
- 2861 Mayer, Michael, Haimberger, L., Edwards, J. M., & Hyder, P. (2017). Toward Consistent
 2862 Diagnostics of the Coupled Atmosphere and Ocean Energy Budgets. *Journal of Climate*,
 2863 30(22), 9225–9246. <https://doi.org/10.1175/JCLI-D-17-0137.1>
- 2864 Meng, L., Liu, J., Tarasick, D. W., Randel, W. J., Steiner, A. K., Wilhelmsen, H., Wang, L., &
 2865 Haimberger, L. (2022). Continuous rise of the tropopause in the Northern Hemisphere over
 2866 1980–2020. *Science Advances*, 7(45), eabi8065. <https://doi.org/10.1126/sciadv.abi8065>
- 2867 Meyssignac, B., Boyer, T., Zhao, Z., Hakuba, M. Z., Landerer, F. W., Stammer, D., Köhl, A.,
 2868 Kato, S., Leuycy, T., Ablain, M., Abraham, J. P., Blazquez, A., Cazenave, A., Church, J.
 2869 A., Cowley, R., Cheng, L., Domingues, C. M., Giglio, D., Gouretski, V., ... Zilberman, N.
 2870 (2019). Measuring Global Ocean Heat Content to Estimate the Earth Energy Imbalance.

- 2871 *Frontiers in Marine Science*, 6, 432–
 2872 <https://www.frontiersin.org/article/10.3389/fmars.2019.00432>
 2873 Mierueh, S., Demirel, S., Simoneelli, S., Schlitzer, R., & Seitz, S. (2021). SalaciaML: A Deep
 2874 Learning Approach for Supporting Ocean Data Quality Control. In *Frontiers in Marine*
 2875 *Science* (Vol. 8). <https://www.frontiersin.org/articles/10.3389/fmars.2021.611742>
 2876 Millan, R., Mouginit, J., Rabatel, A., & Morlighem, M. (2022). Ice velocity and thickness of the
 2877 world's glaciers. *Nature Geoscience*, 15(2), 124–129. [https://doi.org/10.1038/s41561-021-](https://doi.org/10.1038/s41561-021-00885-z)
 2878 00885-z
 2879 Moltmann, T., Turton, J., Zhang, H.-M., Nolan, G., Gouldman, C., Griesbauer, L., Willis, Z.,
 2880 Piniella, A. M., Barrell, S., Andersson, E., Gallage, C., Charpentier, E., Belbeoch, M., Poli,
 2881 P., Rea, A., Burger, E. F., Legler, D. M., Lumpkin, R., Meinig, C., ... Zhang, Y. (2019). A
 2882 Global Ocean Observing System (GOOS), Delivered Through Enhanced Collaboration
 2883 Across Regions, Communities, and New Technologies. In *Frontiers in Marine Science*—
 2884 (Vol. 6, p. 291). <https://www.frontiersin.org/article/10.3389/fmars.2019.00291>
 2885 Moon, T., & Joughin, I. (2008). Changes in ice front position on Greenland's outlet glaciers from
 2886 1992 to 2007. *Journal of Geophysical Research: Earth Surface*, 113(F2).
 2887 <https://doi.org/https://doi.org/10.1029/2007JF000927>
 2888 Moore, G. W. K., Våge, K., Renfrew, I. A., & Piekart, R. S. (2022). Sea-ice retreat suggests re-
 2889 organization of water mass transformation in the Nordic and Barents Seas. *Nature*
 2890 *Communications*, 13(1), 67. <https://doi.org/10.1038/s41467-021-27641-6>
 2891 Motyka, R. J., Truffer, M., Fahnestock, M., Mortensen, J., Rysgaard, S., & Howat, I. (2011).
 2892 Submarine melting of the 1985 Jakobshavn Isbræ floating tongue and the triggering of the
 2893 current retreat. *Journal of Geophysical Research: Earth Surface*, 116(F1).
 2894 <https://doi.org/https://doi.org/10.1029/2009JF001632>
 2895 Mouginit, J., Rignot, E., Bjørk, A., van den Broeke, M., Millan, R., Morlighem, M., Noël, B.,
 2896 Scheuchl, B., & Wood, M. (2019). Forty-six years of Greenland Ice Sheet mass balance
 2897 from 1972 to 2018. *Proceedings of the National Academy of Sciences*, 116(19), 9239–9244.
 2898 <https://doi.org/10.1073/pnas.1904242116>
 2899 Mouginit, J., Rignot, E., Scheuchl, B., Fenty, I., Khazendar, A., Morlighem, M., Buzzi, A., &
 2900 Paden, J. (2015). Fast retreat of Zachariae Isstrøm, northeast Greenland. *Science*, 350(6266),
 2901 1357–1361. <https://doi.org/10.1126/science.aac7111>
 2902 Münchow, A., Padman, L., & Fricker, H. A. (2014). Interannual changes of the floating ice shelf
 2903 of Petermann Gletscher, North Greenland, from 2000 to 2012. *Journal of Glaciology*,
 2904 60(221), 489–499. <https://doi.org/DOI:10.3189/2014JoG13J135>
 2905 Nauels, A., Meinshausen, M., Mengel, M., Lorbacher, K., & Wigley, T. M. L. (2017).
 2906 Synthesizing long-term sea level rise projections—the MAGICC sea level model v2.0.
 2907 *Geosci. Model Dev.*, 10(6), 2495–2524. <https://doi.org/10.5194/gmd-10-2495-2017>
 2908 Nicolaus, M., Hoppmann, M., Arndt, S., Hendricks, S., Katlein, C., Nicolaus, A., Rossmann, L.,
 2909 Schiller, M., & Schwegmann, S. (2021). Snow Depth and Air Temperature Seasonality on
 2910 Sea-Ice Derived From Snow Buoy Measurements. In *Frontiers in Marine Science* (Vol.
 2911 8). <https://www.frontiersin.org/article/10.3389/fmars.2021.655446>
 2912 Nitzbon, J., Krinner, G., Schneider von Deimling, T., Werner, M., & Langer, M. (2022).
 2913 Quantifying the Permafrost Heat Sink in Earth's Climate System. Submitted. *Geophysical*
 2914 *Research Letters*.
 2915 Nitzbon, Jean; Krinner, Gerhard; Langer, Moritz (2022b). Quantifying the Permafrost Heat Sink
 2916 in Earth's Climate System, doi:/10.1002/essoar.10511600.1, submitted to Geophysical

- 2917 Research Letters (2022). World Data Center for Climate (WDCC) at DKRZ.
 2918 https://www.wdc-climate.de/ui/entry?acronym=GCOS_EH1_1960-2020_PHC
 2919 Palmer, M. D., & McNeall, D. J. (2014). Internal variability of Earth's energy budget simulated
 2920 by CMIP5 climate models. *Environmental Research Letters*, 9(3), 034016.
 2921 <https://doi.org/10.1088/1748-9326/9/3/034016>
 2922 Palmer, M. D., Roberts, C. D., Balmaseda, M., Chang, Y.-S., Chepurin, G., Ferry, N., Fujii, Y.,
 2923 Good, S. A., Guinchut, S., Haines, K., Hernandez, F., Köhl, A., Lee, T., Martin, M. J.,
 2924 Masina, S., Masuda, S., Peterson, K. A., Storto, A., Toyoda, T., ... Xue, Y. (2017). Ocean
 2925 heat content variability and change in an ensemble of ocean reanalyses. *Climate Dynamics*,
 2926 49(3), 909–930. <https://doi.org/10.1007/s00382-015-2801-0>
 2927 Palmer, Matthew D., Boyer, T., Cowley, R., Kizu, S., Reseghetti, F., Suzuki, T., & Thresher, A.
 2928 (2018). An Algorithm for Classifying Unknown Expendable Bathythermograph (XBT)
 2929 Instruments Based on Existing Metadata. *Journal of Atmospheric and Oceanic Technology*,
 2930 35(3), 429–440. <https://doi.org/10.1175/JTECH-D-17-0129.1>
 2931 Palmer, Matthew D., Domingues, C. M., Slangen, A. B. A., & Bocira Dias, F. (2021). An
 2932 ensemble approach to quantify global mean sea-level rise over the 20th century from tide-
 2933 gauge reconstructions (13507, trans.). *Environmental Research Letters*, 16(4), 044043.
 2934 <https://doi.org/10.1088/1748-9326/abdae>
 2935 Park, H., Fedorov, A. N., Zheleznyak, M. N., Konstantinov, P. Y., & Walsh, J. E. (2015). Effect
 2936 of snow cover on pan-Arctic permafrost thermal regimes. *Climate Dynamics*, 44(9), 2873–
 2937 2895. <https://doi.org/10.1007/s00382-014-2356-5>
 2938 Perovich, D., Polashenski, C., Arntsen, A., & Stwertka, C. (2017). Anatomy of a late spring
 2939 snowfall on sea ice. *Geophysical Research Letters*, 44(6), 2802–2809.
 2940 <https://doi.org/https://doi.org/10.1002/2016GL071470>
 2941 Piekler, C., Beltrami, H., & Mareschal, Jean-Claude. (2016). Laurentide Ice Sheet basal
 2942 temperatures during the last glacial cycle as inferred from borehole data. *Climate of the
 2943 Past*, 12, 115–127. <https://doi.org/10.5194/ep-12-115-2016>
 2944 Pisoft, P., Sacha, P., Polvani, L. M., Añel, J. A., de la Torre, L., Eichinger, R., Foelsehe, U.,
 2945 Huszar, P., Jacobi, C., Karlicky, J., Kuehar, A., Miksovsky, J., Zak, M., & Rieder, H. E.
 2946 (2021). Stratospheric contraction caused by increasing greenhouse gases. *Environmental
 2947 Research Letters*, 16(6), 64038. <https://doi.org/10.1088/1748-9326/abfe2b>
 2948 Purkey, S. G., & Johnson, G. C. (2010). Warming of Global Abyssal and Deep Southern Ocean
 2949 Waters between the 1990s and 2000s: Contributions to Global Heat and Sea Level Rise
 2950 Budgets. *Journal of Climate*, 23(23), 6336–6351. <https://doi.org/10.1175/2010JCLI3682.1>
 2951 Qu, X., & Hall, A. (2007). What Controls the Strength of Snow-Albedo Feedback? *Journal of
 2952 Climate*, 20(15), 3971–3981. <https://doi.org/10.1175/JCLI4186.1>
 2953 Rhein, M., Rintoul, S., Aoki, S., Campos, E., Chambers, D., Feely, R., Gulev, S., Johnson, G.,
 2954 Josey, S., Kostianoy, A., Mauritzen, C., Roemmich, D., Talley, L., & Wang, F. (2013).
 2955 Chapter 3: Observations: Ocean. In: *Climate Change 2013: The Physical Science Basis.
 2956 Contribution of Working Group I to the Fifth Assessment Report of the Intergovernmental
 2957 Panel on Climate Change.* (T. Stocker, D. Qin, G.-K. Plattner, M. Tignor, S. Allen, J.
 2958 Boscung, A. Nauels, Y. Xia, V. Bex, & P. Midgley (eds.)). Cambridge University Press.
 2959 Rignot, E., Mouginot, J., Scheuchl, B., van den Broeke, M., van Wessel, M. J., & Morlighem,
 2960 M. (2019). Four decades of Antarctic Ice Sheet mass balance from 1979–2017. *Proceedings
 2961 of the National Academy of Sciences*, 116(4), 1095–
 2962 <https://doi.org/10.1073/pnas.1812883116>

- 2963 Riser, S. C., Freeland, H. J., Roemmich, D., Wijffels, S., Troisi, A., Belbéoch, M., Gilbert, D.,
 2964 Xu, J., Pouliquen, S., Thresher, A., Le Traon, P.-Y., Maze, G., Klein, B., Ravichandran, M.,
 2965 Grant, F., Poulain, P.-M., Suga, T., Lim, B., Sterl, A., ... Jayne, S. R. (2016). Fifteen years
 2966 of ocean observations with the global Argo array. *Nature Climate Change*, 6(2), 145–153.
 2967 <https://doi.org/10.1038/nclimate2872>
- 2968 Roemmich, D., Alford, M. H., Claustre, H., Johnson, K., King, B., Moum, J., Oke, P., Owens,
 2969 W. B., Pouliquen, S., Purkey, S., Seanderbeg, M., Suga, T., Wijffels, S., Zilberman, N.,
 2970 Bakker, D., Baringer, M., Belbeoch, M., Bittig, H. C., Boss, E., ... Yasuda, I. (2019). On
 2971 the Future of Argo: A Global, Full-Depth, Multi-Disciplinary Array. In *Frontiers in*
 2972 *Marine Science* (Vol. 6, p. 439).
 2973 <https://www.frontiersin.org/article/10.3389/fmars.2019.00439>
- 2974 Roemmich, D., Church, J., Gilson, J., Monselesan, D., Sutton, P., & Wijffels, S. (2015).
 2975 Unabated planetary warming and its ocean structure since 2006 (13631, trans.). *Nature*
 2976 *Climate Change*, 5, 240. <https://doi.org/10.1038/nclimate2513>
- 2977 Roemmich, D., & Gilson, J. (2009). The 2004–2008 mean and annual cycle of temperature,
 2978 salinity, and steric height in the global ocean from the Argo Program. *Progress in*
 2979 *Oceanography*, 82(2), 81–100. <https://doi.org/https://doi.org/10.1016/j.pocan.2009.03.004>
- 2980 Santer, B. D., Wigley, T. M. L., Doutriaux, C., Boyle, J. S., Hansen, J. E., Jones, P. D., Meehl, G.-
 2981 A., Roeckner, E., Sengupta, S., & Taylor, K. E. (2001). Accounting for the effects of
 2982 volcanoes and ENSO in comparisons of modeled and observed temperature trends. *Journal*
 2983 *of Geophysical Research: Atmospheres*, 106(D22), 28033–28059.
 2984 <https://doi.org/https://doi.org/10.1029/2000JD000189>
- 2985 Santer, Benjamin D., Po-Chedley, S., Feldl, N., Fyfe, J. C., Fu, Q., Solomon, S., England, M.,
 2986 Rodgers, K. B., Stuecker, M. F., Mears, C., Zou, C.-Z., Bonfils, C. J. W., Pallotta, G.,
 2987 Zelinka, M. D., Rosenbloom, N., & Edwards, J. (2022). Robust anthropogenic signal
 2988 identified in the seasonal cycle of tropospheric temperature. *Journal of Climate*, 1–51.
 2989 <https://doi.org/10.1175/JCLI-D-21-0766.1>
- 2990 Santer, Benjamin D., Po-Chedley, S., Mears, C., Fyfe, J. C., Gillett, N., Fu, Q., Painter, J. F.,
 2991 Solomon, S., Steiner, A. K., Wentz, F. J., Zelinka, M. D., & Zou, C.-Z. (2021). Using
 2992 Climate Model Simulations to Constrain Observations. *Journal of Climate*, 34(15), 6281–
 2993 6301. <https://doi.org/10.1175/JCLI-D-20-0768.1>
- 2994 Savita, A., Domingues, C. M., Boyer, T., Gouretski, V., Ishii, M., Johnson, G. C., Lyman, J. M.,
 2995 Willis, J. K., Marsland, S. J., Hobbs, W., Church, J. A., Monselesan, D. P., Dobrohotoff, P.,
 2996 Cowley, R., & Wijffels, S. E. (2022). Quantifying Spread in Spatiotemporal Changes of
 2997 Upper-Ocean Heat Content Estimates: An Internationally Coordinated Comparison. *Journal*
 2998 *of Climate*, 35(2), 851–875. <https://doi.org/10.1175/JCLI-D-20-0603.1>
- 2999 Schweiger, A. J., Wood, K. R., & Zhang, J. (2019). Arctic Sea Ice Volume Variability over
 3000 1901–2010: A Model-Based Reconstruction. *Journal of Climate*, 32(15), 4731–4752.
 3001 <https://doi.org/10.1175/JCLI-D-19-0008.1>
- 3002 Schweiger, A., Lindsay, R., Zhang, J., Steele, M., Stern, H., & Kwok, R. (2011). Uncertainty in
 3003 modeled Arctic sea ice volume. *Journal of Geophysical Research: Oceans*, 116(C8).
 3004 <https://doi.org/10.1029/2011JC007084>
- 3005 Shen, P. Y., Wang, K., Beltrami, H., & Mareschal, J.-C. (1992). A comparative study of inverse
 3006 methods for estimating climatic history from borehole temperature data. *Palaeogeography,*
 3007 *Palaeoclimatology, Palaeoecology*, 98(2), 113–127.
 3008 [https://doi.org/https://doi.org/10.1016/0031-0182\(92\)90192-8](https://doi.org/https://doi.org/10.1016/0031-0182(92)90192-8)

- 3009 Shen, X., Ke, C.-Q., & Li, H. (2022). Snow depth product over Antarctic sea ice from 2002 to
3010 2020 using multisource passive microwave radiometers. *Earth Syst. Sci. Data*, *14*(2), 619–
3011 636. <https://doi.org/10.5194/essd-14-619-2022>
- 3012 Shepherd, A., Frieker, H. A., & Farrell, S. L. (2018). Trends and connections across the
3013 Antarctic cryosphere. *Nature*, *558*(7709), 223–232. <https://doi.org/10.1038/s41586-018-0171-6>
- 3015 Shepherd, A., Ivins, E., Rignot, E., Smith, B., van den Broeke, M., Velicogna, I., Whitehouse, P.,
3016 Briggs, K., Joughin, I., Krinner, G., Nowicki, S., Payne, T., Seambos, T., Sehlegel, N.,
3017 Geruo, A., Agosta, C., Ahlström, A., Babonis, G., Barletta, V. R., ... Team, T. I. (2019).
3018 Mass balance of the Greenland Ice Sheet from 1992 to 2018. *Nature*.
3019 <https://doi.org/10.1038/s41586-019-1855-2>
- 3020 Slater, T., Lawrence, I. R., Ootosaka, I. N., Shepherd, A., Gourmelen, N., Jakob, L., Tepez, P.,
3021 Gilbert, L., & Nienow, P. (2021). Review article: Earth's ice imbalance. *The Cryosphere*,
3022 *15*(1), 233–246. <https://doi.org/10.5194/te-15-233-2021>
- 3023 Smith, B., Frieker, A. H., Gardner, S. A., Medley, B., Nilsson, J., Paolo, S. F., Holschuh, N.,
3024 Adusumilli, S., Brunt, K., Csatho, B., Harbeck, K., Markus, T., Neumann, T., Siegfried, M.,
3025 & Zwally, J. H. (2020). Pervasive ice sheet mass loss reflects competing ocean and
3026 atmosphere processes. *Science*, *368*(6496), 1239–1242.
3027 <https://doi.org/10.1126/science.aaz5845>
- 3028 Smith, D. M., Allan, R. P., Coward, A. C., Eade, R., Hyder, P., Liu, C., Loeb, N. G., Palmer, M.
3029 D., Roberts, C. D., & Seaife, A. A. (2015). Earth's energy imbalance since 1960 in
3030 observations and CMIP5 models. *Geophysical Research Letters*, *42*(4), 1205–1213.
3031 <https://doi.org/10.1002/2014GL062669>
- 3032 Staten, P. W., Grise, K. M., Davis, S. M., Karnauskas, K. B., Waugh, D. W., Maycock, A. C.,
3033 Fu, Q., Cook, K., Adam, O., Simpson, I. R., Allen, R. J., Rosenlof, K., Chen, G.,
3034 Ummenhofer, C. C., Quan, X.-W., Kossin, J. P., Davis, N. A., & Son, S.-W. (2020).
3035 Tropical Widening: From Global Variations to Regional Impacts. *Bulletin of the American*
3036 *Meteorological Society*, *101*(6), E897–E904. <https://doi.org/10.1175/bams-d-19-0047.1>
- 3037 Steiner, A. K., Ladstädter, F., Ao, C. O., Gleisner, H., Ho, S.-P., Hunt, D., Schmidt, T., Foelsehe,
3038 U., Kirchengast, G., Kuo, Y.-H., Lauritsen, K. B., Mannucci, A. J., Nielsen, J. K.,
3039 Schreiner, W., Schwärz, M., Sokolovskiy, S., Syndergaard, S., & Wickert, J. (2020).
3040 Consistency and structural uncertainty of multi-mission GPS radio occultation records
3041 (11695, trans.). *Atmospheric Measurement Techniques*, *13*(5), 2547–2575.
3042 <https://doi.org/10.5194/amt-13-2547-2020>
- 3043 Steiner, Andrea K., Ladstädter, F., Randel, W. J., Maycock, A. C., Fu, Q., Claud, C., Gleisner,
3044 H., Haimberger, L., Ho, S.-P., Keckhut, P., Leblanc, T., Mears, C., Polvani, L. M., Santer,
3045 B. D., Schmidt, T., Sofieva, V., Wing, R., & Zou, C.-Z. (2020). Observed Temperature
3046 Changes in the Troposphere and Stratosphere from 1979 to 2018 (13342, trans.). *Journal of*
3047 *Climate*, *33*(19), 8165–8194. <https://doi.org/10.1175/JCLI-D-19-0998.1>
- 3048 Storto, A., Alvera-Azcárate, A., Balsaseda, M. A., Barth, A., Chevallier, M., Counillon, F.,
3049 Domingues, C. M., Drevillon, M., Drillet, Y., Forget, G., Garric, G., Haines, K., Hernandez,
3050 F., Iovino, D., Jackson, L. C., Lellouche, J.-M., Masina, S., Mayer, M., Oke, P. R., ... Zuo,
3051 H. (2019). Ocean Reanalyses: Recent Advances and Unsolved Challenges. *Frontiers in*
3052 *Marine Science*, *6*, 418. <https://doi.org/10.3389/fmars.2019.00418>
- 3053 Storto, A., Masina, S., Simonecelli, S., Iovino, D., Cipollone, A., Drevillon, M., Drillet, Y.,
3054 Schueckman, K., Parent, L., Garric, G., Greiner, E., Desportes, C., Zuo, H., Balsaseda, M.,

- 3055 & Peterson, K. (2018). The added value of the multi-system spread information for ocean
 3056 heat content and steric sea level investigations in the CMEMS GREP ensemble reanalysis
 3057 product. *Climate Dynamics*. <https://doi.org/10.1007/s00382-018-4585-5>
- 3058 Filling, R. L., Ridout, A., & Shepherd, A. (2018). Estimating Arctic sea ice thickness and
 3059 volume using CryoSat-2 radar altimeter data. *Advances in Space Research*, *62*(6), 1203–
 3060 1225. <https://doi.org/https://doi.org/10.1016/j.asr.2017.10.051>
- 3061 Trenberth, K. E., & Fasullo, J. T. (2010). Tracking Earth's Energy. *Science*, *328*(5976), 316–
 3062 <https://doi.org/10.1126/science.1187272>
- 3063 Trenberth, K. E., Fasullo, J. T., von Schuckmann, K., & Cheng, L. (2016). Insights into Earth's
 3064 Energy Imbalance from Multiple Sources. *Journal of Climate*, *29*(20), 7495–7505.
 3065 <https://doi.org/10.1175/JCLI-D-16-0339.1>
- 3066 Vanderkelen, Inne; Thiery, Wim (2022). Global Heat Uptake by Inland Waters. *Geophysical*
 3067 *Research Letters*, *47*(12). e2020GL087867. D O I: <https://doi.org/10.1029/2020GL087867>.
 3068 (2020). World Data Center for Climate (WDCC) at DKRZ.
 3069 https://www.wdc-climate.de/ui/entry?acronym=GCOS_EHI_1960-2020_IWHC
- 3070 Vanderkelen, I., van Lipzig, N. P. M., Lawrence, D. M., Droppers, B., Golub, M., Gosling, S. N.,
 3071 Janssen, A. B. G., Marcé, R., Schmied, H. M., Perroud, M., Pierson, D., Pokhrel, Y., Satoh,
 3072 Y., Schewe, J., Seneviratne, S. I., Stepanenko, V. M., Tan, Z., Woolway, R. I., & Thiery,
 3073 W. (2020). Global Heat Uptake by Inland Waters. *Geophysical Research Letters*, *47*(12),
 3074 e2020GL087867. <https://doi.org/https://doi.org/10.1029/2020GL087867>
- 3075 Verver, G., Fujiwara, M., Dolmans, P., Becker, C., Fortuin, P., & Miloshevich, L. (2006).
 3076 Performance of the Vaisala RS80A/H and RS90 Humicap Sensors and the Meteorolabor
 3077 “Snow White” Chilled-Mirror Hygrometer in Paramaribo, Suriname. *Journal of*
 3078 *Atmospheric and Oceanic Technology*, *23*(11), 1506–1518.
 3079 <https://doi.org/10.1175/JTECH1941.1>
- 3080 Vömel, H., Selkirk, H., Miloshevich, L., Valverde-Canossa, J., Valdés, J., Kyrö, E., Kivi, R.,
 3081 Stolz, W., Peng, G., & Diaz, J. A. (2007). Radiation Dry Bias of the Vaisala RS92 Humidity
 3082 Sensor. *Journal of Atmospheric and Oceanic Technology*, *24*(6), 953–963.
 3083 <https://doi.org/10.1175/JTECH2019.1>
- 3084 von Schuckmann, Karina; Minière, Audrey; Gues, Flora; Cuesta-Valero, Francisco; Kirehengast,
 3085 Gottfried; Adusumilli, Susheel; Straneo, Fiammetta; Allan, Richard; Barker, Paul M.;
 3086 Beltrami, Hugo; Boyer, Tim; Cheng, Lijing; Church, John; Desbruyeres, Damien; Dolman,
 3087 Han; Domingues, Catia; Gareía-Gareía, Almudena; Gilson, John; Gorfer, Maximilian;
 3088 Haimberger, Leopold; Hendrieks, Stefan; Hosoda, Shigeeki; Johnson, Gregory; Killiek,
 3089 Rachel; King, Brian; Kolodziejczyk, Nicolas; Korosov, Anton; Krinner, Gerhard; Kuusela,
 3090 Mikael; Langer, Moritz; Lavergne, Thomas; Lawrence, Isobel; Li, Yuehua; Lyman, John;
 3091 Marzeion, Ben; Mayer, Michael; MacDougall, Andrew; McDougall, Trevor; Monselesan,
 3092 Didier; Nitzbon, Jean; Otosaka, Inès; Peng, Jian; Purkey, Sarah; Roemmich, Dean; Sato,
 3093 Kanako; Sato, Katsunari; Savita, Abhishek; Schweiger, Axel; Shepherd, Andrew;
 3094 Seneviratne, Sonia; Slater, Donald; Slater, Thomas; Smith, Noah; Steiner, Andrea; Szekely,
 3095 Tanguy; Suga, Toshio; Thiery, Wim; Timmermanns, Mary-Louise; Vanderkelen, Inne;
 3096 Wijffels, Susan; Wu, Tonghua; Zemp, Michael; Simons, Leon (2022). Heat stored in the
 3097 Earth system 1960–2020: Where does the energy go?. World Data Center for Climate
 3098 (WDCC) at DKRZ. [https://www.wdc-climate.de/ui/entry?acronym=GCOS_EHI_1960-
 3099 2020_OHC](https://www.wdc-climate.de/ui/entry?acronym=GCOS_EHI_1960-2020_OHC)
- 3100 von Schuckmann, K., Palmer, M. D., Trenberth, K. E., Cazenave, A., Chambers, D.,

- 3101 Champollion, N., Hansen, J., Josey, S. A., Loeb, N., Mathieu, P.-P., Meyssignac, B., &
 3102 Wild, M. (2016). An imperative to monitor Earth's energy imbalance. *Nature Climate*
 3103 *Change*, 6(2), 138–144. <https://doi.org/10.1038/nclimate2876>
- 3104 von Schuckmann, K., Cheng, L., Palmer, M. D., Hansen, J., Tassone, C., Aich, V., Adusumilli,
 3105 S., Beltrami, H., Boyer, T., Cuesta-Valero, F. J., Desbruyères, D., Domingues, C., García-
 3106 García, A., Gentile, P., Gilson, J., Gorfer, M., Haimberger, L., Ishii, M., Johnson, G. C., ...
 3107 Wijffels, S. E. (2020). Heat stored in the Earth system: where does the energy go? *Earth*
 3108 *Syst. Sci. Data*, 12(3), 2013–2041. <https://doi.org/10.5194/essd-12-2013-2020>
- 3109 von Schuckmann, K., & Le Traon, P.-Y. (2011). How well can we derive Global Ocean
 3110 Indicators from Argo data? *Ocean Sci.*, 7(6), 783–791. [https://doi.org/10.5194/os-7-783-](https://doi.org/10.5194/os-7-783-2011)
 3111 2011
- 3112 von Schuckmann, Karina, Le Traon, P.-Y., Smith, N., Pascual, A., Brasseur, P., Fennel, K.,
 3113 Djavidnia, S., Aaboe, S., Fanjul, E. A., Autret, E., Axell, L., Aznar, R., Benincasa, M.,
 3114 Bentamy, A., Boberg, F., Bourdallé-Badie, R., Nardelli, B. B., Brando, V. E., Bricaud, C.,
 3115 ... Zuo, H. (2018). Copernicus Marine Service Ocean State Report. *Journal of Operational*
 3116 *Oceanography*, 11(sup1), S1–S142. <https://doi.org/10.1080/1755876X.2018.1489208>
- 3117 Wanders, N., Thober, S., Kumar, R., Pan, M., Sheffield, J., Samaniego, L., & Wood, E. F.
 3118 (2019). Development and Evaluation of a Pan-European Multimodel Seasonal Hydrological
 3119 Forecasting System. *Journal of Hydrometeorology*, 20(1), 99–115.
 3120 <https://doi.org/10.1175/JHM-D-18-0040.1>
- 3121 Wang, X., Key, J., Kwok, R., & Zhang, J. (2016). Comparison of Arctic Sea Ice Thickness from
 3122 Satellites, Aircraft, and PIOMAS Data. In *Remote Sensing* (Vol. 8, Issue 9).
 3123 <https://doi.org/10.3390/rs8090713>
- 3124 WCRP Global Sea Level Budget Group. (2018). Global sea-level budget 1993–present. *Earth*
 3125 *Syst. Sci. Data*, 10(3), 1551–1590. <https://doi.org/10.5194/essd-10-1551-2018>
- 3126 Webster, M. A., DuVivier, A. K., Holland, M. M., & Bailey, D. A. (2021). Snow on Arctic Sea
 3127 Ice in a Warming Climate as Simulated in CESM. *Journal of Geophysical Research:*
 3128 *Oceans*, 126(1), e2020JC016308. <https://doi.org/https://doi.org/10.1029/2020JC016308>
- 3129 Weihs, P., Laimighofer, J., Formayer, H., & Olefs, M. (2021). Influence of snow making on
 3130 albedo and local radiative forcing in an alpine area. *Atmospheric Research*, 255, 105448.
 3131 <https://doi.org/https://doi.org/10.1016/j.atmosres.2020.105448>
- 3132 WGMS. (2021). *Fluctuations of Glaciers Database*. World Glacier Monitoring Service, Zurich,
 3133 Switzerland. <https://doi.org/DOI:10.5904/wgms-fog-2021-05>
- 3134 Wijffels, S., Roemmich, D., Monselesan, D., Church, J., & Gilson, J. (2016). Ocean temperatures
 3135 chronicle the ongoing warming of Earth. *Nature Climate Change*, 6(2), 116–118.
 3136 <https://doi.org/10.1038/nclimate2924>
- 3137 Willis, J. K., Roemmich, D., & Cornuelle, B. (2004). Interannual variability in upper ocean heat
 3138 content, temperature, and thermocline expansion on global scales. *Journal of Geophysical*
 3139 *Research: Oceans*, 109(C12). <https://doi.org/10.1029/2003JC002260>
- 3140 Wilson, N., Straneo, F., & Heimbach, P. (2017). Satellite-derived submarine melt rates and mass
 3141 balance (2011–2015) for Greenland's largest remaining ice tongues. *The Cryosphere*, 11,
 3142 2773–2782. <https://doi.org/10.5194/te-11-2773-2017>
- 3143 WMO. (2022). *The State of the Global Climate 2021*. [https://library.wmo.int/index.php?](https://library.wmo.int/index.php?lvl=notice_display&id=22080)
 3144 [lvl=notice_display&id=22080](https://library.wmo.int/index.php?lvl=notice_display&id=22080)
- 3145 Wunsch, C. (2020). Is the Ocean Speeding Up? Ocean Surface Energy Trends. *Journal of*
 3146 *Physical Oceanography*, 50, 3205–3217. <https://doi.org/10.1175/JPO-D-20-0082.1>

- 3147 Zanna, L., Khatiwala, S., Gregory, J. M., Ison, J., & Heimbach, P. (2019). Global reconstruction
3148 of historical ocean heat storage and transport. *Proceedings of the National Academy of*
3149 *Sciences*, *116*(4), 1126. <https://doi.org/10.1073/pnas.1808838115>
- 3150 Zemp, M., Huss, M., Thibert, E., Eckert, N., McNabb, R., Huber, J., Barandun, M., Machguth,
3151 H., Nussbaumer, S. U., Gärtner-Roer, I., Thomson, L., Paul, F., Maussion, F., Kutuzov, S.,
3152 & Cogley, J. G. (2019). *Global and regional glacier mass changes from 1961 to 2016.*
3153 <https://doi.org/10.5281/ZENODO.3557199>
- 3154 Zemp, Michael, Huss, M., Eckert, N., Thibert, E., Paul, F., Nussbaumer, U. S., & Gärtner-Roer,
3155 I. (2020). Brief communication: Ad hoc estimation of glacier contributions to sea-level rise
3156 from the latest glaciological observations (15946, trans.). *Cryosphere*, *14*(3).
3157 <https://doi.org/10.5194/te-14-1043-2020>
- 3158 Zhang, J., & Rothrock, D. A. (2003). Modeling Global Sea Ice with a Thickness and Enthalpy
3159 Distribution Model in Generalized Curvilinear Coordinates. *Monthly Weather Review*,
3160 *131*(5), 845–861. [https://doi.org/10.1175/1520-0493\(2003\)131<0845:MGSIWA>2.0.CO;2](https://doi.org/10.1175/1520-0493(2003)131<0845:MGSIWA>2.0.CO;2)
- 3161 Zhang, R., Wang, H., Fu, Q., Rasch, J. P., & Wang, X. (2019). Unraveling driving forces
3162 explaining significant reduction in satellite-inferred Arctic surface albedo since the 1980s.
3163 *Proceedings of the National Academy of Sciences*, *116*(48), 23947–23953.
3164 <https://doi.org/10.1073/pnas.1915258116>
- 3165 Zou, C.-Z., Xu, H., Hao, X., & Fu, Q. (2021). Post-Millennium Atmospheric Temperature
3166 Trends Observed From Satellites in Stable Orbits. *Geophysical Research Letters*, *48*(13),
3167 e2021GL093291. <https://doi.org/https://doi.org/10.1029/2021GL093291>
3168